

HOST CELL VIRUS ENTRY MEDIATED BY AUSTRALIAN BAT LYSSAVIRUS  
ENVELOPE G GLYCOPROTEIN

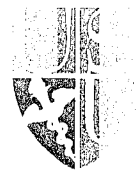
by

Dawn Lynette Weir

Dissertation submitted to the Faculty of the  
Emerging Infectious Diseases Graduate Program  
Uniformed Services University of the Health Sciences  
In partial fulfillment of the requirements for the degree of  
Doctor of Philosophy 2013



UNIFORMED SERVICES UNIVERSITY, SCHOOL OF MEDICINE GRADUATE PROGRAMS  
Graduate Education Office (A 1045), 4301 Jones Bridge Road, Bethesda, MD 20814



DISSERTATION APPROVAL FOR THE DOCTORAL DISSERTATION IN THE EMERGING  
INFECTIOUS DISEASES GRADUATE PROGRAM

Title of Dissertation: "Host cell virus entry mediated by Australian bat lyssavirus envelope glycoprotein G"

Name of Candidate: Dawn L. Weir  
Doctor of Philosophy Degree  
October 24, 2013

DISSERTATION AND ABSTRACT APPROVED:

DATE:

10-24-13

Dr. Chou-Zen Giam  
DEPARTMENT OF MICROBIOLOGY AND IMMUNOLOGY  
Committee Chairperson

10-24-13

Dr. Christopher Broder  
DEPARTMENT OF MICROBIOLOGY AND IMMUNOLOGY  
Dissertation Advisor

10/24/13

Dr. Joseph Mattapallil  
DEPARTMENT OF MICROBIOLOGY AND IMMUNOLOGY  
Committee Member

10-24-13

Dr. Ann E. Jerse  
Department of MICROBIOLOGY AND IMMUNOLOGY  
Committee Member

10/24/13

Dr. Robert Lowy  
PRINCIPLE INVESTIGATOR, AFRI, USU  
Committee Member

## ACKNOWLEDGMENTS

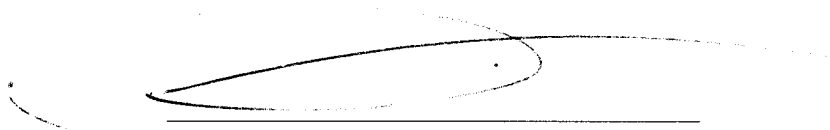
First, I thank my advisor Dr. Christopher C. Broder for his guidance and support over the last six years. I feel very fortunate to have been afforded the opportunity to be mentored by such a great scientist. Second, I thank my committee members Dr. Joe Giam, Dr. Joseph Mattapallil, Dr. Ann Jerse, and Dr. Joel Lowy for their guidance. Third, I thank my classmates Diana Riner, Paige Sachs, Tonia Zangari, Deborah Fusco, and Suman Paul for their friendship and support, particularly during the first two years and throughout the dreaded qualifying exam process. I can't imagine getting through the 1<sup>st</sup> winter quarter without our weekly post-biochem HHs. I also thank past and present members of the Broder Lab and our collaborators, especially those in Australia, who made this work possible. I especially thank Lianying Yan (Linda) for making me smile on a daily basis. Finally, I thank my family for their tremendous support and encouragement throughout this great endeavor. The decision to leave Texas to pursue a Ph.D. in Maryland was not an easy one, but my family's enthusiasm and unwavering support helped give me the courage to accept this challenge. My life is forever changed for the better as result. THANK YOU. 香港萬歲

## **DEDICATION**

For PaPa “Pops” Richard and Granny Rene. I know you both would be proud.

## **COPYRIGHT STATEMENT**

The author hereby certifies that the use of any copyrighted material in the dissertation manuscript entitled: Host cell virus entry mediated by Australian bat lyssavirus envelope G glycoprotein is appropriately acknowledged and, beyond brief excerpts, is with the permission of the copyright owner.

A handwritten signature in black ink, appearing to read 'Dawn Lynette Weir', is written over a horizontal line.

Dawn Lynette Weir

October 24, 2013

## ABSTRACT

Host cell virus entry mediated by Australian bat lyssavirus envelope G glycoprotein:

Dawn L. Weir, Doctor of Philosophy, 2013

Thesis directed by: Dr. Christopher C. Broder, Professor, Department of Microbiology

Australian bat lyssavirus (ABLV) is a recently emerged rhabdovirus of the genus lyssavirus considered endemic in Australian bat populations that causes a neurological disease in people indistinguishable from clinical rabies. There are two distinct variants of ABLV, one that circulates in frugivorous bats (genus *Pteropus*) and the other in insectivorous microbats (genus *Saccolaimus*). Three fatal human cases of ABLV infection have been reported, the most recent in 2013, and each manifested as acute encephalitis but with variable incubation periods. Importantly, two equine cases also arose recently in 2013; the first occurrence of ABLV in a species other than bats or humans. ABLV infects host cells through receptor-mediated endocytosis and subsequent pH-dependent fusion facilitated by its single fusogenic envelope glycoprotein (G), but the specific host factors and pathways involved in ABLV entry have not been determined. To explore the cross-species transmission potential of ABLV and to characterize the ABLV entry pathway, we developed maxGFP-encoding recombinant vesicular stomatitis viruses that express ABLV G glycoproteins to examine ABLV host cell tropism and virus entry as a function of G. Target cell lines derived from numerous mammalian species

were permissive to ABLV, indicating that the ABLV host cell receptor(s) is broadly conserved. Interestingly, the two ABLV variants exhibited distinct *in vitro* tropisms, suggesting that they can utilize alternate host factors for entry. In further support of this distinction, we found that dextran sulfate was a potent inhibitor of viral entry mediated by the *Pteropus* variant, but not entry mediated by the *Saccolaimus* variant. Proposed rabies virus (RV) receptors were not sufficient to permit ABLV entry into resistant cells, suggesting that ABLV utilizes a unique receptor or co-receptor for host cell entry that has yet to be identified. Disruption of lipid raft integrity through sequestration of cholesterol with methyl- $\beta$ -cyclodextrin significantly inhibited ABLV G-mediated entry into HEK293T cells, suggesting that the unknown ABLV receptor(s) may be localized or enriched in lipid rafts. Using a combination of chemical and molecular approaches, we also provide evidence that the predominant pathway utilized by ABLV to enter HEK293T cells is clathrin-mediated and that actin is required for productive infection. We also show that ABLV-G mediated entry is Rab5 dependent, but Rab7 and Rab11 independent, indicating that ABLV likely enters cells through an early endosomal compartment.

# TABLE OF CONTENTS

LIST OF TABLES .....	xii
LIST OF FIGURES .....	xiii
CHAPTER 1: Introduction .....	1
Discovery of Australian Bat Lyssavirus .....	1
Host Reservoirs and Geographic Distribution .....	3
Prevalence of ABLV .....	4
Susceptible Species .....	6
Natural infections in humans and animals .....	7
Bats .....	7
Humans .....	8
Horses .....	10
Experimental infections in animal species .....	11
Flying foxes .....	11
Cats and dogs .....	13
Clinical rabies .....	14
Etiology .....	14
Transmission .....	16
Infection .....	16
Disease .....	18
Pathology .....	19
Treatment and prophylaxis .....	20
Vaccines .....	21
Pre-exposure prophylaxis .....	21
Post-exposure prophylaxis .....	22
The Milwaukee protocol .....	22
Lyssavirus virion structure and molecular biology .....	24
Virus life cycle .....	26
Attachment to host cells .....	26
Internalization .....	29
Clathrin-mediated endocytosis .....	29
Approaches to study CME as a viral entry pathway .....	33
Uncoating .....	35
Approaches to study endosomal trafficking .....	40
Aims and objectives of the present study .....	40
CHAPTER 2: Host cell tropism mediated by Australian bat lyssavirus envelope glycoproteins .....	42
Abstract .....	42
Introduction .....	42
Results and discussion .....	46



<i>In vitro</i> tropism of ABLV-G mediated viral entry.....	46
Low molecular weight dextran sulfate is a potent inhibitor of viral entry mediated by ABLVp G, but not ABLVs G .....	52
Low ABLV infectivity of resistant cell lines is not due to post-entry VSV inhibition or lack of host cell attachment .....	56
ABLV and rabies virus require alternate host factors for entry.....	58
Disruption of lipid rafts significantly reduces ABLV G-mediated viral entry into 239T cells.....	62
Conclusions.....	63
Materials and methods .....	65
Cell lines and culture conditions.....	65
Reagents and antibodies.....	66
Plasmids .....	66
Recovery, purification and titration of rVSV .....	67
Cell infection assays .....	68
Virus binding assay.....	69
Western blot analysis .....	70
Cell ELISA to detect NCAM surface expression .....	70
Expression of human NCAM1 in CHOK1 cells.....	71
Statistical analysis.....	71
Acknowledgements.....	71
CHAPTER 3: Host cell virus entry mediated by Australian bat lyssavirus envelope G glycoprotein occurs through a clathrin-mediated endocytic pathway that requires actin and Rab5. ....	72
Abstract.....	72
Introduction.....	72
Results and discussion .....	76
Dynamin is required for ABLV G-mediated viral entry.....	76
Inhibition of clathrin-mediated endocytosis inhibits ABLV G-mediated viral entry.....	77
Caveolar-dependent endocytosis and macropinocytosis are not involved in ABLV G-mediated viral entry .....	83
Actin polymerization is required for ABLV G-mediated viral entry .....	86
Rab5, but not Rab7 or Rab11, is required for ABLV G-mediated viral entry.....	88
Conclusions.....	92
Materials and methods .....	93
Cells and viruses .....	93
Drug treatments and cell infection assays.....	94
Analysis of dominant negative mutants of Eps15, Rab5, Rab7, and Rab11 .....	95
Cholera toxin B subunit uptake.....	96
Confocal microscopy .....	96
Statistical analysis.....	96
Acknowledgements.....	96
CHAPTER 4: Induction of cross-reactive neutralizing antibodies by a soluble G glycoprotein of Australian bat lyssavirus. ....	97

Abstract .....	97
Introduction .....	98
Results and discussion .....	99
Construction and transient expression of soluble ABLV G glycoproteins .....	99
Large scale production and purification of ABLV Gs .....	105
Immunogenicity of recombinant Gs .....	106
Isolation and characterization of mouse anti-ABLVs G MAbs .....	112
Conclusions .....	116
Materials and methods .....	116
Cells, viruses, and antibodies .....	116
Design of ABLV Gs constructs .....	117
Transient expression and generation of ABLV Gs-expressing stable cell lines .....	118
Large scale expression and purification of ABLV Gs .....	118
Western blot analysis .....	119
Generation of ABLVs G-specific MAbs .....	119
ELISA .....	120
Generation of rabbit antiserum raised against ABLVs Gs .....	121
Virus neutralization assay .....	121
Acknowledgements .....	122
CHAPTER 5: Discussion .....	123
Preface .....	123
Experimental results in the context of project aims .....	124
Review of Chapter 2 results .....	124
In vitro entry tropism of ABLV .....	125
ABLV variants can exploit alternate host factors for entry .....	127
Identification of cell lines resistant to ABLV G-mediated entry .....	129
ABLV and RABV utilize alternate host factors for entry .....	131
Review of Chapter 3 results .....	131
ABLV G-mediated viral entry occurs through a clathrin-mediated pathway that is dependent on actin .....	132
Caveolar-dependent endocytosis and macropinocytosis are not involved in ABLV G-mediated viral entry .....	133
Rab5, but not Rab7 or Rab11, is required for ABLV G-mediated viral entry .....	134
Review of Chapter 4 results .....	135
Construction, expression, and purification of ABLV Gs .....	135
Immunogenicity of ABLVs Gs and isolation of mouse anti-ABLVs G MAbs .....	137
Contributions to the field of lyssavirus entry .....	138
Unanswered questions .....	140
What is cellular receptor(s) for ABLV? Are different receptors used for initial replication in muscle and epithelial cells, entry into neurons at the NMJ, and neuronal spread within the CNS? .....	140
Is it possible that multiple lyssavirus species utilize a common receptor for host cell entry? .....	141
What additional host factors are required for entry? What about post-entry? .....	143
Future directions .....	143

Conclusions .....	146
APPENDICES .....	147
REFERENCES .....	150

## LIST OF TABLES

Table 1. Genotype and phylogroup classifications for the lyssaviruses.....	15
Table 2. Strategies to improve the secretion of ABLV Gs.....	102
Table 3. Neutralization of VSV-ABLV G-GFP infection by anti-ABLVs G polyclonal sera .....	111
Table 4. Neutralization of VSV-ABLV G-GFP infection by mouse anti-ABLVs G MAbs .....	115

## LIST OF FIGURES

Figure 1. Geographic distribution of ABLV host reservoir species. ....	5
Figure 2. The rabies virus virion.....	25
Figure 3. Rabies virus life cycle. ....	27
Figure 4. Endocytic mechanisms.. ....	30
Figure 5. The clathrin-coated vesicle cycle.....	32
Figure 6. A model for rhabdovirus fusion .....	39
Figure 7. Comparison of the amino acid sequences of <i>Saccolaimus</i> and <i>Pteropus</i> ABLV G mature protein ectodomains.....	47
Figure 8. ABLV <i>in vitro</i> entry tropism.....	50
Figure 9. Anti-clumping agents are potent inhibitors of entry mediated by <i>Pteropus</i> , but not <i>Saccolaimus</i> ABLV G.....	54
Figure 10. ABLV entry block in resistant cells is not due to lack of host cell attachment.....	57
Figure 11. ABLV resistant cells express proposed rabies virus receptors. ....	59
Figure 12. The rabies virus receptor neural cell adhesion molecule (NCAM) is not a receptor for ABLV. ....	61
Figure 13. Disruption of lipid rafts significantly reduces ABLV G-mediated viral entry into 293T cells .....	64
Figure 14. Chemical inhibition of dynamin inhibits ABLV G-mediated viral entry into HEK293T cells. ....	78
Figure 15. Chemical inhibition of CME inhibits ABLV G-mediated viral entry into HEK293T cells. ....	80
Figure 16. Inhibition of CME with a DN form of Eps15 significantly reduces ABLV G- mediated viral entry into HEK293T cells.....	81
Figure 17. CavME endocytosis and macropinocytosis are not required for ABLV G- mediated viral entry.....	84
Figure 18. Actin is required for ABLV G-mediated viral entry .....	87
Figure 19. Effect of dominant negative Rab GTPases on ABLV G-mediated viral entry. .....	90
Figure 20. Transient expression of ABLV Gs glycoprotein constructs. (A) Schematic representation of Gs constructs. ....	101
Figure 21. Transient expression of ABLV Gs T4 constructs .....	104
Figure 22. SDS PAGE (A) and Native PAGE (B) analysis of purified ABLVs Gs. ....	107
Figure 23. Schematic for mouse and rabbit immunization schedules with purified ABLVs Gs protein.....	108
Figure 24. Anti-ABLVs Gs polyclonal antibody response in mice (A) and rabbits (B) immunized with ABLVs Gs as measured by ELISA.....	109
Figure 25. Anti-ABLVs Gs-GS3T4 immune sera binds native full-length ABLV G.....	110
Figure 26. Isolation and purification of mouse anti-ABLVs G MAbs.....	113
Figure 27. Anti-ABLVs G MAbs bind native full-length ABLVs G.....	114
Appendix A. Plasmid map of the full-length cDNA clone of VSVΔG-ABLVG-maxGFP. .....	147

Appendix B. Rescue of recombinant VSV-ABLV G and WT VSV-reporter viruses...	148
Appendix C. Mouse anti-ABLVs G MAb DW11C7 potentially neutralizes ABLVs G-, but not ABLVp G-mediated viral entry.. .....	149

## CHAPTER 1: Introduction

### DISCOVERY OF AUSTRALIAN BAT LYSSAVIRUS

The discovery of Hendra virus (HeV), a lethal paramyxovirus that emerged in Australia in 1994 (194), indirectly led to the discovery of Australian bat lyssavirus (ABLV), the first endemic lyssavirus isolated in Australia. In 1996, a retrospective study to identify the natural host of HeV was initiated. Serological evidence pointed to pteropid bats, also known as flying foxes, as the likely host reservoir of HeV (296); indeed HeV was subsequently isolated from these bats (113). Brain tissue samples from two female black flying foxes collected from Ballina, northern New South Wales (NSW) tested negative for HeV antibodies (93). One sample, collected in 1996, was from a juvenile female black flying fox (*Pteropus alecto*) that was found under a tree and unable to fly; the other was a fixed paraffin-embedded tissue sample from a female black flying fox collected the previous year that had been euthanized and necropsied due to its unusually aggressive behavior (93). Histological analyses of brain tissue from the 1996 bat showed severe nonsuppurative encephalitis. Encephalitis was mild in the 1995 bat brain sections but numerous cytoplasmic inclusion bodies, indicative of lyssavirus infection, were present. Immunohistochemical analyses revealed the presence of lyssavirus nucleocapsid antigen throughout the brain of both bats, particularly in the hippocampus, the mesenchymal cells of the trigeminal nucleus, and the larger motor neurons of the medulla oblongata (93). Inclusion bodies were evident within the cell bodies of the large neurons of the 1996 bat and specific labeling with an anti-rabies (RABV) monoclonal antibody (MAb) and gold-labeled rabbit anti-mouse anti-serum

indicated that the inclusion bodies contained ribonucleoprotein (RNP) complexes typical of lyssaviruses (106).

Blood from the 1996 bat tested negative for anti-RABV neutralizing antibodies and virus could not be isolated by direct culture. In further attempts to isolate virus, lung, kidney, and spleen tissue homogenates were individually injected by intracerebral route into 3 week old mice and injected as pooled tissue samples intracerebrally into day old suckling mice. All mice remained healthy except for one weanling mouse injected with kidney homogenate; the affected mouse developed hind limb paralysis 16 days post-inoculation and brain smears tested positive for lyssavirus antigen (93). Brain material from this mouse was repassaged intracerebrally into 3 week old mice, which developed neurologic symptoms 8 to 11 days post-inoculation; the brain material was also passaged in mouse neuroblastoma cells. The virus was shown to be neutralized by anti-RABV (Evelyn-Rokitnicki-Abelseth [ERA] strain) sera; however, the pattern of MAb binding of a panel of lyssavirus nucleoprotein (N) antibodies revealed that this lyssavirus was serologically distinct from RABV and other known lyssaviruses (93). The new lyssavirus was provisionally named pteropid lyssavirus (93), but was renamed Australian bat lyssavirus (ABLV) following its isolation from an insectivorous microbat (see below) (129).

The ABLV N gene was amplified by polymerase chain reaction (PCR) from the tissue cultured virus and paraffin-embedded formalin-fixed brain tissues from both the 1995 and 1996 bats; sequence analysis revealed that the PCR products were identical. Sequence comparisons of the ABLV N and other lyssavirus N proteins showed that ABLV was most closely related to European bat lyssavirus-1 (EBLV1) and RV with 93%



and 92% amino acid identity, respectively (93; 106). Based on these results, as well as the anti-N MAb binding data, ABLV was designated as a new lyssavirus genotype. Duvenhage virus (DUVV), EBLV-1, and European bat lyssavirus 2 (EBLV-2) were separated as three distinct lyssavirus species based on similar serological data (39; 106).

A few months after the initial isolation of ABLV from the black flying fox, ABLV was isolated from an insectivorous microbat, the yellow-bellied sheath-tail bat (*Saccolaimus flaviventris*) (129). Nucleoprotein sequence comparisons revealed that the *Saccolaimus* N protein shared 96% amino acid homology with the *Pteropus* isolate and 90% amino acid homology with RABV. Phylogenetic analyses showed that *Saccolaimus* and *Pteropus* isolates separated into two clades and thus represented two distinct variants of ABLV: ABLVs and ABLVp for *Saccolaimus* and *Pteropus* variants, respectively. Additionally, MAb binding profiles were distinct for ABLVs and ABLVp and could be used to differentiate between the two ABLV variants (107).

#### **HOST RESERVOIRS AND GEOGRAPHIC DISTRIBUTION**

Unlike RABV which has both terrestrial and bat reservoirs, only bats are known reservoirs of ABLV. Bats (order *Chiroptera*) are the second largest class of mammals with greater than 1,200 known species (285). They are classified into two suborders, *Megachiroptera* (large Old World fruit bats; navigate by sight) and *Microchiroptera* (small bats, mostly insectivorous, found worldwide; navigate by echolocation). Australia has one family of Megachiropteran represented by five genera and 13 species (112). ABLV has been isolated from all four species of flying foxes found on mainland Australia (suborder *Megachiroptera*, genus *Pteropus*): the black flying fox (*Pteropus alecto*), the grey-headed flying fox (*P. poliocephalus*), the little red flying fox (*P.*

*scapulatus*) and the spectacled flying fox (*P. conspicillatus*) (129; 172). The combined host range of these four species extends from northwest Western Australia, through the Northern Territory, Queensland, New South Wales, and Victoria (Figure 1). The grey-headed flying fox is the only species restricted to Australia. The black flying fox, little red flying fox, and spectacled flying fox are also found in Papua New Guinea (PNG), and both the black flying fox and spectacled flying fox occur in parts of Indonesia (112). Despite the extended geographic range of these three species outside of mainland Australia, ABLV has not been detected in PNG or Indonesian bat samples to date. However, the detection of neutralizing antibodies in six different bat species in the Philippines indicates the presence of ABLV or a closely related virus in Asia (12).

The Australian microchiroptera are much more diverse than the Australian megachiroptera, with six families containing 20 genera and 65 species identified on mainland Australia (112). ABLV has been isolated from a single species of *Microchiroptera*, the yellow-bellied sheath-tail bat (*Saccolaimus flaviventris*). The *Saccolaimus* strain is genetically distinct from the *Pteropus* strain (107). The yellow-bellied sheath-tail bat is widely distributed throughout mainland Australia (Figure 1) and is also native to PNG (112). Despite the lack of additional virus isolations from other microbat species, serological evidence of ABLV infection has been reported in seven genera, representing five of the six families of microchiroptera found in Australia; all Australian bat species are considered as potential host reservoirs of ABLV (88).

#### **PREVALENCE OF ABLV**

The prevalence of ABLV in healthy bats is estimated to be less than 1%. However, in sick, injured and/or orphaned flying foxes the prevalence of viral antigen as

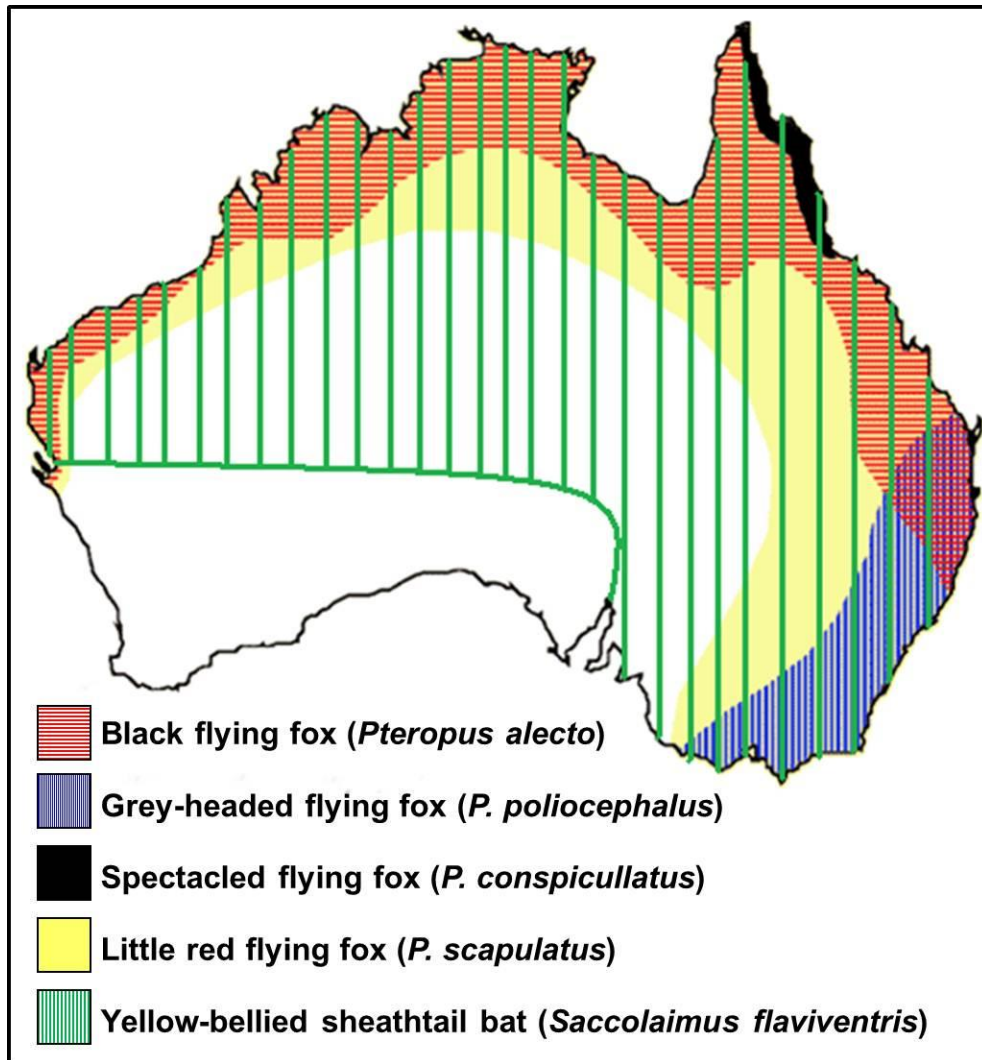


Figure 1. Geographic distribution of ABLV host reservoir species. Adapted from (112; 270).

detected by the fluorescent antibody test (FAT) is typically 5-10%, but may be as high as 17% or as low as 1% depending on the species (16.9% in little red flying fox, 7.8% in black flying fox, 4.6% in grey-headed flying fox, and 1% in spectacled flying fox) (88). The prevalence of ABLV is significantly higher in flying foxes displaying central nervous system (CNS) clinical signs. In one study, approximately 60% of sick or injured little red flying foxes with CNS symptoms tested positive for ABLV antigen (18). ABLV seroprevalence in sick, injured and/or orphaned bats can be as high as 20% in flying foxes and 5% in microbats. However, injured yellow-bellied sheath-tail microbats had an antibody prevalence as high as 62.5% (88).

#### **SUSCEPTIBLE SPECIES**

Natural ABLV infections have been reported in bats, humans, and horses; there have been no confirmed reports of ABLV in any other species despite known contacts of domestic dogs with infected flying foxes (173). RABV and other bat lyssaviruses productively infect numerous mammalian species (17), suggesting that occasional spillover of ABLV into other mammalian species is likely. However, due to limited experimental studies of ABLV pathogenesis, the cross-species transmission potential of ABLV into additional mammal species is not clear. ABLV host cell infection tropism data obtained in the present study and described in Chapter 2 suggest that terrestrial mammals other than humans and horses may be susceptible to ABLV infection. The following sections summarize the natural and experimental ABLV infections reported to date.

## Natural infections in humans and animals

### *Bats*

There are numerous documented reports of observed clinical disease in flying foxes naturally infected with ABLV. Field et al. (1999) describe a nine-day clinical disease course in an orphaned juvenile male black flying fox (*P. alecto*) that was being raised by a volunteer wildlife animal caregiver. After six weeks of good health, the bat began to display clinical signs of neurological disease. On the first day of illness, the bat suddenly became aggressive towards its companion bat and began experiencing repeated muscle spasms during which it vocalized loudly. The next day, the bat was no longer experiencing spasms but was still vocal and was attempting to bite objects, but eating little food. By the third day of illness, the bat was no longer aggressive and was only able to eat pulped food. A veterinarian was called in the next day and noted severe pharyngitis and the bat was given a steroid injection to reduce inflammation. By that evening, the bat was alert and eating solid food. The bat was given another injection the following day and remained alert and continued to eat well. On day 6 of illness, the bat experienced difficulty swallowing and again was given pulped food. During the following two days, the bat could no longer roost properly and was found lying down face up. The bat developed worsening throat spasms, diarrhea, and began losing weight. On the ninth day of illness, its condition rapidly deteriorated and the bat died. Necropsy revealed nonsuppurative meningoencephalitis and numerous neurons contained eosinophilic inclusion bodies indicative of lyssavirus infection. FAT on fresh brain tissue confirmed ABLV infection; viral antigen was detected by immunoperoxidase staining in numerous sections of the brain, including the frontal cortex, hippocampus, brainstem, and cerebellum. Natural in utero infection with lyssaviruses is not known to occur, thus the

authors postulate that the bat was infected within the 2-3 weeks between its birth and when it was taken into care, indicating an incubation period of 6-9 weeks (87).

### ***Humans***

ABLV has caused three fatal human infections; all occurred in Queensland. The first case occurred in late October of 1996. A 39 year old female from Rockhampton developed pain and numbness in her left arm. She reported that she had received several scratches from flying foxes in her care in the preceding 2-4 week period, but had not been bitten (4; 229). She had also been caring for numerous other animals including dogs, cats, cockatoos, marsupials, and insectivorous bats. Over the next 2-3 days, she developed dizziness and vomiting followed by headache and fever and was admitted to the hospital. The initial differential diagnosis included bacterial meningitis, viral encephalitis, and Guillain-Barre syndrome; lumbar puncture was performed but no organisms were seen with microscopy and cultures were negative (4; 229). Intravenous treatment with broad spectrum antibiotics was started but her condition deteriorated and she developed diplopia, cerebellar signs, slurred speech, and had difficulty swallowing. She was intubated and transferred to Royal Brisbane Hospital (4). By the 8<sup>th</sup>-10<sup>th</sup> days of illness, she had developed progressive weakness in all limbs and bilateral facial palsy; additionally, her level of consciousness began to fluctuate. By day eleven she was unresponsive and ventilator dependent; an electroencephalogram indicated diffuse encephalitis. Serum and cerebrospinal fluid (CSF) were analyzed by the Commonwealth Scientific and Industrial Research Organization (CSIRO) Australian Animal Health Laboratory (AAHL) in Geelong. The serum was positive for anti-lyssavirus antibodies but negative for anti-Hendra virus antibodies. Serology for several other local viruses

including Kunjin, dengue, Sinbis, Ross River, and Murray Valley encephalitis, and Barmah Forest virus were also negative. PCR to amplify part of the N gene of ABLV from the CSF resulted in a 250 base pair product, confirming that the patient was infected with ABLV. She was administered rabies immunoglobulin, but her condition continued to deteriorate and she died approximately 20 days after symptom onset (4; 229). It was later determined that the patient was likely bitten or scratched by a yellow-bellied sheath-tail bat (*Saccolaimus flaviventris*) approximately 4.5 weeks prior to symptom onset (116). Monoclonal antibody binding profiles and genetic sequencing of virus isolated from fresh brain tissues of the patient confirmed that the *Saccolaimus* variant of ABLV was the likely source of infection (107).

The second fatal human ABLV infection occurred in late November 1998. A 37 year old female was admitted to Mackay Base Hospital following a five day history of fever, vomiting, pain in her left shoulder and left hand, and difficulty swallowing. She was well oriented, but febrile and was unable to fully open her mouth, had difficulty speaking and was drooling. When her throat was examined, spasmodic attempts to swallow ensued. Her condition rapidly deteriorated within the next 12 hours, with increased agitation, and more frequent and severe muscle spasms; she was sedated and ventilated. It was soon discovered that she had a history of a bat bite and CSF, serum, and saliva were submitted for ABLV testing. By day 2 of hospitalization, she was no longer able to communicate or understand verbal commands and thereafter was ventilator-dependent. Two days later, a PCR product specific for ABLV was detected in the saliva and ABLV infection was confirmed four days later. On day 14 of hospitalization, artificial ventilation was ceased; she died 19 days after symptom onset

(116). Virus was isolated post-mortem from brain and spinal cord tissues. Sequencing of ABLV specific PCR product from infected cell cultures confirmed that the isolate was the *Pteropus* variant of ABLV.

A detailed medical history revealed that the patient had attended a barbeque in late August of 1996 where a flying fox landed on the back of a small child. While removing the bat, the patient had been bitten on the base of her fifth left finger. She sought medical treatment two days after the bite and was administered antibiotics and tetanus toxoid. She returned to her doctor six months later, in early March, and inquired about a blood test for the “bat virus”. It was advised that she receive post-exposure prophylaxis (PEP) for RABV because of potential exposure to ABLV, but she declined treatment and succumbed to ABLV infection 27 months after initial exposure. The child and four other people exposed to the flying fox at the barbeque were administered PEP as soon as ABLVp infection was confirmed in the patient (116).

The third fatal human ABLV infection occurred in February 2013. An 8 year old boy from Long Island, Queensland was scratched by a bat, but did not tell his parents about the bat encounter. He was admitted to Brisbane’s Mater Children’s Hospital approximately two months later, suffering with convulsions and abdominal pain and fever, followed by progressive brain problems and coma. On day 10 of hospitalization, ABLV infection was confirmed; the patient died 28 days after symptom onset (7).

### ***Horses***

The first confirmed cases of ABLV infection in horses occurred in May 2013, the first spillover of ABLV into a species other than bats and humans. A yearling horse was observed to be off in color and displaying mild ataxia. The horse’s condition deteriorated



over the next few days with increased ataxia, trouble swallowing, and became febrile. Four days after symptom onset, the horse had difficulty standing and would not eat. Blood and nasal, oral and rectal swabs were collected and tested for Hendra virus; PCR results were negative. The following day the horse began convulsing and was euthanized, five days after symptom onset. Necropsy revealed severe sub-acute diffuse non-purulent encephalitis. The horse was tested for ABLV and both PCR and FAT tests were positive. The PCR results indicated that the horse had been infected by the *Saccolaimus* strain of ABLV, suggesting that the horse had been exposed to ABLV through an infected microbat. Prior to the onset of illness of this horse, a paddock mate of the infected horse had displayed similar clinical signs and was euthanized the same day that the ABLV infected horse displayed clinical symptoms. The paddock mate had developed neurological symptoms four days prior to being euthanized. This horse had also tested negative for Hendra virus. Remaining oral swab samples from this horse were tested for ABLV and PCR confirmed that the horse had been infected by the *Saccolaimus* variant of ABLV (219).

## **Experimental infections in animal species**

### ***Flying foxes***

Experimental infection studies of ABLV are limited. McColl et al. (2002) describe a pathogenesis study conducted in grey-headed flying foxes (*P. poliocephalus*). Fifteen flying foxes were obtained from a captive colony; ten were inoculated intramuscularly with  $10^5$  median tissue culture infective dose (TCID<sub>50</sub>) of ABLVp, four were inoculated with an equal dose of a bat variant of RABV, and one remained as an uninfected control. Three ABLVp-inoculated bats and two RABV-inoculated bats

developed clinical signs including muscle weakness, ataxia, and paresis or paralysis between 15-24 days post infection; all five bats had histological lesions consistent with a lyssavirus infection and viral antigen was detected in brain smears by FAT. Virus was recovered from the brain of two ABLVp-infected bats and from one RABV-infected bat. The five infected bats did not develop anti-lyssavirus antibodies, but by the end of the three month study, five of the seven ABLVp-inoculated survivors and one of the two RABV-inoculated survivors had seroconverted (175).

A second study evaluating ABLV pathogenesis in flying foxes was conducted by Barrett (2004). Ten wild-caught pre-breeding young adult grey-headed flying foxes that were seronegative for lyssavirus infection were selected for the study. Nine were inoculated intramuscularly with 0.12 ml of a 20% weight per volume suspension of salivary gland tissue derived from a naturally infected black flying fox (*P. alecto*). The inoculum contained  $10^{5.1}$  90 day mouse footpad mean effective dose (MFP<sub>90</sub>ED<sub>50</sub>) and was equally injected into four inoculation sites: the left footpad, left pectoral muscle, left temporal muscle, and left muzzle. The remaining bat received 0.06 ml ( $10^{4.8}$  MFP<sub>90</sub>ED<sub>50</sub>) divided into two injection sites: the left footpad and left pectoral muscle. Seven of the ten flying foxes, including the bat that received the lower dose, developed clinical signs between 10 and 19 days post inoculation and either died naturally or were euthanized. ABLVp infection was confirmed by FAT on fresh brain smears, detection of viral antigen in formalin-fixed tissues and virus isolation in mice. The three asymptomatic flying foxes were euthanized at day 82 and were negative for ABLVp by FAT, immunohistochemistry, and mouse inoculation; only one had seroconverted (18).

### ***Cats and dogs***

The susceptibility of cats and dogs to ABLVp infection was evaluated by McColl et al (2007). Three adult cats were inoculated intramuscularly (forelimb) with  $10^5$  TCID<sub>50</sub> of ABLVp, one was inoculated with an equivalent dose of bat-variant RABV, and one served as an uninoculated control. All lyssavirus-inoculated cats exhibited mild behavioral changes between 11 and 42 days post inoculation, but none died during the three month trial. At necropsy, no histological lesions were present in the CNS and FAT analyses of the brain tissues of each cat were negative for lyssavirus antigen. All three ABLVp-inoculated cats, but not the RABV-inoculated cat seroconverted during the trial (176).

In the dog trial, three 2-3-month-old pups were inoculated intramuscularly (left gluteal muscle) with  $10^{3.7}$  TCID<sub>50</sub> of ABLVp, two with  $10^5$  TCID<sub>50</sub> of ABLVp, two with  $10^5$  TCID<sub>50</sub> of bat-variant RABV, and two remained as uninoculated controls. Three of the five ABLVp-inoculated pups exhibited mild abnormal clinical signs approximately 2-3 weeks post inoculation, but recovered. All five pups seroconverted during the trial and two had antibodies in the CSF. Both pups inoculated with RABV developed clinical signs 9-12 days post inoculation and were euthanized on the day that clinical signs were first observed. The ABLVp-inoculated pups showed no histopathology of the brain or spinal cord at necropsy, but the CNS tissue of both RABV-inoculated pups revealed non-suppurative meningoencephalomyelitis and viral antigen was detected in the CNS, with the greatest amount detected in the spinal cord (176).

The outcomes of the cat and dog trials suggest that ABLVp causes little to no clinical disease in cats and dogs. However, the studies were terminated after three months and it is possible that this was not sufficient time for the virus to reach the brain;

one of the documented human ABLVp infections had an incubation period greater than 2 years (116). The ability of the *Saccolaimus* variant of ABLV to cause clinical disease in cats and dogs has not been evaluated.

## **CLINICAL RABIES**

### **Etiology**

ABLV is a member of the family *Rhabdoviridae*, genus *Lyssavirus*; all lyssaviruses are capable of causing fatal acute encephalitis indistinguishable from clinical rabies in humans and other mammals. There are currently 12 classified species (genotypes) of lyssaviruses: *Rabies virus* (RABV), *Lagos bat virus* (LBV), *Mokola virus* (MOKV), *Duvenhage virus* (DUVV), *European bat lyssavirus* types 1 and 2 (EBLV-1 and -2), *Australian bat lyssavirus* (ABLV), *Aravan virus* (ARAV), *Khujand virus* (KHUV), *Irkut virus* (IRKV), *West Caucasian bat virus* (WCBV), and *Shimoni bat virus* (SHIBV). Three more recently described bat lyssaviruses have not yet been officially classified as distinct genotypes: Bokeloh bat lyssavirus (BBLV), Ikoma lyssavirus (IKOV), and Lleida bat lyssavirus (LLEBV) (53). Lyssaviruses are also separated into three phylogroups based on their genetic, immunologic, and pathogenic characteristics. Phylogroup I includes RABV, DUVV, EBLV-1, EBLV-2, ABLV, ARAV, IRKV, BBLV, and KHUV, phylogroup II includes LBV, MOKV, and SHIBV, and phylogroup III includes WCBV, IKOV, and LLEBV (Table 1) (53). With the exception of Mokola virus and Ikoma lyssavirus, all lyssavirus species have known bat reservoirs, leading to the speculation that lyssaviruses originated in the order Chiroptera (15). Human clinical rabies cases have been documented for RABV, MOKV, DUVV, EBLV-1, EBLV-2, ABLV, and IRKV (17).

Table 1. Genotype and phylogroup classifications for the lyssaviruses.

Lyssaviruses	Genotype	Phylogroup
*Rabies virus (RABV)	1	I
Lagos Bat virus (LBV)	2	II
*Mokola virus (MOKV)	3	II
*Duvenhage virus (DUVV)	4	I
*European bat lyssavirus 1 (EBLV1)	5	I
*European bat lyssavirus 2 (EBLV2)	6	I
*Australian bat lyssavirus (ABLV)	7	I
Aravan virus (ARAV)	8	I
Khujand virus (KHUV)	9	I
*Irkut virus (IRKV)	10	I
West Caucasian bat virus (WCBV)	11	III
Shimoni bat virus (SHIBV)	12	III
Bokeloh bat lyssavirus (BBLV)	NC	I
Ikoma lyssavirus (IKOV)	NC	III
Lleida bat lyssavirus (LLEBV)	NC	III

NC – Not classified; these viruses are not yet classified as distinct lyssavirus species (genotypes) according to the International Committee on the Taxonomy of Viruses (ICTV) (<http://www.ictvonline.org/virusTaxonomy.asp>; accessed October 29, 2013). \*, human cases have been documented.

## **Transmission**

Lyssaviruses are most commonly transmitted to a new host by a bite from a rabid animal or through the contamination of scratches with virus infected saliva. Dogs are the predominant host and transmitter of classical RABV, the prototype species for the lyssavirus genus, and are responsible for more than 55,000 deaths annually, mostly in Asia and Africa (282). Due to successful vaccination programs for domestic dogs and wildlife carnivores, bats are the main source of human rabies deaths in the United States and Canada (282). With the exception of MOKV, for which the source of infection for the two reported human deaths was not identified, human rabies deaths caused by lyssavirus species other than RABV have been attributed exclusively to exposure to infected bats, including the three human deaths caused by ABLV (4; 7; 20; 36; 82; 83; 92; 116; 163; 216; 233). More rare transmissions of human rabies caused by RABV have been reported and include airborne infections in spelunkers (65) and a laboratory worker (287), infections after human organ transplantation (10; 40; 121; 130; 241), and suspected human to human transmission via bites from the infected patient (9).

## **Infection**

Due to the limited number of experimental ABLV infection studies (see *Experimental infections in animal species*), the exact details on how ABLV infects the body are not known; however, because the clinical presentation of ABLV infection is indistinguishable from that of clinical disease caused by RABV it is assumed that ABLV follows a similar pathway of infection. While some strains enter nerve endings rapidly, replication of rabies virus can occur within muscle and epithelial cells at the site of inoculation before progressing to the CNS (43; 190). After the virus gains entry into the

peripheral nervous system through receptor-mediated endocytosis (see *Virus life cycle*), it travels by retrograde axonal transport at a rate of 50-100 mm per day to the dorsal root ganglia and to the spinal cord (260). After the virus reaches the spinal cord, the brain quickly becomes infected; the most affected areas include the hippocampus, brain stem, ganglionic cells of the pontine nuclei, and Purkinje cells of the cerebellum (28). Virus then spreads throughout the body via afferent neurons to highly innervated sites, such as salivary glands, skin of the head and neck, retina, cornea, kidney, skeletal and cardiac muscle, lungs, bladder, and pancreas (196).

Following initial virus exposure, clinical symptoms typically develop within one to three months, although incubation periods can vary greatly; the three human ABLV infections are a prime example of this variability as the incubation periods ranged from 3-5 weeks to greater than two years (4; 7; 116). Although rare, multi-year incubation periods for RABV infections have been reported. A case of rabies in a Vietnamese girl who immigrated to Australia was reported to have an incubation period of greater than six years and an incubation period of greater than 20 years was reported for a rabies case in an Indian man whose only history of a dog bite had occurred 23 years prior to symptom onset (177; 236). The length of the incubation period depends on several factors including severity of the wound and proximity to the CNS, the type and quantity of virus introduced into the wound, immune status and age (165). For example, a person with a severe wound near the head or neck will likely develop disease symptoms quicker than a person exposed to virus through a scratch on the hand or foot.

## Disease

After the incubation period, a prodromal phase lasting 2 to 10 days occurs with initial influenza-like symptoms including moderate fever and malaise. Other symptoms such as local itching, pain, or paraesthesia at the site of the bite are also common.

Additionally, agitation and insomnia may occur at this early stage (224). Following the prodromal phase, neurologic symptoms specific to clinical rabies appear. At this stage the disease can follow two different courses: furious/classical rabies (more involvement of the brain) or paralytic rabies (extensive involvement of the spinal cord). The furious form of disease occurs in greater than 80% of patients (168), including all three ABLV patients (4; 7; 116).

Furious rabies manifests with intermittent symptoms of increasing anxiety, hyperactivity, hyperventilation, excitation, and disorientation; these symptoms may occur spontaneously or are precipitated by sensory stimuli (274). Signs of autonomic dysfunction including hypersalivation (“frothing at the mouth”) and sweating may also occur. Hydrophobia (fear of water) and aerophobia (fear of air) are the most characteristic symptoms of rabies and occur in about 50% of patients; painful throat spasms which develop into generalized convulsions, are triggered by seeing water or induced by blowing air over the face (224). As a result, patients avoid drinking water for long periods of time and become dehydrated (274). Patients typically become comatose within 10 days following the onset of neurological symptoms, followed by paralysis and cardiac and respiratory arrest; death typically occurs within the next 7 days.

Paralytic or *dumb rabies* is characterized by flaccid paralysis which often begins at the site of inoculation and then disseminates further (123; 185). The disease course is less rapid than the furious form; death occurs from general paralysis. This is the most



frequent form of the disease following a vampire bat bite. During a vampire bat induced RABV outbreak in Trinidad between 1929 and 1937, all 70 patients died from paralytic rabies (132; 200). However, rabies caused by vampire bats does not exclusively present as paralytic rabies; in an outbreak in the Peruvian jungle in 1990, disease manifested as furious rabies (162). It is not known why some patients develop furious rabies and others develop paralytic rabies, although it has been suggested that host immune responses may influence clinical manifestations and disease course (122).

### **Pathology**

Despite the dramatic clinical course of disease and the extensive CNS involvement and impairment of neuronal function, in most cases only mild inflammation, and very little histopathological changes, other than cytoplasmic Negri bodies, are present in affected tissues. Death may occur with no obvious signs of pathology, suggesting that neuronal dysfunction rather than neuronal death is responsible for the fatal outcome of disease (136). When present, the dominant inflammatory lesion is non-specific, nonsuppurative viral encephalitis or meningitis (193), but the severity of inflammatory lesions is highly variable and no single lesion is consistently present. This variation is seen in both principle host species such as dogs and skunks, and in dead end hosts such as humans (56; 74; 84; 191). Lesions associated with ABLV infection in bats are similar to those caused by RABV both in distribution and in variation of severity (128). A postmortem evaluation of the first two human ABLV infections revealed widespread advanced nonsuppurative meningoencephalitis with particularly severe inflammation and necrosis present in the brainstem and hippocampi; numerous intraneural cytoplasmic inclusion bodies were also noted (116; 129). The advanced

pathology seen in the human ABLV infections as opposed to bat infections is likely due to prolonged infection as a result of life-support procedures. Similar pathology has been observed for human RABV infections following prolonged and aggressive medical treatment (74).

### **Treatment and prophylaxis**

Clinical rabies is near 100% fatal once clinical signs begin; there have only been eight well-documented reports of individuals that have survived clinical RABV infection, five of which had received rabies vaccinations either pre- or post-exposure (5; 48-51; 118; 204). However, with proper post-exposure prophylaxis (PEP) it is possible to prevent clinical disease from developing. Administration of PEP should be administered as soon as possible following exposure and should include immediate cleansing and disinfection of the wound, passive immunization with human rabies immunoglobulin (HRIG) and administration of a rabies vaccine. Even after a lengthy delay following exposure PEP is recommended, though delays in starting the treatment may result in death if bite wounds occurred in highly innervated regions such as the head, neck, or hands (281). Depending on the type of contact and extent of exposure, none or all of the above PEP is administered. There are three categories of exposure: category I consists of feeding or touching animals and receiving licks on intact skin, category II includes nibbling of uncovered skin or receiving minor abrasions/scratches without bleeding, and category III, the most severe exposure, involves single or multiple transdermal bites or scratches, saliva contamination of broken skin or mucous membranes, and exposure to bat bites or scratches. Category I exposures require no treatment, category II exposures require immediate vaccination, and category III exposures require administration of RIG

and immediate vaccination (281). In the case of potential lyssavirus exposure from bats, both category II and III exposures require administration of HRIG. In all cases wounds should be thoroughly cleansed; proper wound care alone following RABV exposure was shown to reduce the incidence of rabies by 90% in mice and guinea pigs (69).

### ***Vaccines***

Three different types of inactivated vaccines prepared from fixed RABV vaccine strains have proven efficacious in preventing clinical disease: human diploid cell vaccine (HDCV), purified chick embryo cell vaccine (PCECV), and purified Vero cell vaccine (PVCV) (281). In Australia both HDCV and PCECV preparations are available. All commercial vaccines strains are derived from RABV strains (genotype I) and if administered correctly offer complete protection against rabies caused by RABV variants; however, they are less efficient against the RABV-related lyssaviruses. In general, some level of protection, although variable depending on the vaccine strain tested, is seen against phylogroup I, but not against phylogroup II or III lyssaviruses (41; 72; 85; 115; 144; 145; 259). For ABLV, rabies vaccine efficacy studies yielded different results for *Pteropus* and *Saccolaimus* strains. Mice were completely protected against intracerebral challenge with 80 LD<sub>50</sub> ABLVp two months after vaccination with a human rabies PVCV (129); however, mice vaccinated with a human rabies HDCV and then challenged one month later with 25 MLD<sub>50</sub> ABLVs, only 50% and 79% survived intracranial and peripheral challenge, respectively (41).

### ***Pre-exposure prophylaxis***

Pre-exposure prophylaxis is recommended for anyone with high risk of exposure to lyssaviruses including laboratory personnel working with live virus, bat handlers,

veterinarians, wildlife officers, and other individuals who come into direct contact with bats. Vaccination consists of three doses administered by intramuscular (IM) route on days 0, 7, and 28. Individuals that work with live ABLV should have their serum rabies antibody titer determined every six months; other high risk individuals should be evaluated every two years. A booster dose of vaccine is required for individuals with a rabies antibody titer below 0.5 International units per milliliter (52; 281).

### ***Post-exposure prophylaxis***

Immunocompetent individuals not previously vaccinated should receive four doses by IM injection on days 0, 3, 7, and 14; immunocompromised individuals should receive a fifth injection on day 28. For all potential bat exposures, a single dose of HRIG should be administered as soon as possible after PEP is initiated and is not indicated beyond seven days after the first vaccination. For individuals previously vaccinated, two doses of rabies vaccine should be given on days 0 and 3; HRIG is not indicated (52).

### ***The Milwaukee protocol***

The experimental medical treatment employed in the first recorded case of human survival after the onset of rabies symptoms without prior rabies vaccination or HRIG is collectively termed “the Milwaukee protocol”. In 2004, a 15 year old girl from Fond du Lac, Wisconsin was bit on the left index finger by a bat. The wound was cleaned with hydrogen peroxide but no other treatment was sought. Approximately one month later, she developed neurological signs indicative of clinical rabies. She was admitted to the hospital where her condition continued to deteriorate. History of a bat bite was elicited on the 6<sup>th</sup> day of illness and rabies virus-specific antibodies were detected in the CSF and serum. She was put in a drug-induced coma and ventilator support and was treated with

intravenous ribavirin. Anti-rabies antibodies in the CSF increased from 1:32 to 1:2,048 after seven days and the medications were slowly tapered so that the patient became increasingly alert. She was discharged after 76 days; five months after initial hospitalization she was able to dress herself, ate a normal diet, and attended high school part-time, though her speech was slurred and she had an unsteady gait (49; 284). More than two years after initial exposure, her speech and gait abnormalities had improved and she returned to high-school full-time; she had no difficulties in learning or with daily activities such as driving (131).

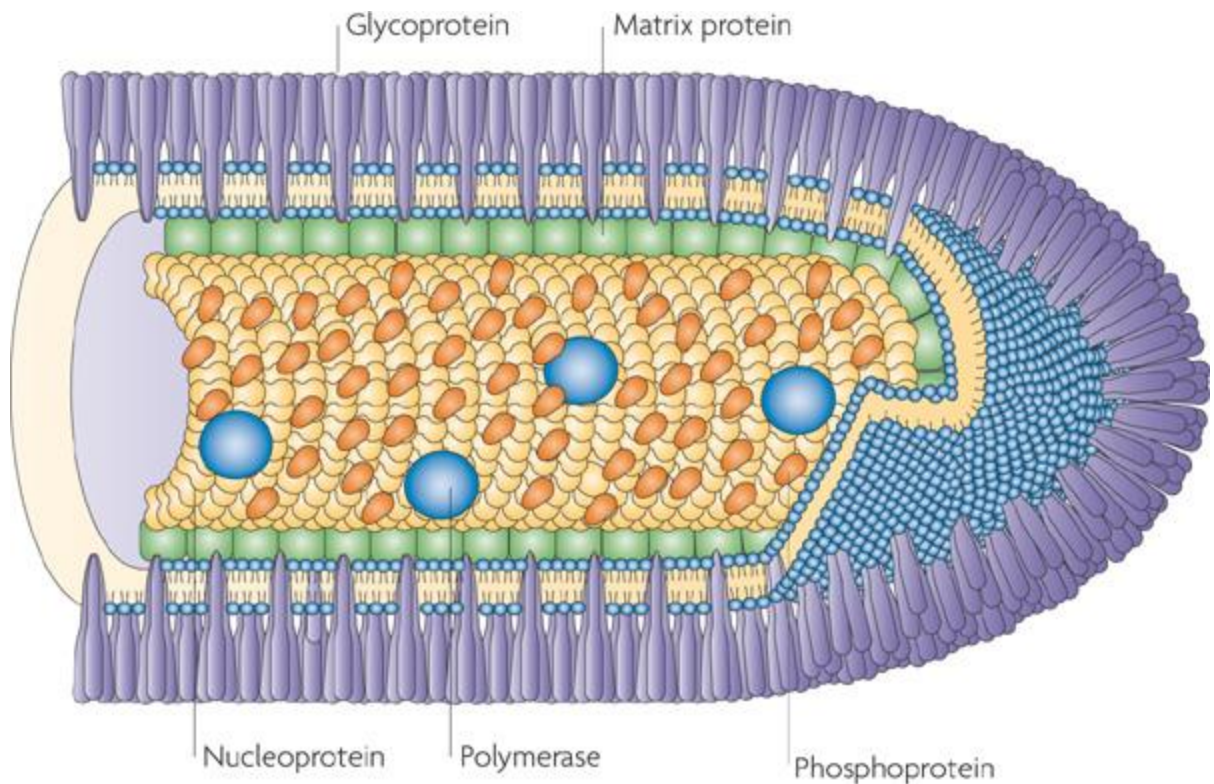
The Milwaukee protocol has since been attempted on 33 additional patients, four of which survived (<http://www.chw.org/display/PPF/DocID/33223/router.asp>). The protocol has undergone several revisions and it is now recommended that ribavirin be excluded due to its immunosuppressive effects and the administration of rabies vaccine or RIG is not recommended after rabies symptoms appear due to “early death” phenomena based on animal studies of bat derived rabies and human case reports (6; 283).

Due to its low success rate, the idea that the Milwaukee protocol is directly responsible for patient recovery from clinical rabies is not universally accepted. Critics argue that it is more likely that patients survived due to other factors such as an especially strong immune response or a weak form of the virus. A study of two Peruvian Amazon rural populations suggests that non-fatal rabies encounters may not be as rare as previously believed. Researchers found that 11% (7 of 63) of blood samples collected from individuals that reported a history of a bat bite(s) tested positive for rabies virus neutralizing antibodies; only one of the seven individuals reported having received a rabies vaccine suggesting non-fatal rabies exposure for the remaining six (103).

Additionally, a presumptive abortive case of clinical rabies was reported for an adolescent girl from Texas (50). The 17 year old patient was admitted to two different hospitals with a severe headache, paresthesia of face and forearms, neck pain, and dizziness. During the second admission, a history of bat exposure was elicited and serum and CSF tested positive for RABV IgG, with titers of 1:2,048 and 1:32, respectively, despite no history of rabies vaccination or receipt of HRIG; no virus neutralizing antibodies (VNA) were detected until after administration of HRIG and a single dose of vaccine. Symptoms resolved without the need for intensive care. Based on the low RABV IgG titers in the CSF and serum compared to previous rabies survivors (49), the relatively mild clinical signs, and the absence of VNA, and no alternative infectious etiology for the displayed clinical symptoms, it was concluded that perhaps the patient's innate immune system cleared the infection before the production of VNA and was therefore an abortive case of clinical rabies (50).

#### **LYSSAVIRUS VIRION STRUCTURE AND MOLECULAR BIOLOGY**

Lyssaviruses are enveloped, bullet-shaped viruses with a single-stranded, negative sense RNA genome of about 12 kb that encodes five viral proteins: nucleoprotein (N), phosphoprotein (P), matrix (M), glycoprotein (G), and RNA polymerase (L) (Figure 2). The RNA genome is encapsidated by the N protein, forming the ribonucleoprotein (RNP) complex. Only the RNP is a functional template for transcription and replication. The L and P proteins associate with the RNP, forming the viral capsid. A host cell derived membrane surrounds the viral capsid and is associated with the M and G glycoproteins. The M protein serves as a bridge between the viral capsid and the virion membrane. The



Nature Reviews | Microbiology

Figure 2. The rabies virus virion. The negative-stranded RNA genome is tightly encapsidated into the nucleoprotein (yellow) and is termed the ribonucleoprotein (RNP). Two other viral proteins are associated with the RNP, the viral polymerase (blue) and the phosphoprotein (orange), which make up the internal core or capsid. The capsid is engulfed by the host cell-derived membrane, which is associated with two additional viral proteins: the matrix protein (green), which functions as a bridge between the capsid and the virion membrane, and the single transmembrane glycoprotein, which is organized as a trimer (purple).

From (231). Figure and legend reprinted with permission from Nature Publishing Group.

G glycoproteins associate into trimers on the virion surface and mediate viral attachment to and fusion with the host cell membrane (100). Following host cell attachment, lyssaviruses are internalized by means of receptor-mediated endocytosis; the low pH of the endosome triggers G-mediated fusion of the viral and host cell membranes.

### **Virus life cycle**

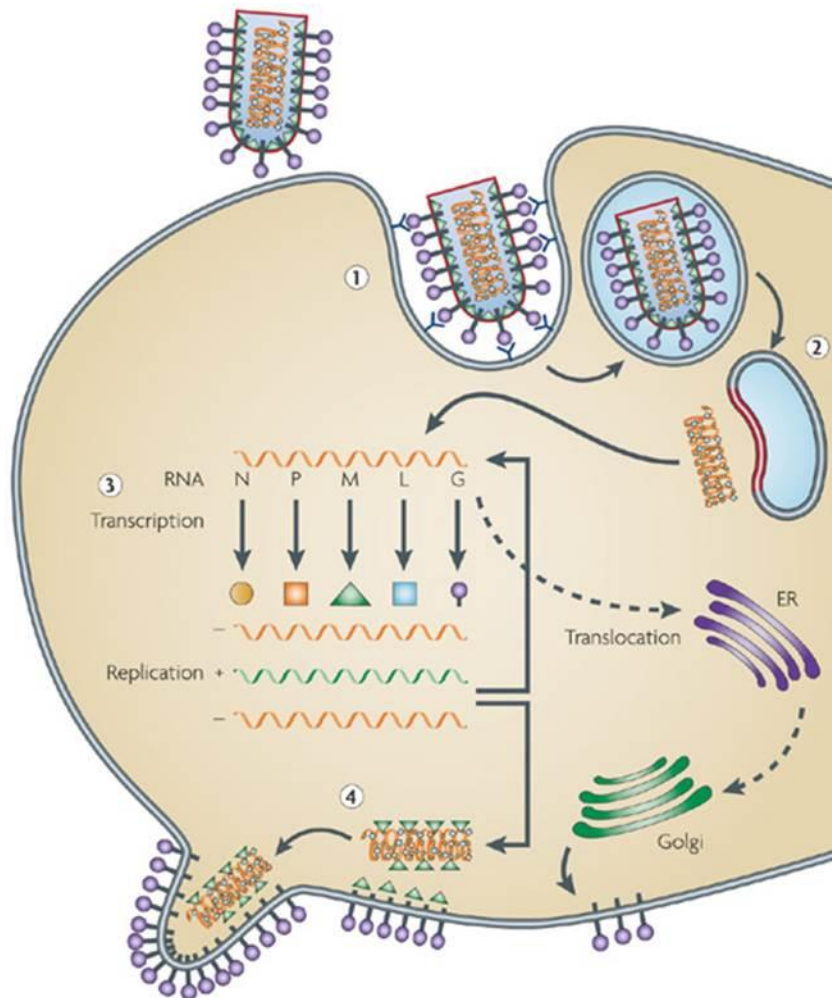
A simplified lyssavirus life cycle can be divided into three phases (Figure 3). The first phase includes G-mediated binding to the host cell receptor(s) and entry by receptor-mediated endocytosis followed by low pH induced fusion of the viral and endosomal membranes and subsequent release of the viral genome into the cytoplasm. Lyssaviruses most likely enter motor neurons at the neuromuscular junction; however, a study using a bat-derived RABV variant demonstrated that the virus was able to spread in the blood and enter the CNS at the neurovascular junction of the hypothalamus (205). After entry into the neuron, virus particles are transported through the axon in a retrograde direction (265) to the cell body where the second phase of the life cycle begins. In this phase, transcription, translation, and replication occur to produce the viral components. The last phase of the life cycle includes assembly and transport of the viral components to the plasma membrane for subsequent budding and release of mature virions which can then initiate a new round of infection.

### **Attachment to host cells**

The first step of the lyssavirus life cycle is attachment to the host cell which is mediated by the G glycoprotein; however, it is unclear which host cell surface molecule(s) interacts with the G glycoprotein to mediate viral entry into the cell.

Numerous host cell molecules have been proposed as receptors for RABV, but none have





Nature Reviews | Microbiology

Figure 3. Rabies virus life cycle. A simplified rabies virus life cycle in an infected cell can be divided into three different phases. The first phase includes binding and entry into the host cell by endocytosis (step 1), followed by fusion of the viral membrane and endosome membrane to release the viral genome (uncoating; step 2). In the second phase, virion components are produced (transcription, replication and protein synthesis; step 3). The last phase of the life cycle is the assembly of the viral components and budding and release of the rabies virus virions (step 4), which can start a new round of infection. ER, endoplasmic reticulum.

From (231). Figure and legend reprinted with minimal editing with permission from Nature Publishing Group.

been shown to be essential *in vitro*. These include protein receptors such as nicotinic acetylcholine receptor (nAChR) (114; 151; 152), neuronal cell adhesion molecule (NCAM) (258), and p75 neurotrophin receptor (p75NTR) (261), as well as neuraminic acid containing glycolipids (gangliosides) (66; 249). The nAChR is predominantly expressed in muscle cells and is localized to the postsynaptic muscle membrane, not to the presynaptic nerve membrane (143); thus, it is unlikely that initial entry into motor neurons occurs through this receptor. While nAChR is not required for RABV infection of neurons (178), it may account for replication of RABV in muscle cells at the site of inoculation (43). The p75NTR does not bind to most lyssavirus G glycoproteins, including ABLV G (262), and is not essential for RABV infection (264). Similarly, although NCAM was shown to be an *in vitro* receptor for RABV, NCAM knock-out mice were still susceptible to infection by RABV, although clinical onset was delayed by a few days (258).

Prior to the present study, the nature of the host cell receptor(s) for ABLV had not been investigated. Data presented in Chapter 2 indicate that neither nAChR nor NCAM are sufficient to permit ABLV to enter host cells. Additionally, ABLV G-mediated entry was significantly reduced following lipid raft disruption with the cholesterol sequestering drug methyl- $\beta$ -cyclodextrin. Taken together these results suggest that ABLV utilizes a unique receptor or co-receptor for host cell infection that is localized or enriched in lipid rafts. Additionally, we identified three cell lines that were significantly less permissive to ABLV G-mediated viral entry. These cell lines, which are described in Chapter 2, will be valuable tools for future strategies aimed at ABLV receptor identification.

## **Internalization**

Lyssaviruses are internalized into the host cell by receptor-mediated endocytosis. Pinocytic mechanisms of endocytosis, which permit the uptake of fluid, small particles, and solutes into the host cell, are typically exploited by viruses to gain entry into cells. Clathrin-mediated endocytosis (CME), caveolin/raft-dependent endocytosis (CavME), and macropinocytosis are the best studied endocytic mechanisms, but there are several clathrin- and caveolin/raft-independent mechanisms that are less understood. The CME pathway is the most commonly utilized pathway in virus entry, but there are examples of viruses using at least six additional endocytic pathways for host cell entry (Figure 4) [reviewed in (183)]. Additionally, some viruses take advantage of multiple pathways to gain entry into the host cell; examples include Ebola virus (CME and macropinocytosis) (3; 27; 195; 227), influenza A (CME and a novel pathway) (57; 225; 238), and reovirus (CME and CavME) (232). Pertinent to the work presented herein, rhabdoviruses from three different genera have been shown to utilize CME for entry, including vesicular stomatitis virus (VSV) (genus *Vesiculovirus*) (247), infectious hematopoietic necrosis virus (IHNV) (genus *Novirhabdovirus*) (160), and RABV (genus *Lyssavirus*) (201; 248); to date no rhabdovirus has been reported to utilize a clathrin-independent pathway. Data presented in Chapter 3 suggest that ABLV also utilizes CME for host cell entry.

### ***Clathrin-mediated endocytosis***

CME is initiated by the formation of a nucleation module that defines the region on the plasma membrane where clathrin will be recruited; the module is composed of FCH domain only (FCHO) proteins, EGFR pathway substrate 15 (EPS15) and

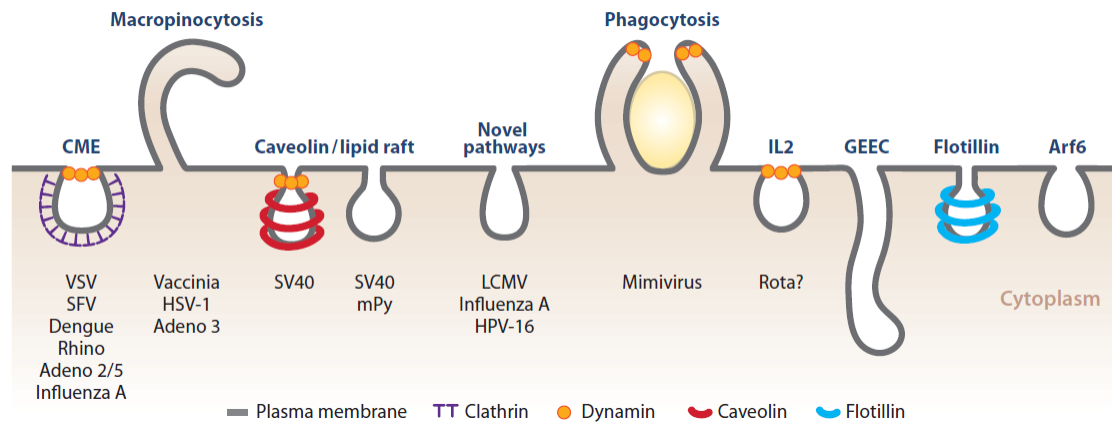


Figure 4. Endocytic mechanisms. Endocytosis in animal cells can occur via several different mechanisms. Multiple mechanisms are defined as pinocytic, i.e., they involve the uptake of fluid, solutes, and small particles. These include clathrin-mediated, macropinocytosis, caveolar/raft-mediated mechanisms, as well as several novel mechanisms. Some of these pathways involve dynamin-2 as indicated by the beads around the neck of the endocytic indentations. Large particles are taken up by phagocytosis, a process restricted to a few cell types. In addition, there are pathways such as IL-2, the so-called GEEC pathway, and the flotillin- and ADP-ribosylation factor 6 (Arf6)-dependent pathways that carry specific cellular cargo but are not yet used by viruses. Abbreviations: Adeno 2/5, adenovirus 2/5; Adeno 3, adenovirus 3; CME, clathrin-mediated endocytosis; HPV-16, human papillomavirus 16; HSV-1, herpes simplex virus 1; LCMV, lymphocytic choriomeningitis virus; mPy, mouse polyomavirus; SFV, Semliki Forest virus; SV40, simian virus 40; VSV, vesicular stomatitis virus.

From (183). Figure and legend reprinted with permission from Annual Reviews, Inc.

intersectins (Figure 5) (124; 244) [reviewed in (180)]. These proteins then recruit AP2, the core plasma membrane adaptor for clathrin as well as additional cargo-specific adaptor proteins (124); AP2 is second only to clathrin in protein abundance within clathrin-coated pits (31). Following recruitment of and cargo selection by AP2 and other cargo-specific adaptor proteins, clathrin is recruited to the plasma membrane by AP2 and polymerizes in hexagonal and pentagonal lattices that stabilize membrane curvature and displace curvature effector proteins such as Eps15 and epsin to the edge of the nascent clathrin-coated pit (CCP) (Figure 5); the curvature effector proteins directly interact with the plasma membrane to sculpt the vesicle (228; 256). Although initially thought to be a constitutive process that occurred whether cargo was present or not, CCP formation has since been shown to be actively initiated by certain cargo. VSV, Influenza A, and reovirus induce de novo CCP formation at the site of viral binding (67; 78; 138; 225). Transient accumulation of clathrin, dynamin-2, and AP2 can be observed underneath or in close proximity to surface bound VSV; the CCP assembly phase lasts about twice as long as normal CCP formation (110 sec versus 50 sec, respectively) (67; 138). Though it is not clear what causes clathrin-coat assembly, it has been postulated that receptor clustering induced by surface bound virus may cause the formation of a microdomain with differing properties than that of the surrounding membrane (183). The final step of CME includes the pinching of the clathrin-coated vesicle from the membrane by dynamin, a self-polymerizing GTPase (19; 125; 252). Clathrin lattices are then disassembled from the detached vesicle, enabling the uncoated vesicle to traffick to and fuse with its target endosome (267).

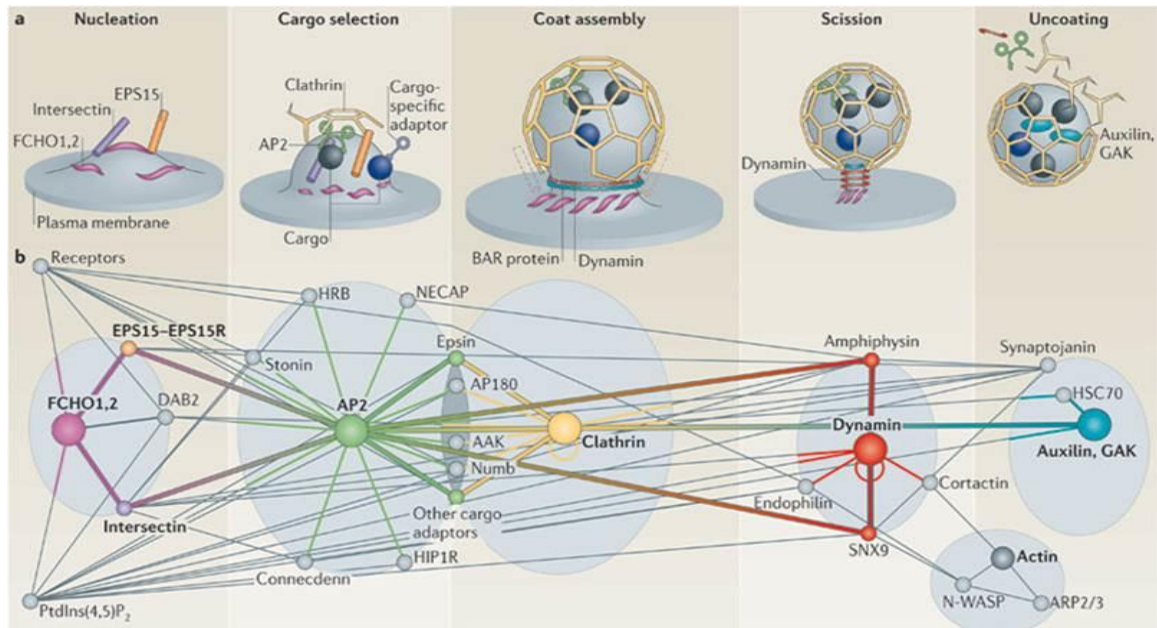


Figure 5. The clathrin-coated vesicle cycle. (a) The proposed five steps of clathrin-coated vesicle formation. Nucleation: FCH domain only (FCHO) proteins bind phosphatidylinositol-4,5-bisphosphate (PtdIns(4,5)P<sub>2</sub>)-rich zones of the plasma membrane and recruit EPS15-EPS15R (EGFR pathway substrate 15-EPS15-replated) and intersectins to initiate clathrin-coated pit formation by recruiting adaptor protein 2 (AP2). Cargo selection: AP2 recruits several classes of receptors directly through its  $\mu$ -subunit and  $\sigma$ -subunit. Cargo-specific adaptors bind to AP2 appendage domains and recruit specific receptors to the AP2 hub. Coat assembly: clathrin triskelia are recruited by the AP2 hub and polymerize in hexagons and pentagons to form the clathrin coat around the nascent pit. Scission: the GTPase dynamin is recruited at the neck of the forming vesicle by BAR domain-containing proteins, where it self-polymerizes and, upon GTP hydrolysis, induces membrane scission. Uncoating: auxilin or cyclin G-associated kinase (GAK) recruits the ATPase heat shock cognate 70 (HSC70) to disassemble the clathrin coat and produce an endocytic vesicle containing the cargo molecules. Synaptojanin probably facilitates this by releasing adaptor proteins from the vesicle membrane through its PtdIns lipid phosphatase activity. The components of the clathrin machinery are then freed and become available for another round of clathrin-coated vesicle formation. (b) The clathrin network. The protein-protein interactions underlying the different stages of vesicle progression are shown. Major hubs are obvious because of their central location in the network and the large number of interacting molecules. They are essential for the pathway progression and are denoted by the central colored circles. Possible pathways of progression between the hubs are shown with thicker lines.

From (180). Figure (a) and (b) and legend reprinted with permission from Nature Publishing Group. Legend reprinted with minimal editing.

### ***Approaches to study CME as a viral entry pathway***

Numerous approaches can be utilized to determine whether clathrin is involved in a given virus entry pathway. Electron microscopy (EM) techniques provide the most direct method for visualizing the interaction of viruses and clathrin-coated pits (59; 179; 202). Another direct approach is the utilization of confocal microscopy in co-localization studies of viral proteins and the clathrin heavy-chain using specific tagged markers. While these direct studies are favorable because they do not disturb normal cellular processes, as often is the case when chemical inhibitors are used to disrupt endocytic pathways, they require large quantities of virus and precise experimental timing is required to visualize co-localization events due to the rapid assembly and disassembly of clathrin-coated pits.

Another traditional approach to studying CME is through chemical inhibition of clathrin-coated pit formation. Chlorpromazine, a cationic amphiphilic drug that is believed to inhibit CME through the translocation of clathrin and the AP2 complex from the cell surface to intracellular vesicles so that clathrin lattice formation occurs on endosomal membranes rather than the cell surface, is the most widely used CME inhibitor in virus entry studies (29; 134; 247; 273). There are no reports in the literature of chlorpromazine affecting lipid raft/caveolae mediated endocytosis; furthermore, several studies have demonstrated that viral entry inhibited by chlorpromazine was not inhibited by agents that block lipid raft/caveolae mediated internalization, and vice versa (45; 134; 160). However, phagocytosis in neutrophils and macrophages and neutrophil degranulation were inhibited by chlorpromazine (79; 276). These data suggest that in addition to blocking CME, the biogenesis of large intracellular vesicles such as phagosomes and macropinosomes may be affected by chlorpromazine, perhaps by

affecting actin dynamics which are critical for both phagocytosis and macropinocytosis (149; 171; 186). Therefore, while chlorpromazine is useful for the initial discrimination between CME and other endocytic pathways, the role of CME in a viral entry pathway should be confirmed with an alternative method such as RNA interference (RNAi) or overexpression of dominant negative (DN) mutants of a CME accessory protein, such as Eps15.

Clathrin is abundant in cells, thus it is difficult to achieve substantial depletion using siRNA techniques; high concentrations of siRNA as well as sequential transfections of siRNA are often required (67). Furthermore, even if knockdown of clathrin is shown to reduce viral entry, additional experiments are required to confirm that CME is the entry mechanism because clathrin is involved in cellular processes other than endocytosis. Clathrin plays crucial roles in protein secretion from the *trans*-Golgi network, endosomal sorting complex required for transport (ESCRT)-dependent cargo sorting at endosomes, and mitotic spindle formation (70; 209; 223). Thus, a perceived reduction in viral entry may actually be an indirect effect of clathrin RNAi. For example, depletion of clathrin could result in defective *trans*-Golgi export or endosomal recycling of the viral host cell receptor, leading to an indirect decrease in virus internalization.

Overexpression of DN Eps15 mutants in target cells is an alternative approach to RNAi for specifically examining CME. Eps15 is constitutively associated with AP2 and is required for an early step within the CME pathway (23). The DN Eps15 mutants, such as EH29 which lacks a portion of the Eps15 homology (EH) domains required for CCP targeting but retains the ability to bind to AP2, have been shown to inhibit CME by preventing efficient targeting of AP2 and clathrin to CCPs without adversely affecting



other endocytic pathways (22-24). This approach has been used to confirm CME as a viral entry pathway for numerous viruses including VSV (63; 150; 246; 247).

In the present study, both chemical inhibition of CME by chlorpromazine and overexpression of Eps15 EH29 in HEK293T cells were used to examine the role of clathrin in the viral entry pathway of ABLV. Data presented in Chapter 3 demonstrate that both approaches significantly reduced ABLV-G mediated viral entry into HEK293T cells. Inhibition of both dynamin, a scission factor involved in CME, and actin dynamics also significantly reduced ABLV-G mediated viral entry. In contrast, chemical inhibition of macropinocytosis and caveolae-dependent endocytosis had no effect on ABLV entry, suggesting that the predominant endocytic pathway utilized by ABLV to gain entry into HEK293T cells is clathrin-mediated and is dependent upon actin.

## **Uncoating**

Once internalized by endocytosis, viruses follow the same intracellular vesicular trafficking pathways as physiological ligands and membrane components, such as hormones, growth factors, and plasma membrane factors. These endosomal systems are responsible for molecular sorting, recycling, degradation, and transcytosis of incoming cargo. The primary organelles in the endosomal network are early endosomes (EEs), maturing endosomes (MEs), late endosomes (LEs), recycling endosomes (REs) and lysosomes (183). The low-pH of the endosome triggers a conformational change in the viral glycoprotein spike that facilitates viral and endosomal membrane fusion and the subsequent release of the viral genome into the cytosol. The pH required to trigger fusion typically correlates with the pH of the endosome; EEs (pH 6.5-6.0) for VSV, or LEs (pH 6.0-5.0) for influenza viruses (146; 280).

Viruses delivered from the surface by CME are typically delivered to EEs in less than two minutes and to the LEs within 10-12 minutes, with viral and host membrane fusion taking place within 1-5 minutes (VSV) or 10-20 minutes (influenza and dengue viruses), respectively (32; 146; 147; 183; 269). Selective vesicular trafficking and sorting is determined by functionally distinct domains localized on the cytosolic face of the endosomal membrane that are defined by different Rab GTPases and their effectors. In their active states, Rab proteins are GTP-bound and are recognized by multiple effector proteins; in inactive states they are GDP-bound. A guanine exchange factor (GEF) catalyzes the GDP to GTP exchange. The active Rab is converted back to the GDP-bound inactive state by the release of an inorganic phosphate by GTPase-activating protein (GAP) (243). Active Rab GTPases coordinate cargo trafficking within the endosomal network. For example, clathrin-coated vesicles are transported to EEs through the interactions of Rab5 (a marker of EEs) with AP2 to facilitate the uncoating of clathrin-coated vesicles and subsequent fusion with EEs (234). Once delivered to the EEs, the Rab defined domains either target cargo back to the plasma membrane (Rab4), to LEs (Rab7), to REs (Rab22/Rab11), or to the *trans*-Golgi network (Rab9) (183). To facilitate vesicular transport towards the microtubule organizing center (MTOC), Rab GTPase proteins interact with dynein or dynactin, whereas interaction with kinesin-1 results in the recycling of vesicles back to the cell surface along microtubules (90; 159; 169; 212).

Lyssaviruses require vacuolar acidification for G glycoprotein-mediated viral fusion with host cell membranes (184), but few studies have examined the endosomal trafficking of these viruses. RABV G was shown to co-localize with Rab5a (EEs) but not

Rab9 (LEs); this same study demonstrated that internalization of an anti-RABV G antibody/RABV G complex was dependent on the presence of functional Rab5a suggesting that RABV G fuses with EEs (242). Separate studies showed that RABV co-localized with endocytic tracers for early endosomes within nerve cells (154; 155). Furthermore, the optimal pH for RABV G-mediated fusion is pH 5.8-6.0, which correlates with the pH of EEs (99; 183). Indeed, the fusion activity of RABV G is completely abolished following pre-incubation of virus at a pH below pH 6.75 in the absence of a target membrane. However, in contrast to other viruses that fuse at low pH, the aforementioned fusion inhibition is reversible upon readjustment of pH to above 7, with full recovery of fusion activity (96; 102). The pre- and post-fusion states of G exist in a pH-dependent thermodynamic equilibrium that is shifted towards the post-fusion conformation at low pH (214); the reversibility of G conformational states is required for the recovery of its native pre-fusion state following its transport through the acidic compartments of the Golgi apparatus before it is incorporated into newly synthesized virions (101).

Viral membrane fusion proteins are grouped into one of three classes based on key structural features of the proteins. The structural features of class I proteins resemble influenza virus hemagglutinin (286). The fusogenic domain is predominantly composed of  $\alpha$ -helices which contain the N-terminal hydrophobic fusion peptides; in the post-fusion form, the fusogenic domain is composed of a trimeric  $\alpha$ -helical coiled coil. Class II proteins share structural features with the tick borne encephalitis virus E fusion protein (211); these proteins are predominantly composed of  $\beta$ -sheets with fusion peptides located in internal loops and their conformational change involves the transition from

pre-fusion dimers to post-fusion trimers, unlike class I proteins which remain trimeric. Class III proteins, which share structural similarities to VSV G and Herpes Simplex virus-1 glycoprotein B, combine some features of both class I and class II proteins (120; 213); similar to class I proteins, they contain a trimeric coiled-coil in the post-fusion conformation, but, similar to class II proteins, three of their domains are predominantly composed of  $\beta$ -sheets and they contain an internal fusion peptide. Amino acid sequence alignments of VSV G and G glycoproteins from other rhabdovirus genera, including lyssaviruses, suggest that all rhabdovirus G glycoproteins share the structure and folding features of VSV G and are also likely class III fusion proteins (1; 213).

Due to the pH-dependent equilibrium of pre- and post-fusion conformations of rhabdovirus G glycoproteins, several G spikes must cooperate to complete the fusion reaction; for RABV an estimated minimum of 15 spikes are required for a functional fusion complex (214). The crystal structure of the pre-fusion form of VSV G revealed a hexagonal lattice of G composed of six trimers; a similar organization has been implied for RABV G (98; 215). Electron microscopy studies revealed that VSV fusion is initiated at the flat base of the VSV virion, likely through activated G glycoproteins with their fusion domains exposed at the top of the protein, facilitating the formation of stalks and initial fusion pores (Figure 6). G glycoproteins outside of the contact zone in their post-fusion form then reorganize into regular arrays which are thought to induce membrane constraints which drive pore enlargement and allow the fusion reaction to complete (1; 158).

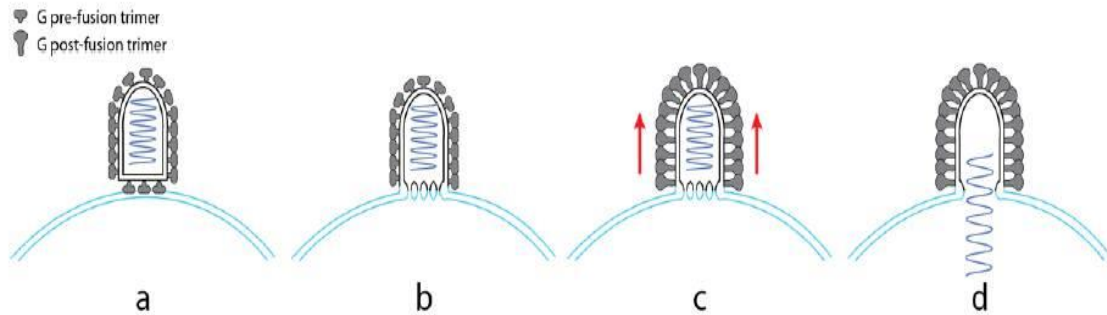


Figure 6. A model for rhabdovirus fusion. (a) The flat base of the virion interacts with the target membrane most likely via activated glycoproteins that expose their fusion domain at their top. (b) The local organization of G in this region may facilitate the formation of stalks and initial fusion pores. (c) A helical network of G in their post-fusion conformations is then formed on the lateral part of the viral particle. The formation of this regular array likely induces tension in the membrane (red arrows) that (d) drives pore enlargement and leads to complete fusion.

From (1). Figure and legend reprinted with permission from MDPI (open access).  
Legend reprinted with minimal editing.

### ***Approaches to study endosomal trafficking***

Numerous strategies can be used to identify which endosomal compartment a given virus fuses with. One of the most common methods for studying viral endosomal trafficking is through overexpression of dominant negative Rab GTPases specific for EE, LE, and RE (64; 138; 140; 199; 217; 227). Dominant negative Rab proteins contain single amino acid changes (Rab5 S34N, Rab7 T22N, Rab11 S25N) that cause the proteins to have a much greater affinity for GDP than GTP, thus maintaining the protein in an inactive state (86; 156; 266). Overexpression of the mutant Rab proteins in host cells elicit a dominant negative effect over the endogenous wild-type protein; thus, a virus that requires a specific endosome for trafficking and fusion will be adversely affected by the overexpression of a dominant negative Rab protein specific for that endosome. Alternative methods for studying endosomal trafficking include siRNA knockdown of Rab proteins in host cells (127; 141) or co-localization studies of virus or viral protein with an EE marker such as Rab5 or EEA-1, or a LE marker such as Rab7 or LAMP-1 by microscopy (25; 62; 272).

In the present study, dominant negative forms of Rab5, Rab7, and Rab11 were used to investigate the endosomal trafficking of ABLV G. Data presented in Chapter 3 indicate that ABLV G-mediated viral entry is dependent on Rab5 and that ABLV G fuses with early endosome membranes to gain entry into the host cell cytosol. Inhibition of functional Rab7 or Rab11 had no effect on ABLV G-mediated viral entry.

### **AIMS AND OBJECTIVES OF THE PRESENT STUDY**

The goal of the present study was to characterize host cell virus entry mediated by Australian bat lyssavirus G glycoprotein. This goal was divided into two separate aims:

in Aim 1 the host cell infection tropism for ABLV G-mediated viral entry was characterized (described in Chapter 2); these studies indicate that the host cell receptor for ABLV is broadly conserved among mammalian species and that it utilizes a unique receptor or co-receptor that has yet to be identified, as proposed rabies virus receptors were not sufficient to permit ABLV entry into host cells. In Aim 2 the endocytic pathway and endosomal compartment utilized by ABLV to gain entry into the host cell cytosol were identified (described in Chapter 3); these studies indicate that ABLV G-mediated viral entry into HEK293T cells primarily occurs through clathrin-mediated endocytosis that is dependent upon actin and that ABLV G fuses with early endosomes to gain entry into the host cell cytosol.

To further characterize ABLV G and to explore its immunogenicity in animal models, an S-peptide tagged soluble version of ABLVs G (Gs) was developed (described in Chapter 4); these studies show that Gs is highly immunogenic and induces a potent cross-reactive neutralizing antibody response in both mice and rabbits. These results indicate that ABLVs Gs retains important native structural features, suggesting that it may be a useful diagnostic reagent and could also be used as antigen for the panning and isolation of anti-ABLV G human MAbs, which could lead to more effective PEP treatments for individuals exposed to ABLV.

## **CHAPTER 2: Host cell tropism mediated by Australian bat lyssavirus envelope glycoproteins**

Published as: **Weir DL, Smith IL, Bossart KN, Wang LF, Broder CC.** 2013. Host cell tropism mediated by Australian bat lyssavirus envelope glycoproteins. *Virology* **444**:21-30.

### **ABSTRACT**

Australian bat lyssavirus (ABLV) is a rhabdovirus of the lyssavirus genus capable of causing fatal rabies-like encephalitis in humans. There are two variants of ABLV, one circulating in pteropid fruit bats and another in insectivorous bats. Three fatal human cases of ABLV infection have been reported with the third case in 2013. Importantly, two equine cases also arose in 2013; the first occurrence of ABLV in a species other than bats or humans. We examined the host cell entry of ABLV, characterizing its tropism and exploring its cross-species transmission potential using maxGFP-encoding recombinant vesicular stomatitis viruses that express ABLV G glycoproteins. Results indicate that the ABLV receptor(s) is conserved but not ubiquitous among mammalian cell lines and that the two ABLV variants can utilize alternate receptors for entry. Proposed rabies virus receptors were not sufficient to permit ABLV entry into resistant cells, suggesting that ABLV utilizes an unknown alternative receptor(s).

### **INTRODUCTION**

Until the discovery and isolation of Australian bat lyssavirus (ABLV) from a black flying fox (*Pteropus alecto*) in 1996, Australia was considered free of endemic lyssaviruses, a group of globally important zoonotic viral pathogens that continue to threaten human health (93). Capable of causing fatal acute rabies-like encephalitis in



humans, ABLV has since been a cause of considerable concern to wildlife, veterinary, and health-care workers. There are two genetically distinct variants of ABLV, one which circulates in frugivorous bats (suborder Megachiroptera, genus *Pteropus* (ABLVp)) and the other in the insectivorous yellow-bellied sheath-tail microbat (suborder Microchiroptera, genus *Saccolaimus*) (ABLVs)) (107). While the prevalence of ABLV in healthy bats is estimated to be less than 1%, in sick or injured bats it may be as high as 20% in flying foxes, depending on the species, and up to 62.5% in the yellow-bellied sheath-tail bat (88). ABLV has caused three fatal human infections and each manifested as acute encephalitis; however, incubation periods were variable. The first fatal case occurred in November 1996 approximately 5 weeks after a 39-year-old female animal handler was bitten presumably by a yellow-bellied sheath-tail bat (4). A second fatal case was reported in November 1998, more than 2 years after a 37-year-old female was bitten by a flying fox (116). The most recent case occurred in an 8-year old boy in February 2013, when he began to suffer convulsions, abdominal pain and fever, followed by progressive brain problems and coma. He died approximately 12 weeks after he was scratched (7).

ABLV is a member of the family *Rhabdoviridae*, genus *Lyssavirus*. The *Lyssavirus* genus is divided into 12 classified species (<http://www.ictvonline.org/virusTaxonomy.asp>; accessed 02 May 2013) and three recently described bat lyssaviruses not yet classified (39); all species are capable of causing fatal neurological disease indistinguishable from clinical rabies in humans and other mammals. Except for Mokola virus, all lyssavirus species have known bat reservoirs, leading to the speculation that lyssaviruses originated in bats (15). Of the

lyssavirus species, ABLV is most closely related to classical rabies virus (RABV) (107). Lyssaviruses are enveloped, bullet-shaped viruses with a single-stranded, negative sense RNA genome that encodes five viral proteins: nucleoprotein (N), phosphoprotein (P), matrix (M), glycoprotein (G), and RNA polymerase (L). The G glycoproteins associate into trimers on the virion surface and mediate viral attachment to and fusion with the host cell membrane (100). Following host cell attachment, lyssaviruses are internalized by means of receptor-mediated endocytosis; the low pH of the endosome triggers G-mediated fusion of the viral and host cell membranes.

Studies aimed at identifying host factors required for lyssavirus entry have thus far been limited to RABV. Lyssaviruses are highly neurotropic *in vivo*, but can replicate at sites of inoculation such as muscle tissue and epithelial cells (43; 190) and do exhibit a broad *in vitro* tropism (261). For RABV, several host cell molecules have been proposed as receptors, but none have been shown to be essential *in vitro*. These include protein receptors such as nicotinic acetylcholine receptor (nAChR) (114; 151; 152), neuronal cell adhesion molecule (NCAM) (258), and p75 neurotrophin receptor (p75NTR) (261), as well as neuraminic acid containing glycolipids (gangliosides) (66; 249). The nAChR, predominantly located in muscle cells, is not required for RABV infection of neurons (178), but may account for replication of RABV in myotubes at the site of inoculation (43). The p75NTR does not interact with the majority of lyssavirus glycoproteins, including ABLV G (262), and is not essential for RABV infection (264). Similarly, although NCAM has been shown to be an *in vitro* receptor for a fixed strain of RABV, NCAM knock-out mice were still susceptible to RABV infection, although the disease

was delayed by a few days (258). The nature of the ABLV receptor(s) has not been investigated.

In contrast to RABV which has both bat and terrestrial mammal reservoirs, only bats are known reservoirs for ABLV. ABLV has been isolated from five bat species including all four common species of flying fox present in mainland Australia (*Pteropus alecto*, *P. poliocephalus*, *P. scapulatus* and *P. conspicillatus*) and the insectivorous microbat *Saccolaimus flaviventris*; however, it is likely that all Australian bats may potentially serve as host reservoirs of the virus (129; 172). The first ABLV spillover into a terrestrial species other than humans was recently reported in May of 2013, when two ill horses in Queensland tested positive for ABLV infection and were euthanized, and presently the infections are presumably caused by exposure to infected microbats (53). The fatal human and recent equine infections clearly demonstrate that ABLV can infect other non-bat species. Furthermore, molecular evidence suggests that terrestrial RABV evolved from bat lyssaviruses (15). Although the risk of human exposure to ABLV is currently believed to be limited to contact with infected bats, the establishment of ABLV in terrestrial animal populations would significantly increase this risk. To understand the cross-species transmission potential of ABLV, infection tropism should be better defined. Characterization of ABLV tropism will also provide important data for ABLV receptor identification.

In the present study, we developed fluorescent protein-encoding recombinant vesicular stomatitis viruses (rVSV) that express ABLV G envelope glycoproteins and have used them to examine ABLV entry and infectivity as a function of G. Target cell lines derived from numerous mammalian species were permissive to ABLV, indicating

that the ABLV host cell receptor(s) is broadly conserved. Notably, the two ABLV variants exhibited distinct *in vitro* tropisms, suggesting that they can utilize alternate host factors for entry. Also, cell lines resistant to ABLV G-mediated infection were identified, and these also expressed proposed RABV receptors, indicating that a receptor(s) required for ABLV host cell entry remains to be identified.

## **RESULTS AND DISCUSSION**

### ***In vitro* tropism of ABLV-G mediated viral entry**

The *Saccolaimus* and *Pteropus* ABLV variant G glycoproteins are highly homologous, sharing 92% amino acid identity within the G ectodomain (Figure 7). However, because a single amino acid change within a viral glycoprotein can alter cellular tropism (263; 268), it is very possible that ABLVs and ABLVp, which differ by 33 amino acids within the G ectodomains, exhibit distinct tropisms. The very different incubation periods of human infections caused by the two variants, as well as the lack of overlapping host reservoir species, also point to possible tropism differences between ABLVs and ABLVp. To investigate ABLV tropism we developed and recovered maxGFP-encoding replication competent recombinant vesicular stomatitis viruses (rVSV) that express the G glycoproteins from both ABLVs and ABLVp and used them as infection screening tools to examine infectivity and tropism, as a function of ABLV G. This approach has several advantages over using WT ABLV. First, rVSV-ABLV G viruses are safer and easier to manipulate than WT ABLV. Second, the incorporation of GFP into the viral genome eliminates the need for traditional fluorescent antibody staining to detect infected cells. Third, the inclusion of rVSV-VSV G as a positive

```

ABLVs  1  KFPLYTIPDKLGPWSPIDIHHLSCPNNLIVEDEGCTSLSGFSYMELKVGFIITTIKVSQFT
ABLvp  1  .....V.....

ABLVs  61  CTGVVTESEYTYTNFFGYVTTTFKRKHFRPTPESCRKAYNWKIAGDPRIEESLHNPYPDYH
ABLvp  61  .....F..N....V.....

ABLVs 121  WLRTVTTTKESLLIISPSVVDMDPYDKSLHSRMFPGKSCSGASIPSVFCSTNHDYTLWMP
ABLvp 121  .....K.....T....V..I.....

ABLVs 181  EDSNSGMSCDIFTMSKGGKASKGGKVCGFVDERGLYKSLKGACKLKLKCGISGLRLMDGSW
ABLvp 181  .NPKP.....T.....

ABLVs 241  VSIQNHEEVKWCSPNQLVNIHDFNADEIEHLIVEELIKEREELDALESIIITTKSVSFRR
ABLvp 241  .....A.....D.....HS.....VRK.....M.....

ABLVs 301  LSHLRKLVPGFGKAYTIINKTLMEADAHYKSVRTWDEIIPSKGCLKVREKCHPPNNGVFF
ABLvp 301  .....V.....N.....R....Y....

ABLVs 361  NGIILSPDGQVLIPEMQSLLHQHTELLESSVIPLIHPLADPSTIFRGDDEAEGFIEVHL
ABLvp 361  .....H.....Q..I.....V.KR....D.....

ABLVs 421  PDIQKQVSGIDLGLSEWER
ABLvp 421  ..V.....

```

Figure 7. Comparison of the amino acid sequences of *Saccolaimus* and *Pteropus* ABLV G mature protein ectodomains. Scoring matrix: BLOSUM62.

control in all infection assays enables us to distinguish between actual ABLV G entry blocks and post-entry VSV inhibition. Previous studies that examined *in vitro* RABV tropism and receptor usage did not control for post-entry inhibition (258; 261).

Furthermore, because the viral backbones of the rVSV reporter viruses are identical except for the envelope glycoproteins, the tropism differences exhibited by the different viruses can be attributed directly to differences among the G glycoproteins themselves.

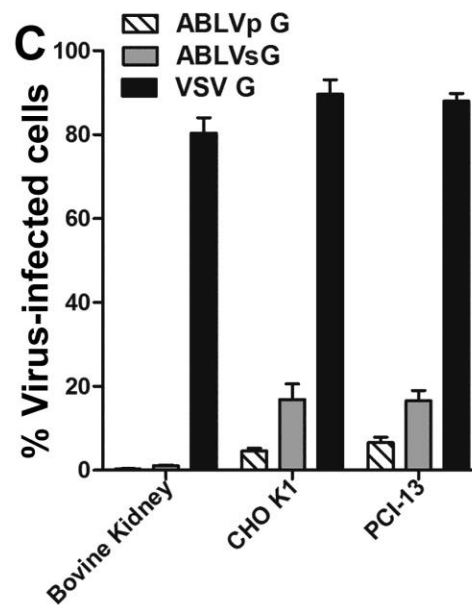
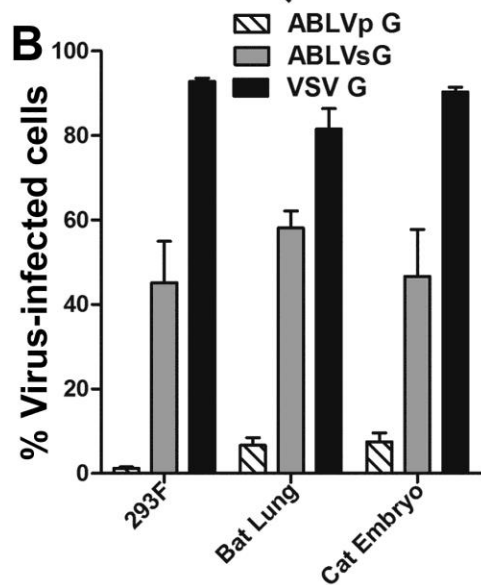
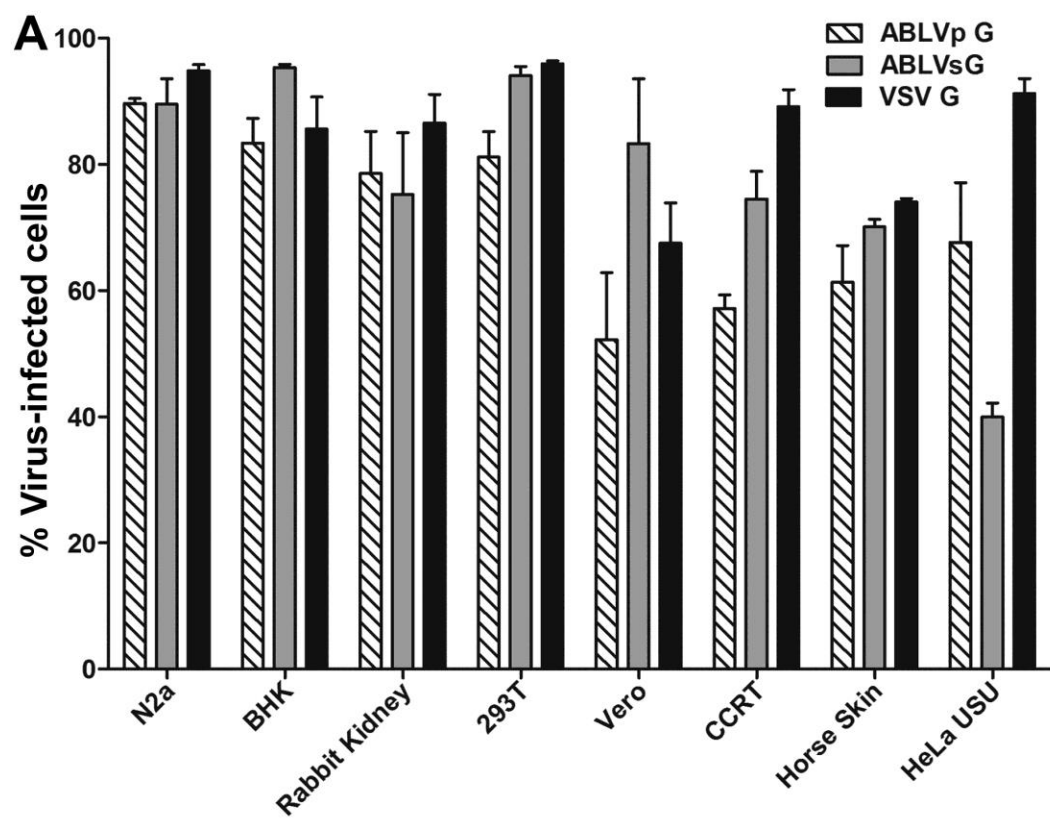
Diverse target cell populations were infected with the rVSV-maxGFP viruses at a multiplicity of infection (MOI) of 1 and the percent of maxGFP positive cells, indicative of productive infection, was determined 18-20 hrs post infection. As shown in Figure 8A, several target cell lines derived from both neuronal and non-neuronal tissues of numerous mammalian species, including multiple species of small rodents, rabbit, human, monkey, and horse, were permissive to viral entry mediated by the G glycoproteins of both ABLV variants. This is in agreement with the broad *in vitro* tropism reported for RABV (258). To date, except for the three human infections and the two recent equine cases, there have been no confirmed reports of ABLV infection in other terrestrial mammals despite known contacts of domestic dogs with infected bats (173). Dogs and cats experimentally infected with a laboratory adapted strain of ABLVp exhibited mild behavioral changes and seroconverted within the three month study, but none succumbed to ABLV and no viral antigen was detected at necropsy (176). However, this study was only carried out for three months and it is possible that this was not sufficient time for the virus to reach the brain; one of the documented human ABLVp infections had an incubation period of more than two years (116). The ability of ABLVs to cause clinical disease in dogs and cats has not been evaluated. Nevertheless, the

tropism data described here indicates that the ABLV receptor(s) is highly conserved among mammals and suggests that species other than bats, humans, and horses could potentially be susceptible to ABLV infection.

Interestingly, we also identified three cell lines derived from human (293F), insectivorous bat, and cat embryonic tissues that exhibited a 6-45 fold difference in infectivity mediated by the G glycoproteins of ABLVs and ABLVp (Figure 8B). All three cell lines were moderately permissive to ABLVs G-mediated (> 45% total cells infected), but resistant to ABLVp G-mediated viral entry (< 10% total cells infected), suggesting that ABLV variants can utilize alternate host factors for entry. It was surprising that the 293F cells, which are a derivative of HEK293 cells that have been adapted for growth in serum-free medium as suspension cells, were resistant to ABLVp (< 5% total cells infected) (Figure 8B) given that adherent 293T cells are highly permissive to both ABLV variants (Figure 8A). Dube et al. reported that 293F cells grown as adherent, rather than suspension cultures were significantly more susceptible to Ebola virus envelope glycoprotein (GP) pseudotyped virus infection (76). To determine whether a similar phenomenon may exist for ABLVp G-mediated viral entry, 293F cells were grown in serum-supplemented medium to allow the cells to form adherent monolayers prior to infection with rVSV-ABLV G reporter viruses. As shown in Figure 9A, although 293F cells grown in suspension were resistant to ABLVp G-mediated infection, cells grown as adherent monolayers were highly permissive to infection; thus, it appeared that cell adhesion promoted ABLVp infection. However, because adherent and suspension cultures of 293F cells were grown in the presence or absence of serum,

Figure 8. ABLV *in vitro* entry tropism. (A-C) Target cells infected with recombinant VSV-maxGFP reporter viruses at a MOI=1 were harvested 18-20 hrs post infection and fixed with 2% paraformaldehyde. GFP expression, indicative of productive infection, was analyzed by flow cytometry. The percent of virus-infected cells was calculated by dividing the number of GFP positive cells by the total number of cells in the parent population. (A) Numerous mammalian cell lines are permissive to ABLV G-mediated host cell entry. (B) *Saccolaimus* and *Pteropus* ABLV variants display unique *in vitro* entry tropisms. (C) Low ABLV infectivity of resistant cell lines is not due to post-entry VSV inhibition. Data are the means from 3 independent experiments and error bars represent the standard error of the mean (SEM). Reporter viruses that express VSV G were included as a positive control. N2a, mouse neuroblastoma; BHK, baby hamster kidney; 293T and 293F, human embryonic kidney; Vero, African green monkey kidney; CCRT, cotton rat osteogenic sarcoma; HeLa USU, human cervical adenocarcinoma; CHO K1, Chinese hamster ovary; PCI-13, human head and neck sarcoma.





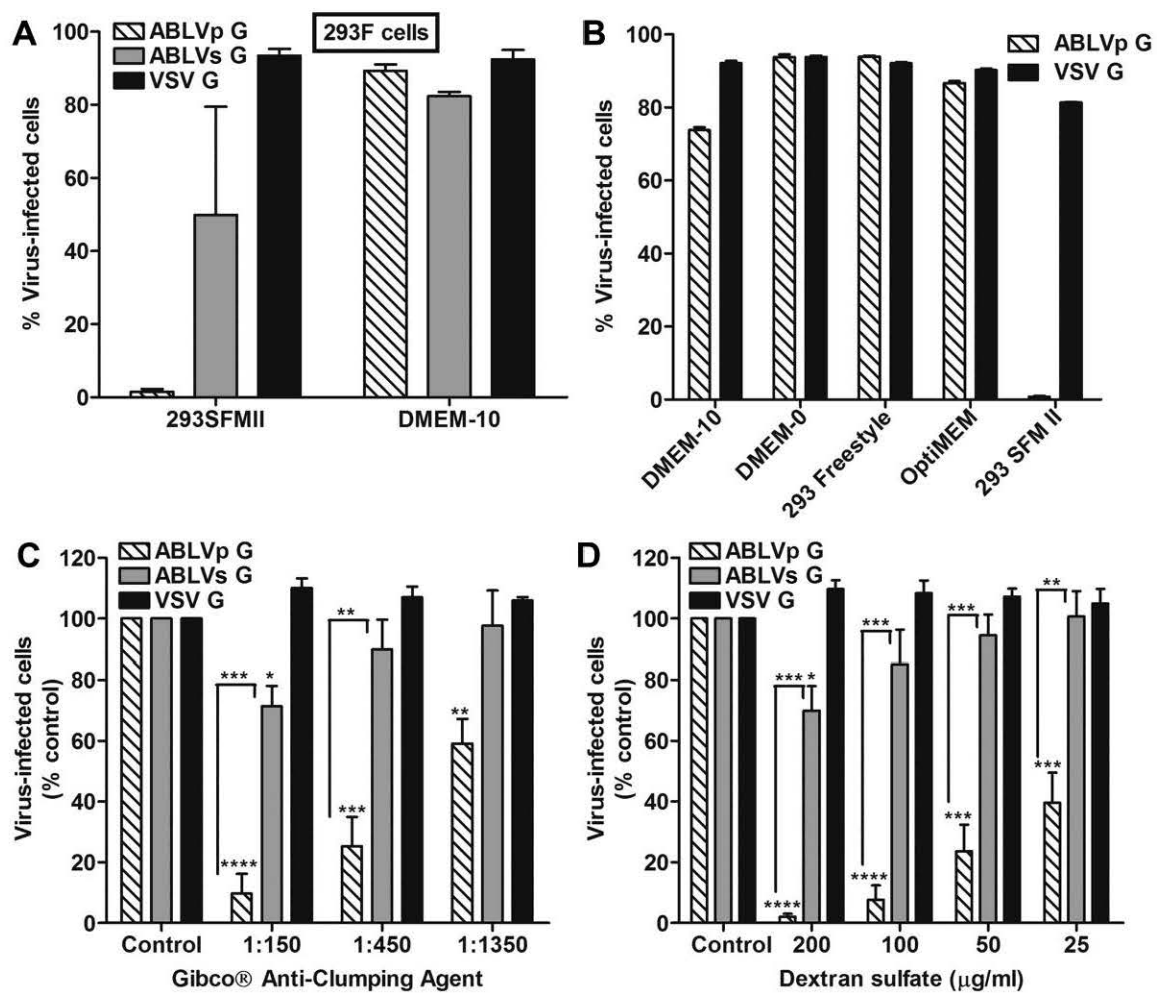
respectively, it was possible that it was the addition of serum, rather than cell adhesion that promoted ABLVp infection of 293F cells. To address this, 293T cells kept in suspension by continuous rotation in microcentrifuge tubes were infected with rVSV-ABLVp G in the presence or absence of serum in several commercially available media. Reporter virus that expressed VSV G was included as a positive control. As shown in Figure 9B, suspension cultures of 293T cells were highly permissive to ABLVp infection regardless of whether serum was present (DMEM-10) or not (DMEM-0, Gibco® 293 Freestyle™, OptiMEM®); only cells cultured in Gibco® 293 SFMII medium, the standard culture medium used for 293F cell maintenance, were resistant to ABLVp G-mediated viral infection. VSV G-mediated infection was not inhibited, demonstrating that the antiviral component within 293 SFMII medium blocks ABLVp G-mediated infection at the level of entry.

**Low molecular weight dextran sulfate is a potent inhibitor of viral entry mediated by ABLVp G, but not ABLVs G**

The complete formulations of 293 SFMII and OptiMEM® serum-free media, which inhibits and supports ABLVp infection, respectively, are not publicly available. However, the manufacturer acknowledged that 293 SFMII medium contains a proprietary anti-clumping reagent that is not present in OptiMEM®. To determine whether the anti-clumping agent was responsible for the ABLVp G-mediated viral inhibition, 293T cell culture medium was supplemented with Gibco® anti-clumping agent prior to infection with rVSV reporter viruses. As shown in Figure 9C, the anti-clumping agent significantly inhibited ABLVp G-mediated infection in a dose-dependent manner. Although ABLVs G-mediated infection was significantly reduced at the lowest dilution of anti-clumping agent tested, only 20-30% inhibition was observed compared to >80%

inhibition of ABLVp infection relative to untreated controls. As expected, the agent had no effect on VSV G-mediated infection. Low molecular weight dextran sulfate (5 kDa) is a conventional anti-clumping agent that has been used by the manufacturer of 293 SFMII in past serum-free media formulations (104). To determine whether dextran sulfate inhibited ABLVp G-mediated viral infection, culture medium supplemented with 2-fold serial dilutions of 5 kDa molecular weight dextran sulfate was added to 293T cell monolayers prior to infection with rVSV reporter viruses. Results paralleled what was seen with the anti-clumping agent: dextran sulfate reduced ABLVp G-mediated infection by up to 97% in a dose dependent manner (Figure 9D). At the highest dose, ABLVs G-mediated infection was significantly inhibited but the percent of inhibition was significantly lower than that observed for ABLVp at the same dose (20-30% versus 97%, respectively). ABLVs was not inhibited at lower concentrations of dextran sulfate and VSV was not inhibited at the concentrations tested. Dextran sulfate has been reported to have antiviral activity against numerous enveloped RNA and DNA viruses; the mechanism of antiviral action is thought to be mediated by a direct interaction of dextran sulfate with the viral envelope glycoproteins (288). In contrast to previous studies which reported a potent antiviral effect of dextran sulfate on VSV (13; 164; 288), in our experiments VSV entry was not inhibited at any concentration of dextran sulfate tested (Figure 9D). However, the aforementioned studies used higher molecular weight dextran sulfate and different cell lines, which may account for the different experimental outcomes. The potent inhibition of ABLVp G-, but not of ABLVs G-mediated viral entry by dextran sulfate strengthens the argument that the two ABLV variants can exploit alternate receptors to gain entry into host cells.

Figure 9. Anti-clumping agents are potent inhibitors of entry mediated by *Pteropus*, but not *Saccolaimus* ABLV G. (A-D) Cells were infected and analyzed as described in Figure 8. (A) HEK 293F cells grown in Gibco® 293 SFMII serum-free medium (suspension cells), but not serum supplemented DMEM (adherent cells), are resistant to ABLVp G-mediated infection. (B) Inhibition of ABLVp infection of suspension cultures of 293T is restricted to cells grown in 293 SFMII medium. 293T cells ( $5 \times 10^5$ ) in 1.5 ml microcentrifuge tubes were pelleted by centrifugation at  $2000 \times g$  for 5 min. Cells were washed once with PBS, pelleted, and then were resuspended in 500 ml of culture medium as designated. (C) Proprietary Gibco® anti-clumping agent in 293 SFMII medium inhibits ABLVp G-mediated entry into 293T cells. (D) Low molecular weight dextran sulfate (5 kDa) is a potent inhibitor of ABLVp G-mediated viral entry into 293T cells. 293T monolayers were washed once with PBS prior to addition of culture medium supplemented with 3-fold dilutions of Gibco® anti-clumping agent beginning at 1:150 (C) or with 2-fold serial dilutions of low molecular weight dextran sulfate (5kDa) beginning with 200  $\mu\text{g/ml}$  (D). Results are expressed as percent virus-infected cells relative to that of untreated controls. Data represent three independent experiments and error bars represent SEM. \*\*\*\*,  $p < 0.0005$ ; \*\*\*,  $p < 0.005$ ; \*\*,  $p < 0.01$ ; \*,  $p < 0.05$ .



### **Low ABLV infectivity of resistant cell lines is not due to post-entry VSV inhibition or lack of host cell attachment**

Cell lines that were resistant to ABLV G-mediated infection, with only 1-20% of total cells infected after 20 hrs, were also identified in our *in vitro* tropism studies (Figure 8C). These included bovine kidney (MDBK), CHOK1, and a human head and neck sarcoma cell line (PCI-13). VSV G expressing control viruses infected greater than 80% of these cells, indicating that the low ABLV infectivity was not due to post-entry VSV inhibition. To examine whether the lower susceptibilities corresponded to decreased viral binding, paraformaldehyde fixed monolayers of cells were incubated for 1 hr at 37°C with rVSV-ABLV viruses (MOI=20). Bound ABLV virus was detected by cell ELISA with anti-ABLV G sera (see Materials and Methods). BHK cells were included as positive controls for viral binding. Although there was significantly ( $p < 0.01$ ) less binding of ABLVs G to PCI-13 and MDBK cells than BHK cells, ABLVs G was able to bind to all three resistant cell lines and binding to CHOK1 was similar to permissive BHK cells (Figure 10A). Likewise, binding of ABLVp G to MDBK cells was significantly ( $p < 0.03$ ) less than BHK cells; however, ABLVp G bound to CHOK1, PCI-13, and BHK cells equally (Figure 10B). Thus, with the possible exception of ABLVp G-mediated infection of MDBK cells, the decreased susceptibility of CHOK1, PCI-13, and MDBK cells to ABLV G-mediated viral infection was not due to lack of host cell attachment, suggesting that host cell entry of ABLV may require interaction with two or more co-receptors. Dual- or multi-receptor models have been proposed for a number of viruses (239) as well as the highly neurotropic botulinum and tetanus toxins (203).

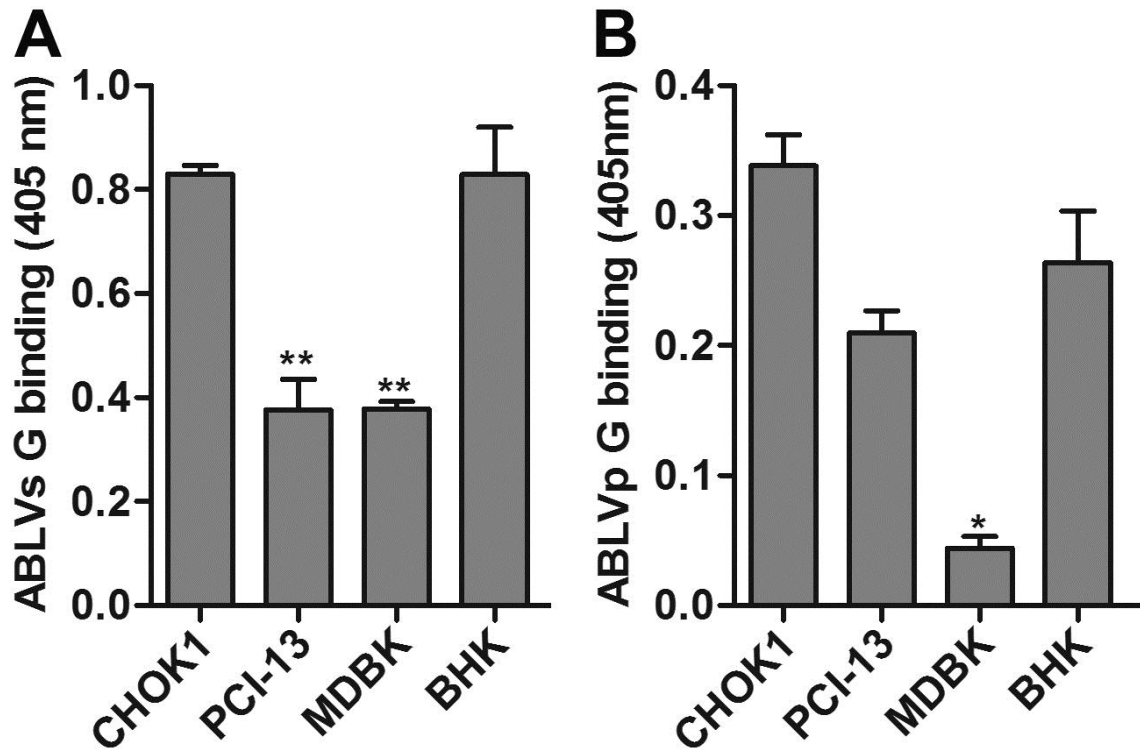


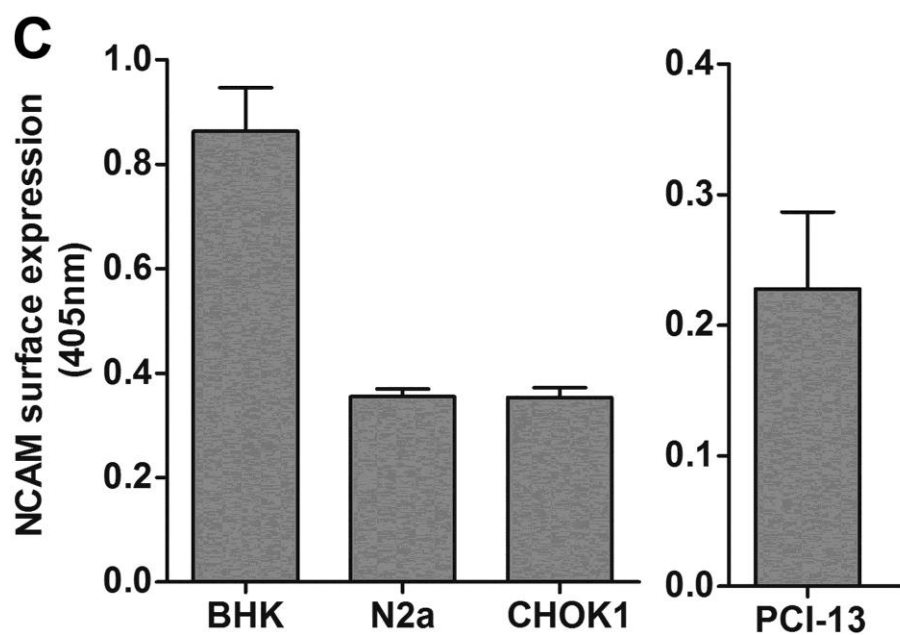
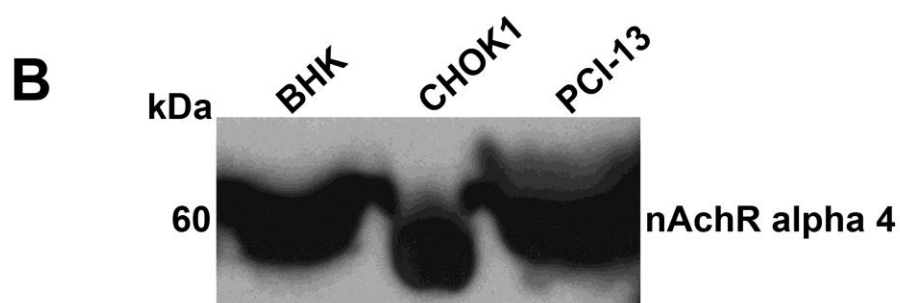
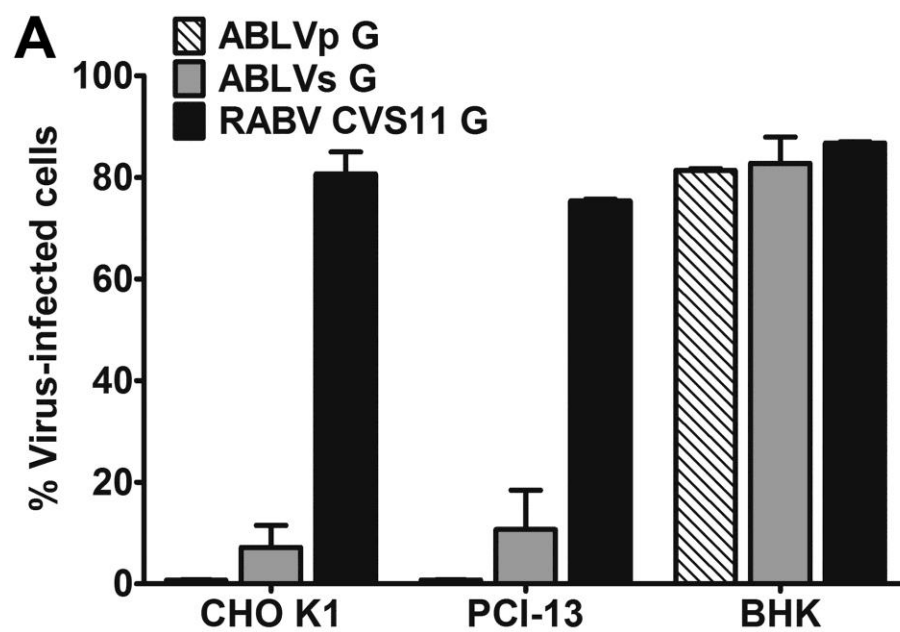
Figure 10. ABLV entry block in resistant cells is not due to lack of host cell attachment. (A) ABLVs G binding. (B) ABLVp G binding. Cell monolayers fixed with 2% PFA were blocked with 3% BSA in PBS and incubated with rVSV virus ( $5 \times 10^6$  IU) for 1 hr at 37°C. For detection of bound virus, cells were incubated overnight at 4°C with either rabbit or mouse anti-ABLVs Gs polyclonal serum (see Materials and Methods), followed by incubation with HRP-conjugated secondary antibodies for 1 hr at 37°C. Reactions were developed with ABTS substrate for 30 min at room temperature and absorbance was measured at 405 nm. The average value was calculated from duplicates. Background absorbance, determined by incubation of target cells with primary and secondary antibodies only, was subtracted from plotted data. Data represent the mean of two independent experiments and error bars represent SEM. BHK cells were included as a positive control. \*\*,  $p < 0.01$ ; \*,  $p < 0.03$ .

### **ABLV and rabies virus require alternate host factors for entry**

The identification of CHOK1 cells as an ABLV resistant cell line was particularly interesting as these cells have been reported to be highly permissive to the CVS-11 fixed strain of RABV (258), suggesting that ABLV and RABV may utilize alternate receptors for host cell entry. To confirm this possible *in vitro* tropism difference between ABLV and RABV, we rescued a recombinant VSV reporter virus that encodes the CVS-11 G glycoprotein and tested the ability of this virus to mediate entry into ABLV resistant CHOK1 and PCI-13 cells. BHK cells were included as a positive control. CHOK1 and PCI-13 cells were highly permissive to VSV-RABV CVS11 G infection, with 70-80% of total cells infected after 20 hrs (Figure 11A). Expression of the proposed RABV protein receptors nAChR (Figure 11B) and NCAM (Figure 11C) was confirmed in both cell lines. MDBK cells were excluded from these experiments due to the lack of reagents to detect bovine nAChR and NCAM. Although NCAM surface expression on CHOK1 cells was approximately 2-fold less than that on ABLV permissive BHK cells, the CHOK1 NCAM levels were similar to those on mouse neuroblastoma cells (N2a) (Figure 11C), which are highly permissive to both ABLV (Figure 8A) and RABV infection (258). However, to verify that the low ABLV infectivity of CHOK1 cells was not due to low expression of NCAM, a human NCAM (hNCAM) cDNA clone was transfected into CHOK1 cells. Over-expression of hNCAM was not sufficient to allow ABLV G glycoproteins to mediate viral entry into transfected CHOK1 cells (Figure 12A). This was not due to lack of hNCAM expression in transfected cells (Figure 12B). Furthermore, HeLa-USU cells, which do not express NCAM on the cell surface (data not shown), are permissive to ABLV G- mediated infection (Figure 8A). Taken together, these results indicate that the proposed RABV receptors nAChR and NCAM are not sufficient to allow host cell entry



Figure 11. ABLV resistant cells express proposed rabies virus receptors. (A) ABLV resistant cell lines are highly permissive to rabies virus G-mediated viral entry. Cells were infected as described in Figure 8. GFP positive cells were counted with a Nexcelom Vision automated cell counter with fluorescence detection and the percent of virus-infected cells was calculated by dividing the number of GFP positive cells by the total number of cells counted. (B) Endogenous nicotinic acetylcholine receptor (nAChR) expression. Cell lysates were prepared in buffer containing Triton X-100, clarified by centrifugation and analyzed by 4-12% BT SDS PAGE. An equivalent of  $1 \times 10^6$  cells per well were analyzed as described in the methods. nAChR was detected by Western blotting with rabbit anti-nAChR alpha 4 polyclonal antibody. BHK cells were included as a positive control. (C) Endogenous surface expression of neural cell adhesion molecule (NCAM). Cell monolayers fixed with 2% PFA were blocked with 3% BSA in PBS and then incubated overnight at 4°C with mouse anti-NCAM mAbs (3 µg/ml) specific for mouse (BHK, N2a and CHOK1) or human (PCI-13) NCAM. Following incubation with HRP conjugated anti-mouse IgG for 1 hr at 37°C, reactions were developed with ABTS substrate for 30 min at room temperature. Absorbance was measured at 405 nm and the average value was calculated from duplicates. Incubation of target cells with secondary antibody only was used to determine background absorbance and was subtracted from plotted data. (A) and (B) Data represent at least two independent experiments and error bars represent SEM. BHK and N2a cells were included as a positive control.



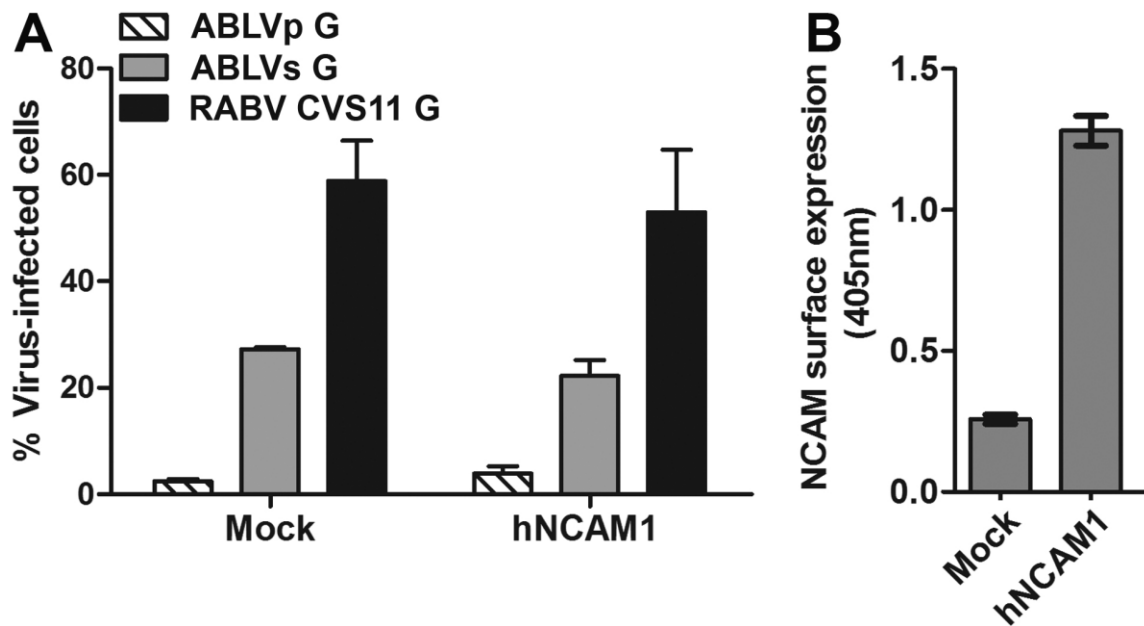


Figure 12. The rabies virus receptor neural cell adhesion molecule (NCAM) is not a receptor for ABLV. (A) Over-expression of human NCAM1 (hNCAM1) does not render CHOK1 cells permissive to ABLV. CHOK1 cells transfected with an hNCAM1 cDNA clone (see Materials and Methods) were infected 24 hrs post-transfection and analyzed as described in Figure 11A. Results shown are the mean from 2 independent experiments and error bars represent standard error of the mean. (B) Human NCAM1 surface expression in hNCAM-transfected CHOK1 cells. Mock and hNCAM-transfected cells were fixed with 2% paraformaldehyde 24 hrs post-transfection. A mouse anti-human NCAM MAbs was used to detect NCAM expression by cell ELISA as described in Materials and Methods.

of ABLV. Rather, ABLV appears to utilize a receptor(s) for host cell entry that has yet to be identified.

### **Disruption of lipid rafts significantly reduces ABLV G-mediated viral entry into 239T cells**

The observation that proposed RABV receptors are not sufficient to allow ABLV G to mediate viral entry into host cells prompted an examination of the nature of the unknown ABLV receptor(s). We treated permissive target cells with increasing doses of neuraminidase or protease (pronase, proteinase K, and trypsin) and in no case was ABLV G-mediated entry inhibited (data not shown). One possible explanation for these results could be that ABLV G interacts with more than one host cell receptor for entry, as is suggested by the ability of rVSV-ABLV G viruses to bind to cells resistant to infection (Figure 10). If the co-receptors belong to different classes of macromolecules, as is the case for several bacterial neurotoxins which utilize glycolipid and protein co-receptors to enter neurons (203), then treatment with protease or neuraminidase alone would not reduce viral infection; surface bound virions would interact with functional co-receptors as soon as the enzyme cleaved receptors were recycled and replaced by native ones. Thus, protein or sialic acid moieties as the ABLV receptor(s) cannot be ruled out.

We next examined whether lipid raft integrity was important for ABLV G-mediated viral entry. To disrupt lipid rafts, 293T cell monolayers were pre-treated with the cholesterol-sequestering drug methyl- $\beta$ -cyclodextrin (M $\beta$ CD) for 1 hr at 37°C. The drug was removed and the cells were washed extensively prior to rVSV infection. Subsequent to depletion of cholesterol with M $\beta$ CD, culture medium was supplemented with mevinolin (4  $\mu$ g/ml) to prevent *de novo* cholesterol synthesis. VSV reporter viruses expressing VSV G, and Ebola virus GP (Ebo GP) were included as negative and positive

controls, respectively. As previously reported, M $\beta$ CD treatment caused a drastic reduction of Ebo GP- mediated infection (227) but enhanced VSV G-mediated infection (up to 40%) (Figure 13) (235). ABLV G-mediated infection was significantly reduced (57% and 35% inhibition for ABLVp and ABLVs, respectively) compared to untreated controls (Figure 13), suggesting that the ABLV receptor(s) is localized or enriched in lipid rafts.

## CONCLUSIONS

In summary, we have developed replication-competent rVSV maxGFP reporter viruses that encode ABLV G envelope glycoproteins and have used them to characterize ABLV entry tropism as a function of G. The results presented here provide the first *in vitro* tropism data for a lyssavirus species other than classical RABV and reveal that although ABLV and RABV are closely related and are capable of causing identical fatal neurological disease in humans, they display distinct *in vitro* tropisms and can utilize alternate host receptors for viral entry. The same is true for *Saccolaimus* and *Pteropus* variants of ABLV. The ABLV receptor(s) appears to be highly conserved among mammalian species and may localize to lipid rafts. A major obstacle to identifying specific host cell receptors required for RABV entry has been the ability of fixed strains of RABV to replicate in most continuous cell lines (258; 261); thus, methods that have been successfully used to identify receptors for other viruses could not be used for RABV. Here however, we were able to identify several cell lines resistant to ABLV G-mediated viral entry. ABLV resistant CHOK1 cells in particular, which are easy to transfect with expression plasmids, will be an invaluable tool for future studies aimed at ABLV receptor identification.

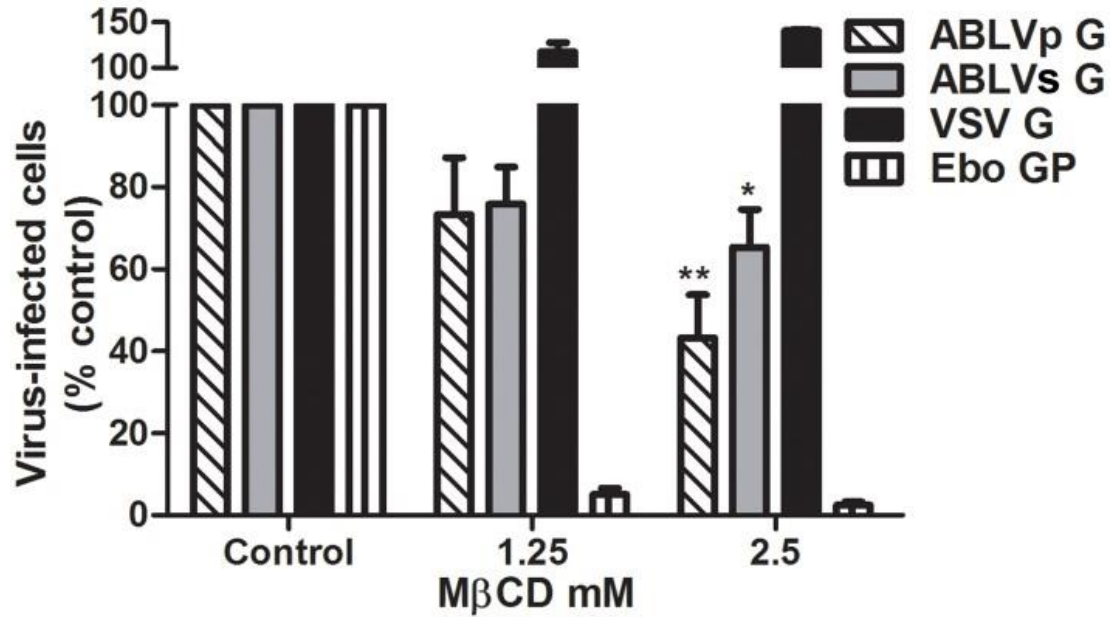


Figure 13. Disruption of lipid rafts significantly reduces ABLV G-mediated viral entry into 293T cells. 293T cell monolayers were treated with methyl- $\beta$ -cyclodextrin (M $\beta$ CD) diluted in OptiMEM® for 1 hr at 37°C. The drug was removed and the cells were washed three times with PBS to remove the drug. Cells were infected with rVSV (MOI=1) diluted in OptiMEM® supplemented with 4  $\mu$ g/ml mevinolin and analyzed as described in Figure 11A. rVSV viruses encoding Ebo GP and VSV G were used as positive and negative controls, respectively, to assess M $\beta$ CD activity. Results are expressed as percent virus-infected cells relative to that of untreated controls and represent three independent experiments; error bars are SEM. \*\*,  $p < 0.01$ ; \*,  $p < 0.05$ .

## **MATERIALS AND METHODS**

### **Cell lines and culture conditions**

The following cell lines were obtained from the American Type Culture Collection (ATCC): N2a (mouse neuroblastoma) (CCL-131); BHK (CCL-10); RK-13 (rabbit) (CCL-37); *Equus caballus* (horse) (CCL-57); *Tadarida brasiliensis* (bat) (CCL-88); MDBK (CCL-22); CHO-K1 (CCL-61). HEK293T cells were provided by Gerald Quinnan (Uniformed Services University). Cat embryo, HeLa-USU, PCI 13, and CCRT cell lines have been described (30; 33; 35). Vero cells were provided by Alison O'Brien (Uniformed Services University). HEK293F cells were purchased from Invitrogen Corp (Carlsbad, CA). N2a, BHK, MDBK, CHO-K1, 293T, HeLa-USU, Vero, and CCRT cells were maintained in Dulbecco's modified Eagle's medium (Quality Biologicals, Gaithersburg, MD) supplemented with 10% cosmic calf serum (CCS) (Hyclone, Logan, UT) and 2 mM L-glutamine (DMEM-10). PCI-13 cells were maintained in DMEM-10 supplemented with 10 mM HEPES (Quality Biologicals). Rabbit and horse cells were maintained in Eagle's minimal essential medium (EMEM) (Quality Biologicals) supplemented with 10% CCS, 2 mM L-glutamine (EMEM-10) supplemented with 1 mM sodium pyruvate. Bat cells were maintained in EMEM-10 supplemented with 0.85 g/L sodium bicarbonate. Cat embryo cells were maintained in RPMI 1640 (Quality Biologicals) supplemented with 10% CCS and 2 mM L-glutamine (RPMI-10). 293F cells were maintained in 293SFMI (Invitrogen) supplemented with 2 mM L-glutamine. All cell cultures were maintained at 37°C in a humidified 5% CO<sub>2</sub> atmosphere.

## Reagents and antibodies

OptiMEM® culture medium, Gibco® Freestyle™ 293 expression medium, and Gibco® anti-clumping agent were purchased from Invitrogen. Dextran sulfate sodium salt (5kDa) methyl- $\beta$ -cyclodextrin (M $\beta$ CD) and mevinolin were purchased from Sigma (St. Louis, MO). Stock solutions were prepared in water (dextran sulfate and M $\beta$ CD) or DMSO (mevinolin) and stored, as per manufacturer's recommendation. Polyclonal rabbit and mouse anti-sera against ABLV G were produced in mice and rabbits (Spring Valley Laboratories, Sykesville, MD). Goat anti-rabbit and anti-mouse IgG (H+L) horse radish peroxidase (HRP) conjugated secondary antibodies were purchased from Pierce, Rockford, IL). Mouse MAbs specific for mouse (catalog no. 60211A) and human (catalog no. 559043) neural cell adhesion molecule (NCAM) were purchased from BD Biosciences, San Jose, CA. Rabbit anti-nicotinic acetylcholine receptor alpha 4 polyclonal antibody [N1C1] (catalog no. GTX113653) was purchased from GeneTex Inc., Irvine, CA.

## Plasmids

Full-length ABLV G cDNA sequences for both the *Pteropus* (ABLVp G) (GenBank accession AF426309.1) and *Saccolaimus* (ABLVs G) (GenBank accession AAN63540.1) variants (111) were codon optimized and synthesized by Genart Inc., Germany and then cloned into the mammalian expression vector pCAGGS (197). The Rabies virus strain CVS-11 G sequence (GenBank accession EU352767.1) was synthesized by GenScript USA Inc., Piscataway NJ, and then cloned into a promoter-modified pcDNA3.1 vector. Plasmids that encode the vesicular stomatitis virus (VSV) nucleoprotein (N), phosphoprotein (P), and RNA polymerase (L) genes and a full-length



anti-genomic VSV Indiana cDNA clone that expresses Ebola Zaire virus GP and the fluorescent mCherry protein were kindly provided by Paul Bates (University of Pennsylvania). Recombinant VSV reporter plasmids that express maxGFP (Lonza Inc., Allendale, NJ) were constructed by replacing the mCherry gene, in the full-length anti-genomic VSV Indiana cDNA clone, with that for maxGFP. To construct full-length VSV-ABLV G- reporter plasmids (Appendix A), standard cloning techniques were used to replace the Ebola GP gene with ABLVs G and ABLVp G genes. VSV-GFP reporter plasmids that express Rabies CVS11 G and native VSV G (Indiana) were similarly constructed. All VSV-GFP reporter plasmids were then used to rescue replication competent recombinant VSV reporter viruses. An open reading frame (ORF) clone of the human neural cell adhesion molecule 1 (phNCAM1), transcript variant 2 (catalog no. RC207890) was purchased from OriGene Technologies, Inc., Rockville, MD.

### **Recovery, purification and titration of rVSV**

Recombinant reporter viruses were recovered using reverse genetics (148) with some modifications. HEK293T cells grown to 70-80% confluence in 6-well culture plates were transfected with plasmids encoding the recombinant VSV antigenomic RNA (2.5 µg) and the VSV N (2.5 µg), P (2.5 µg), and L (0.5 µg) genes under control of the bacteriophage T7 promoter using the Lipofectamine LTX transfection reagent. After 4-5 hrs, the transfection mix was removed and cells were infected with MVA-T7 (250) at a multiplicity of infection of 1. After 1 hr, the viral inoculum was removed, cells were washed 3 times with PBS, and fresh medium was added to the wells. After 48 hrs incubation at 37°C, cells and supernatants were collected and subjected to three rounds of freeze-thawing (-80°C, 37°C) to release cell-associated virus. Cell debris was pelleted

from the lysates by centrifugation for 5 min at 1300 x g. The clarified lysate was slowly filtered through a 0.22  $\mu$ m filter to remove the MVA-T7. Five hundred microliters of the lysate was then added to  $\sim 2 \times 10^6$  293T cells on a 6-well plate in 1.5 ml of DMEM-10. After 48 hrs, cells were observed for fluorescent reporter gene expression and CPE by microscopy (10X objective) (Appendix B).

To prepare viral stocks, 293T cells in T-162 flasks were infected with the rVSV virus and supernatants were collected 24-48 hrs later. Cell debris was removed by centrifugation at 2600 rpm for 10 min. Clarified supernatant was layered on top of 20% sucrose in TNE buffer (10 mM Tris, 135 mM NaCl, 2 mM EDTA) and centrifuged at 27,000 rpm for 2 hrs. Virus pellets were resuspended in 10% sucrose/TNE buffer. Viral titers were determined by adding serial 10-fold dilutions of virus to 293T cells grown on 96-well plates. At 24 hrs post-infection, fluorescent cells were counted under a fluorescent microscope and calculated as infectious units/ml (IU/ml).

### **Cell infection assays**

Target cells were infected with rVSV-GFP virus at a MOI=1. 18-20 hrs post-infection, cells were harvested and fixed with 2% paraformaldehyde (PFA). GFP expression, indicative of productive infection, was analyzed by either flow cytometry or a Nexcelom Vision cellometer (Nexcelom Bioscience LLC., Lawrence, MA) capable of fluorescence detection. The percent of infected cells was calculated by dividing the number of GFP positive cells by the total number of cells in the parent population and multiplying by 100. To determine the effect of anti-clumping agents on ABLV G-mediated infection, cells were treated with Gibco® anti-clumping agent (3-fold dilutions beginning at 1:150) or low molecular weight dextran sulfate (5kDa) (2-fold dilutions

beginning at 200 µg/ml) diluted in OptiMEM® serum free medium (Invitrogen). To determine whether cholesterol enriched lipid raft domains are important for ABLV entry, 293T cell monolayers were treated with the cholesterol sequestering drug methyl-β-cyclodextrin (MβCD) diluted in OptiMEM® for 1 hr at 37°C. Cells were then washed three times with PBS to remove the drug and infected with rVSV (MOI=1) diluted in OptiMEM® supplemented with 4 µg/ml mevinolin to prevent *de novo* synthesis of cholesterol. Pilot experiments indicated that 10 mM MβCD appeared toxic and cells detached from the culture plates; cells treated with 5 mM MβCD initially looked healthy, but cell viability was drastically reduced by the end of the experiment. In the final experiments 2.5 mM MβCD was used. To assess MβCD activity, rVSV viruses encoding Ebo GP and VSV G were used as positive and negative controls, respectively. In all drug treatment experiments, results are expressed as percent virus-infected cells relative to that of untreated controls

### **Virus binding assay**

Target cells ( $2 \times 10^5$ ) grown in 8-well chamber slides were washed once with cold PBS, and then fixed with 2% PFA for 30 min at room temperature. Fixed cell monolayers were blocked with 3% bovine serum albumin in PBS (BSA/PBS) for 1 hr at 37°C and then incubated with rVSV virus ( $5 \times 10^6$  IU) diluted in 200 µl BSA/PBS for 1 hr at 37°C. After washing with PBS (3X) cells were incubated overnight at 4°C with rabbit anti-ABLVs Gs polyclonal serum (1:10,000) to detect bound VSV-ABLVs G virus or with mouse anti-ABLVs Gs polyclonal serum (1:2000) to detect bound VSV-ABLVP G virus. Cells were washed with PBS (3X) and then incubated 1 hr at 37°C with either goat anti-rabbit IgG or goat anti-mouse IgG HRP conjugated antibodies (1:10,000) diluted in

200  $\mu$ l BSA/PBS. After three washes with PBS, cells were incubated with 200  $\mu$ l of ABTS [2,2'-azinobis (3-ethylbenzthiazolinesulfonic acid)] substrate (Roche, Indianapolis, IN) for 30 min at room temperature. The developed substrate (100  $\mu$ l) was transferred to a 96 well plate and absorbance was measured for each well at 405 nm, and the average value was calculated from duplicates. Target cells incubated with primary and secondary antibodies in the absence of virus were used as background controls.

### **Western blot analysis**

Cell lysates were prepared by treatment of  $5 \times 10^6$  cells of each population with lysis buffer (100 mM Tris-HCl (pH 8.0), 100 mM NaCl, 0.5% Triton X-100, 1X complete protease inhibitor cocktail (Roche)). Lysates were clarified by centrifugation at 13,200 rpm for 10 min at 4°C and 20  $\mu$ l of prepared lysate were loaded per well (an equivalent of  $1 \times 10^6$  cells/well) and analyzed by 4-12% Bis-Tris SDS PAGE (Invitrogen) under reducing conditions (2%  $\beta$ -mercaptoethanol in NuPAGE sample buffer). Following transfer to nitrocellulose paper, the blot was probed with rabbit anti-nicotinic acetylcholine receptor alpha 4 polyclonal antibody (1:1000), followed by incubation with HRP-conjugated goat anti-rabbit IgG (1:20,000).

### **Cell ELISA to detect NCAM surface expression**

Cell monolayers grown in 24-well plates were washed once with cold PBS, and then fixed with 2% PFA for 30 min at room temperature. Fixed cell monolayers were blocked with 3% bovine serum albumin in PBS (BSA/PBS) for at least 1 hr at 37°C and then incubated overnight at 4°C with mouse anti-NCAM mAbs (3  $\mu$ g/ml) diluted in 250  $\mu$ l BSA/PBS. Cells were washed three times with PBS and then incubated 1 hr at 37°C with HRP-conjugated goat anti-mouse IgG (1:10,000) diluted in 250  $\mu$ l BSA/PBS. After

three washes with PBS, cells were incubated with 300 µl of ABTS substrate for 30 min at room temperature. The developed substrate (100 µl) was transferred to a 96 well plate and absorbance was measured for each well at 405 nm, and the average value was calculated from duplicates. Target cells incubated with secondary antibody alone were used as background controls.

### **Expression of human NCAM1 in CHOK1 cells**

CHOK1 cells were grown overnight to 60-80% confluence in 24 well culture plates. Cells were transfected with 0.5 µg of phNCAM1 plasmid or empty vector (mock) (8 wells each) using the Lipofectamine LTX transfection reagent (Invitrogen) according to the manufacturer's protocol. Twenty four hours post-transfection, cells were infected in duplicate with rVSV virus and analyzed as described above. Expression of hNCAM1 was assessed 24 hrs post transfection by cell ELISA.

### **Statistical analysis**

Student's *t-test* was used to evaluate the statistical significance levels of the data, with  $p < 0.05$  indicating statistical significance.

### **Acknowledgements**

We thank Dr. Ross Lunt at CSIRO Livestock Industries, Australian Animal Health Laboratory for providing the *Saccolaimus* and *Pteropus* bat brain tissues used for the initial cloning of *Saccolaimus*- and *Pteropus*-derived ABLV G and Dr. Paul Bates at the University of Pennsylvania for kindly providing the VSV full-length and helper plasmids. This work was supported by NIH grant AI057168 to C.C.B.

### **CHAPTER 3: Host cell virus entry mediated by Australian bat lyssavirus envelope G glycoprotein occurs through a clathrin-mediated endocytic pathway that requires actin and Rab5.**

#### **ABSTRACT**

Australian bat lyssavirus (ABLV), a zoonotic virus circulating in both pteropid fruit bats and insectivorous bats in mainland Australia, has caused three fatal human infections manifested as acute neurological disease similar to clinical rabies. ABLV infects host cells through receptor-mediated endocytosis and subsequent pH-dependent fusion mediated by its single envelope glycoprotein (G), but the specific host factors and pathways involved in ABLV entry have not been determined. Here we examined ABLV internalization into HEK293T cells using maxGFP-encoding recombinant vesicular stomatitis viruses (rVSV) that express ABLV G glycoproteins. Using a combination of chemical and molecular approaches, we provide evidence that the predominant pathway utilized by ABLV to enter HEK293T cells is clathrin-mediated and that actin is required for productive infection. We also show that ABLV-G mediated entry is Rab5 dependent, but Rab7 and Rab11 independent, indicating that ABLV likely enters cells through an early endosomal compartment.

#### **INTRODUCTION**

Australian bat lyssavirus (ABLV) is a rhabdovirus endemic in Australian bat populations that is capable of causing a fatal neurological disease in humans indistinguishable from clinical rabies. There are two genetically distinct variants of ABLV, the *Pteropus* strain (ABLVp) which circulates in all four species of frugivorous flying foxes (genus *Pteropus*) present on mainland Australia, and the *Saccolaimus* strain

(ABLVs) present in the insectivorous yellow-bellied sheath-tail bat (genus *Saccolaimus*). ABLV has caused three fatal human infections, the most recent in February of 2013, and each manifested as acute encephalitis; however, incubation periods were variable, ranging from approximately 5 weeks to over 2 years (4; 7; 116). In May 2013, ABLV infected two horses, representing the first spillover of ABLV into a terrestrial species other than humans (8). Although the number of ABLV spillover events have thus far been scarce and limited to only two terrestrial species, *in vitro* tropism studies indicate that the unknown ABLV receptor(s) is broadly conserved among mammals and suggests that terrestrial species other than humans and horses may be susceptible to ABLV infection (277).

ABLV is an enveloped, bullet-shaped, non-segmented, negative sense RNA virus belonging to the genus *Lyssavirus* of the family *Rhabdoviridae* within the order *Mononegavirales*. There are currently 12 species of lyssaviruses and 3 additional species that have not yet been classified (53); ABLV is most closely related to classical rabies virus (RABV), the prototype member of the *Lyssavirus* genus. Lyssaviruses have a single envelope glycoprotein (G) that mediates all internalization steps from cell attachment to pH-dependent fusion with the host cell membrane (100). The lyssavirus G glycoprotein is a key determinant of the neurotropic and neurovirulent properties of lyssaviruses (189).

Rhabdoviruses gain access to the host cell cytoplasm, the site of viral replication, by receptor-mediated endocytosis and subsequent low pH-dependent fusion (184; 280). Viruses internalized by receptor-mediated endocytosis predominantly use trafficking pathways mediated either by clathrin or caveola, but several alternative pathways,

including macropinocytosis, have been reported [reviewed in (183)]. Different viruses utilize different pathways for entry and the endocytic pathway taken by a given virus largely depends on the host receptor it interacts with. Clathrin-mediated endocytosis (CME) is the most commonly utilized pathway in virus entry and is the only pathway reported to be utilized by different rhabdoviruses, including VSV, RABV, and infectious hematopoietic necrosis virus (IHNV) (160; 201; 247; 248). The initial virus-host cell receptor interaction induces de novo clathrin-coated pit (CCP) formation at the site of viral binding (67; 78; 138; 225). Both VSV and RABV were shown to internalize through partially coated clathrin pits that require actin to complete the internalization process (67; 201). Entry of IHNV was also shown to be actin-dependent (160). After invagination, the CCP buds from the plasma membrane forming a clathrin-coated vesicle. The clathrin coat is then shed, enabling the uncoated vesicle to traffick to and fuse with the early endosome. The entry pathway of ABLV has not been examined; however, we recently demonstrated that disruption of lipid rafts via sequestration of cholesterol by methyl- $\beta$ -cyclodextrin (M $\beta$ CD) treatment significantly reduced ABLV G-mediated entry into human embryonic kidney (HEK) 293T cells (277). This finding is compatible with a clathrin- or caveola-dependent entry pathway for ABLV; acute cholesterol depletion with M $\beta$ CD has been shown to inhibit CCP budding (245) and caveolae formation is strictly dependent on cholesterol (210).

Once internalized by endocytosis, the acidic environment of the endosome triggers the conformational changes in the G glycoprotein that lead to fusion of the viral and endosomal membranes and the subsequent release of the viral genome into the cytosol. For most enveloped viruses, membrane fusion occurs either in early endosomes



(EEs) (pH 6.5-6.0) or late endosomes (LEs) (pH 6.0-5.00) [reviewed in (109; 183)]. Recycling endosomes (REs) are responsible for directing vesicular cargo back to the plasma membrane and have been shown to be involved in some virus budding pathways (222) and particle assembly pathways [reviewed in (42)]. The use of dominant negative (DN) Rab GTPases specific for EEs, LEs, and REs, have been used extensively to determine virus exit points from the endosomal network (64; 138; 140; 187; 199). Overexpression of the mutant Rab proteins in host cells elicits a dominant negative effect over the endogenous wild-type protein; thus, a virus that requires a specific endosome for trafficking and fusion will be adversely affected by the overexpression of a DN Rab protein specific for that endosome. Lyssaviruses require vacuolar acidification for G glycoprotein-mediated viral and endosomal membrane fusion (184), but few studies have examined the endosomal trafficking of these viruses. RABV G was shown to co-localize with Rab5a, a marker for EEs, but not Rab9, a marker for LEs; this same study demonstrated that internalization of an anti-RABV G antibody/RABV G complex was dependent on the presence of functional Rab5a suggesting that RABV G fuses with EEs (242). Furthermore, the optimal pH for RABV G-mediated fusion is pH 5.8-6.0, which correlates with the pH of EEs (99; 183). The membrane fusion requirements for ABLV have not been investigated.

In the present study, we used fluorescent protein-encoding recombinant vesicular stomatitis viruses (rVSV) that express ABLV G envelope glycoproteins to examine the ABLV entry pathway using both chemical and molecular approaches. Results indicate that ABLV is internalized into 293T cells by a clathrin-dependent pathway that like VSV, IHNV, and RABV, is dependent upon actin polymerization. Moreover, we show that

ABLV G-mediated entry is Rab5-dependent, but Rab7-independent, indicating that ABLV G-mediated fusion occurs within the early endosomal compartment.

## **RESULTS AND DISCUSSION**

### **Dynamin is required for ABLV G-mediated viral entry**

To examine the endocytic pathway utilized by ABLV for host cell internalization, we used maxGFP-encoding replication competent recombinant vesicular stomatitis viruses (rVSV) that express ABLV G glycoproteins (277). This approach is advantageous over using WT ABLV because not only are rVSV-ABLV G viruses safer and easier to manipulate than WT ABLV, but the incorporation of GFP into the viral genome eliminates the need for traditional fluorescent antibody staining to detect infected cells. We chose HEK293T cells as the cell culture model to investigate the ABLV entry pathway. HEK293 cells, an immortalized cell line derived from primary human embryonic kidney cells in the late 1970s (108), have in recent years been shown to express several genes that are typically found only in cells of neuronal origin, displaying neuronal gene expression patterns similar to those of early differentiating neurons or neuronal stem cells (119; 237). Moreover, a recent study demonstrated that HEK293 cells were just as sensitive as murine neuroblastoma cells for the rapid isolation of street RABV from brain tissue of suspected RABV infected animals (167). Additionally, we previously demonstrated the high susceptibility of HEK293T cells to ABLV G-mediated viral infection (277). The aforementioned neuronal characteristics of HEK293 cells combined with their ease of handling, robust growth rate, and amenability to transfection, make them an ideal model to study ABLV entry.

We first examined whether dynamin was required for ABLV entry. Dynamin, a GTPase that is responsible for the scission of endocytic vesicles from the plasma membrane (19), plays a critical role in several endocytic pathways including, but not limited to, CME (180), CavME (294), and some types of macropinocytosis (135; 192). In contrast, dynamin is dispensable for the macropinocytosis of vaccinia virus (VV) (181), the GPI-anchored protein-enriched endosomal compartment (GEEC) pathway (226), and a novel non-clathrin, non-caveolar entry pathway utilized by lymphocytic choriomeningitis virus (LCMV) (207). Therefore, the effect of dynamin inhibition on viral entry serves as an initial criterion for endocytic pathway classification.

HEK293T cells were pretreated with dynasore, a specific and potent inhibitor of dynamin (166), for 30 min at 37°C and then infected with rVSV-ABLV G reporter viruses; rVSV that expresses VSV G was included as a positive control. Dynasore treatment of HEK293T cells inhibited ABLV G-mediated viral entry in a dose dependent manner, with > 80% inhibition at the highest concentration (Figure 14A). Impaired virus infection was not due to drug toxicity as cells were > 90% viable at the end of the experiment (Figure 14B). These results indicate that ABLV G-mediated entry into HEK293T cells follows a dynamin-dependent pathway.

### **Inhibition of clathrin-mediated endocytosis inhibits ABLV G-mediated viral entry**

CME is the endocytic route most frequently utilized by viruses to gain entry into host cells. Other rhabdoviruses such as VSV, IHNV, and RABV have all been reported to utilize CME for entry (160; 201; 247; 248). To assess whether clathrin is required for ABLV entry, we first employed chemical inhibition studies using chlorpromazine, a drug that inhibits CME by blocking the assembly of clathrin coated pits (273). HEK293T cells

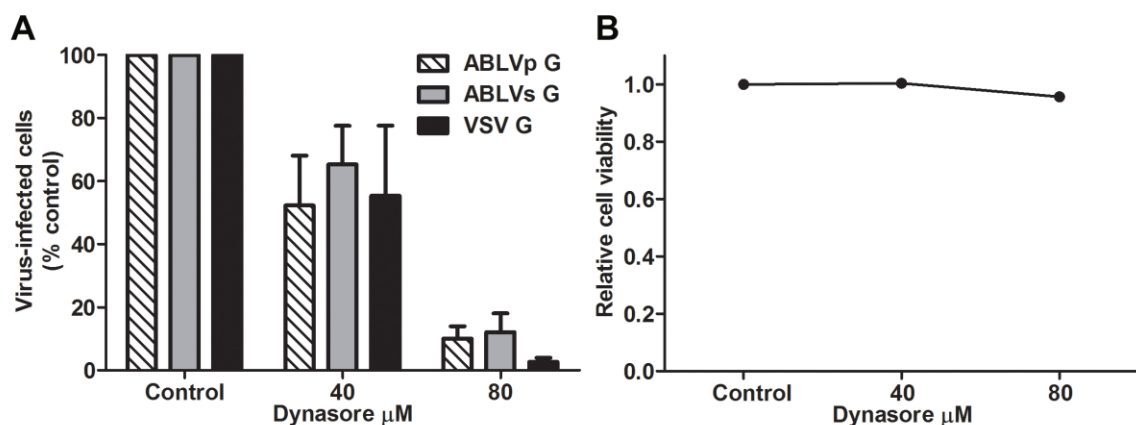


Figure 14. Chemical inhibition of dynamin inhibits ABLV G-mediated viral entry into HEK293T cells. (A) HEK293T cell monolayers were pretreated with dynasore diluted in OptiMEM® for 30 min at 37°C. Cells were then infected with max-GFP encoding rVSV reporter viruses (MOI=1). Cells were harvested 20 hrs post infection, fixed with 2% paraformaldehyde and then analyzed for GFP expression (indicative of productive infection). GFP positive cells were counted with a Nexcelom Vision automated cell counter with fluorescence detection and the percent of virus-infected cells was calculated by dividing the number of GFP positive cells by the total number of cells counted. Under these experimental conditions, a MOI of 1 resulted in the productive infection of 60-70% of untreated cells (control). Drug was maintained for the entire course of infection and its effect on cell viability (B) was determined by trypan blue staining. Reporter viruses that express VSV G were included as a positive control to assess dynasore activity. Results are expressed as percent virus-infected cells relative to that of untreated controls and represent 3 independent experiments; error bars are standard error of the mean (SEM).

were pretreated with chlorpromazine at the indicated concentrations for 30 min at 37°C prior to infection with rVSV-ABLV G reporter viruses in the presence of drug; rVSV-VSV G was included as a positive control. To avoid cell toxicity associated with long-term exposure to chlorpromazine, cells were harvested 8 hrs post infection and analyzed for GFP expression. Chlorpromazine inhibited ABLV G-mediated entry in a dose-dependent manner, with >70% inhibition at the highest concentration (Figure 15A). To monitor potential toxic effects of chlorpromazine treatment, cell viability was assessed in parallel. Under these experimental conditions, no toxicity was noted; greater than 90% of cells treated with the highest concentration were viable at the end of the experiment (Figure 15B).

To confirm CME as an entry pathway for ABLV, we next examined the effect of the expression of a dominant negative (DN) mutant (EH29) of the CME effector protein Eps15. The EH29 mutant blocks CME by preventing clathrin-coated pit formation and does not affect non-clathrin pathways; Eps15 mutant DIIIΔ2, which has no effect on clathrin-coated pit assembly, was included as a negative control for the inhibition of CME (22-24). HEK293T cells were transfected with plasmids encoding eGFP alone or eGFP-tagged Eps15 mutants for 18 hrs; transfection rates, as measured by eGFP expression, consistently reached 50-60% (data not shown). Cells were then infected with VSVΔG-RFP pseudoviruses that express ABLV G or VSV G at a MOI=2. After 20 hrs the cells were harvested and analyzed for RFP expression. As expected, compared to the eGFP control, DIIIΔ2 did not interfere with ABLV entry (Figure 16A); however, ABLV G-mediated viral entry was significantly inhibited by EH29 (60%) compared to eGFP controls (Figure 16B). The uptake of cholera toxin B subunit (CTX-B), which is

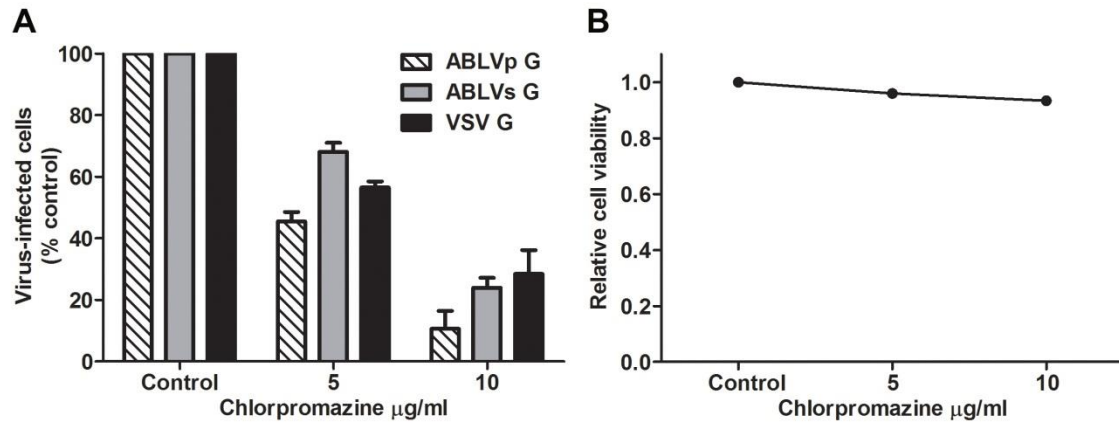
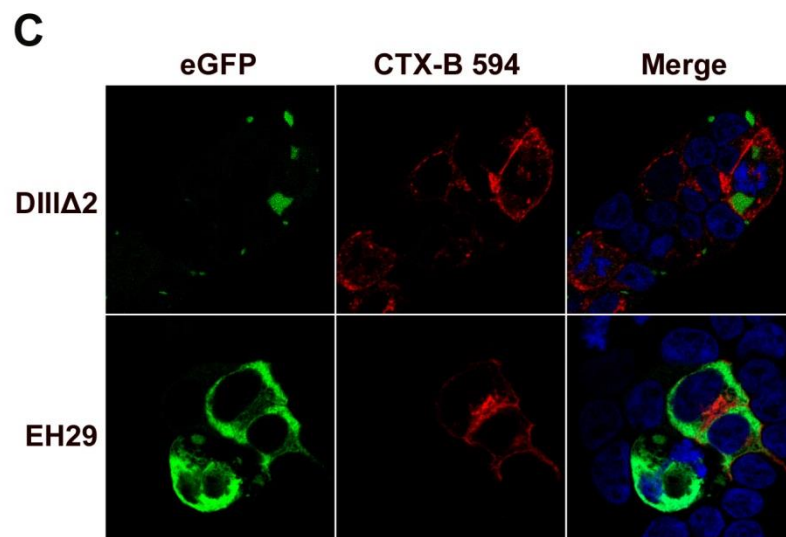
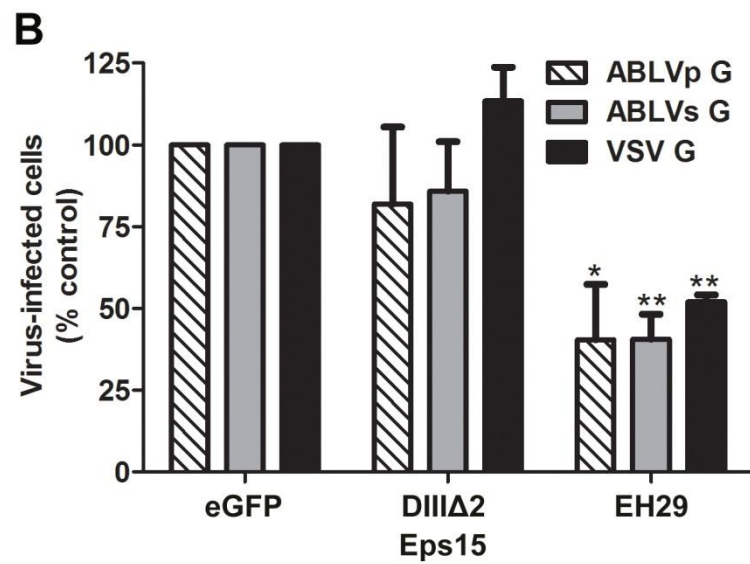
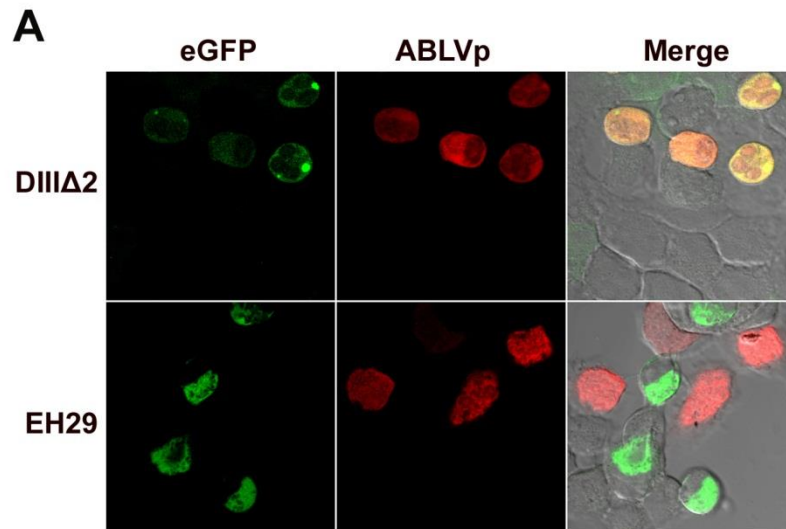


Figure 15. Chemical inhibition of CME inhibits ABLV G-mediated viral entry into HEK293T cells. (A) HEK293T monolayers were pretreated with chlorpromazine diluted in OptiMEM® for 30 min at 37°C. Cells were then infected with rVSV (MOI=3) for 8 hrs and then analyzed as described in Figure 14. Under these experimental conditions, a MOI of 3 resulted in the productive infection of 50-60% of untreated cells (control). Drug was maintained for the entire course of infection and its effect on cell viability (B) was determined by trypan blue staining. rVSV-VSV G reporter virus was included as positive control. Results are expressed as percent virus-infected cells relative to that of controls and represent 3 independent experiments; error bars are SEM.

Figure 16. Inhibition of CME with a DN form of Eps15 significantly reduces ABLV G-mediated viral entry into HEK293T cells. HEK293T cells transfected with an eGFP control plasmid or eGFP-tagged Eps15 mutants were infected with VSVΔG-ABLV G\* or –VSV G\*-RFP pseudoviruses at a MOI=2 for 20 hrs and then analyzed for RFP expression as described in Figure 14. Under these experimental conditions, a MOI of 2 resulted in the productive infection of 25-30% of cells transfected with the eGFP control plasmid. DIIIΔ2, a mutant of Eps15 that does not affect clathrin coated pit formation; EH29, DN Eps15 mutant. (A) Representative microscopic fields of cells transfected with each Eps15 construct and infected with VSVΔG-ABLVp G\*- RFP pseudovirus. Similar results were obtained for ABLVs G-expressing pseudovirus (not shown). (B) Quantitation of virus-infected cells. A minimum of 1000 cells were counted for each sample per experiment. VSVΔG- VSV G\* was included as positive control. Results are expressed as percent virus-infected cells relative to that of controls and represent 3 independent experiments; error bars are SEM. Significance of effect on virus infection was determined using Student's *t-test*. \*\*,  $p < 0.0005$ ; \*,  $p < 0.005$ . (C) Cholera toxin B (CTX-B) subunit uptake into HEK293T cells is not inhibited by EH29. To verify the specificity of EH29 to inhibit CME, 18 hrs post transfection HEK293T cell monolayers grown on 12 mm coverslips were incubated with Alexa Fluor 594-labeled CTX-B (10  $\mu$ g/ml) for 1 hr at 37°C. Cells were then washed twice with PBS, fixed and imaged. Images were taken by confocal microscopy with a mid z-section shown. Nuclei were stained with DAPI (4',6-diamidino-2-phenylindole, dihydrochloride).



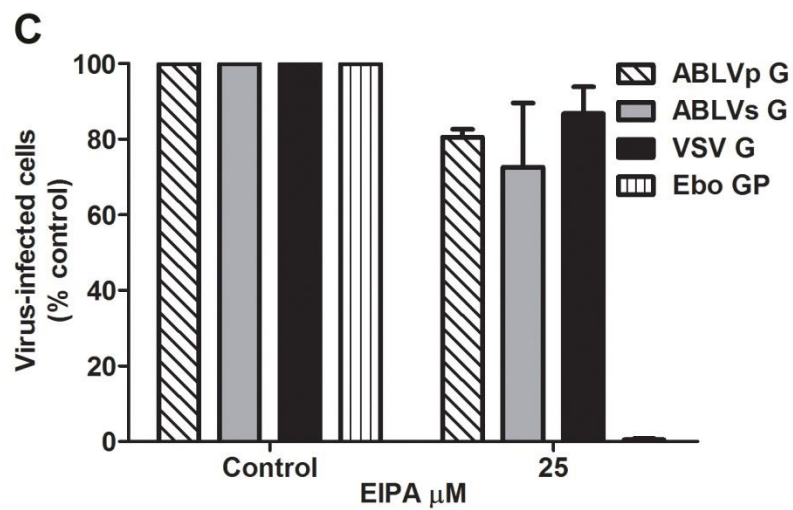
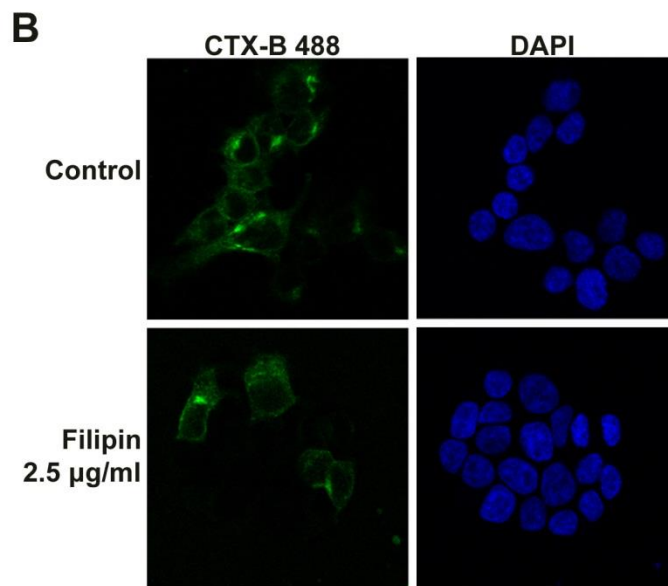
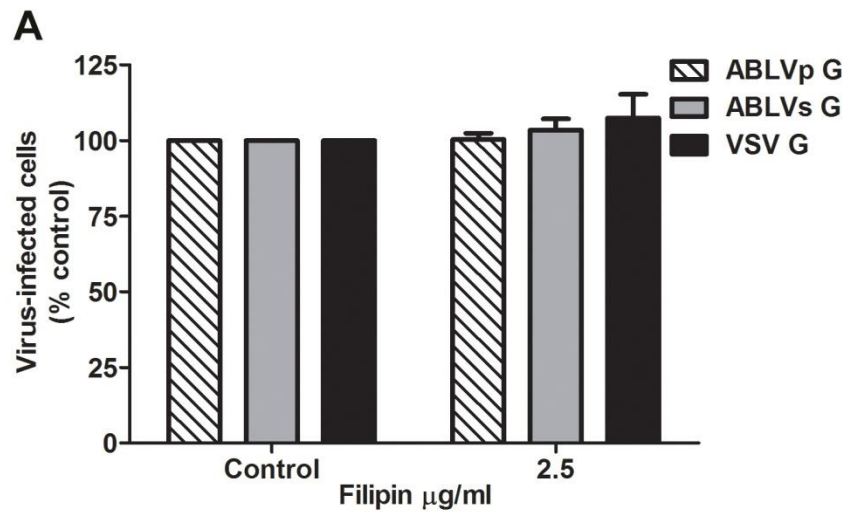


endocytosed by CavME (198), was not inhibited by EH29, demonstrating the specificity of EH29 in inhibiting CME (Figure 16C). Taken together, these data suggest that ABLV G-mediated viral entry into HEK293T cells occurs through a clathrin-dependent pathway.

#### **Caveolar-dependent endocytosis and macropinocytosis are not involved in ABLV G-mediated viral entry**

Some viruses, such as Ebola virus (3; 27; 195; 227), influenza A (57; 225; 238), and reovirus (232), have been reported to utilize more than one type of endocytic pathway to gain entry into host cells. Additionally, we previously showed that the disruption of lipid rafts through cholesterol depletion significantly reduced ABLV G-mediated entry into HEK293T cells (277), a finding compatible with a clathrin- or caveolae-dependent entry pathway. To test the possible contribution of pathways other than CME to ABLV G-mediated viral entry, HEK293T cells were treated with the chemical inhibitors filipin and EIPA (5-(N-ethyl-N-isopropyl amiloride)) to inhibit CavME and macropinocytosis, respectively. A recombinant VSV reporter virus expressing VSV G and fluorescently labeled CTX-B were included as a negative and positive control, respectively for CavME (198); rVSV-EboGP reporter virus was included as a positive control for macropinocytosis (227). Pretreatment of HEK293T cells with filipin, which disrupts CavME by specifically binding to cholesterol abundant in caveolae (220; 221), did not inhibit ABLV G-mediated entry (Figure 17A), but did significantly decrease the uptake of CTX-B into HEK293T cells (Figure 17B). Similarly, pretreatment of HEK293T cells with EIPA, a potent inhibitor of Na<sup>+</sup>/H<sup>+</sup> exchanger activity required for macropinosome formation (182; 279), had no effect on ABLV G-mediated entry but, as previously reported, drastically inhibited Ebo GP-mediated viral entry (>98%) (Figure 17C) (195; 227). Taken together, these data indicate that CavME

Figure 17. CavME endocytosis and macropinocytosis are not required for ABLV G-mediated viral entry. (A) Chemical inhibition of CavME. HEK293T cell monolayers were pretreated with filipin diluted in OptiMEM® for 1 hr at 37°C. Cells were then infected with rVSV (MOI=1) for 20 hrs and analyzed as described in Figure 14. Drug was maintained for the entire course of infection. (B) Cholera toxin B (CTX-B) subunit uptake is inhibited by filipin. Following pretreatment with filipin as described in (A), HEK293T cell monolayers grown on 12 mm coverslips were incubated with Alexa Fluor 488-labeled CTX-B (10 µg/ml) for 1 hr at 37°C. Cells were then washed twice with PBS, fixed and imaged. Images were taken by confocal microscopy with a mid z-section shown. Nuclei were stained with DAPI, (4',6-diamidino-2-phenylindole, dihydrochloride) (C) Chemical inhibition of macropinocytosis. HEK293T cell monolayers were pretreated with EIPA diluted in OptiMEM® for 1 hr at 37°C. Cells were then infected with rVSV (MOI=1) for 20 hrs and analyzed as described in Figure 14. rVSV encoding VSV G (MOI=1) or EboGP (MOI=15) were included as negative and positive controls, respectively, to assess EIPA activity. Drug was maintained for the entire course of infection. For (A) and (C) results are expressed as percent virus-infected cells relative to that of untreated controls and represent 3 independent experiments; error bars are SEM. Under these experimental conditions, the chosen MOIs resulted in the productive infection of 60-70% of untreated cells. EIPA, 5-(N-ethyl-N-isopropyl) amiloride.



and macropinocytosis do not contribute to ABLV G-mediated entry into HEK293T cells. This is in agreement with previous studies that show that CavME and macropinocytosis do not play a role in the entry of other rhabdoviruses (160; 201; 227).

### **Actin polymerization is required for ABLV G-mediated viral entry**

Recent studies have revealed that the rhabdoviruses VSV, RABV, and IHNV are internalized through clathrin-dependent pathways that are also actin-dependent (67; 160; 201). To determine whether ABLV entry is also dependent upon actin, HEK293T cells were pretreated with the actin depolymerizing drug latrunculin B (LatB) at the indicated concentrations for 1 hr at 37°C prior to infection with rVSV-ABLV G reporter viruses in the presence of drug; rVSV-VSV G was included as a positive control. To avoid cell toxicity associated with long-term exposure to LatB, cells were harvested 8 hrs post infection and analyzed for GFP expression. LatB significantly inhibited ABLV G-mediated entry at all concentrations tested with greater than 65% and 90% inhibition of ABLVs G- and ABLVp G-mediated entry, respectively, at the highest concentration tested (Figure 18A). Entry inhibition was not due to drug toxicity as cell viability remained greater than 85% at the highest dose of LatB (Figure 18B).

Actin is not required for the clathrin-mediated uptake of transferrin, the classical ligand used to study CME (37; 95; 201); however, it is required for CME of large cargos such as viruses and bacteria (25; 63; 67; 201; 271). VSV and RABV in particular have been shown to be internalized by partially coated pits that require actin polymerization for envelopment; this dependence on actin is dictated by the size of the particle, as truncated defective-interfering particles of VSV do not require actin (67; 68; 201). Thus,

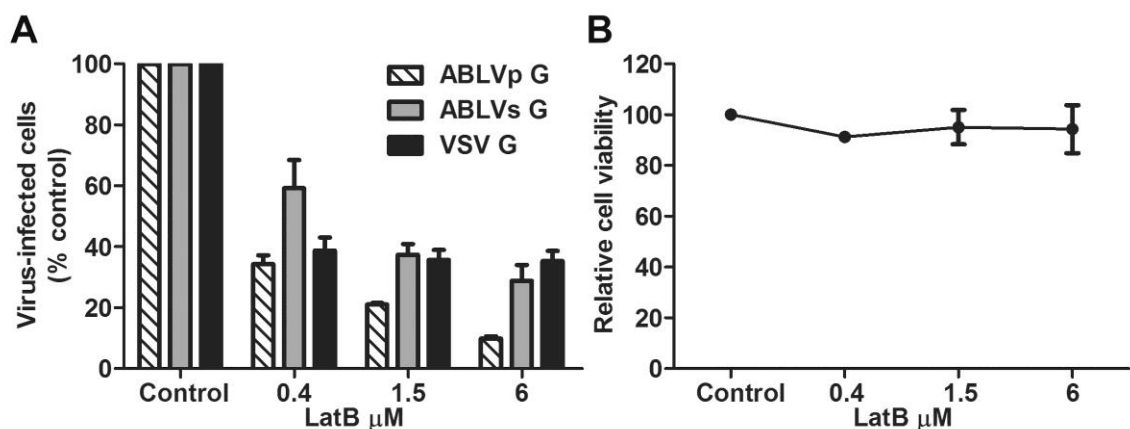


Figure 18. Actin is required for ABLV G-mediated viral entry. (A) HEK293T cell monolayers were pretreated with latrunculin B (LatB) diluted in OptiMEM® for 1 hr at 37°C. Cells were then infected with max-GFP encoding rVSV reporter viruses (MOI=3). Cells were harvested 8 hrs post infection and analyzed as described in Figure 14. Under these experimental conditions, a MOI of 3 resulted in the productive infection of at least 50% of untreated cells. Drug was maintained for the entire course of infection and its effect on cell viability (B) was determined by trypan blue staining. Reporter viruses that express VSV G were included as a positive control to assess LatB activity. Results are expressed as percent virus-infected cells relative to that of untreated controls and represent 3 independent experiments; error bars are standard error of the mean (SEM).

given the shared particle morphology of all rhabdoviruses, it is not surprising that ABLV entry is also actin-dependent. The mechanism by which cell surface bound viral particles induce actin recruitment to the CCPs is not completely understood. However, recent studies have demonstrated that plasma membrane tension induces the actin dependence of clathrin coat assembly; in the case of tense or rigid membranes, actin polymerization may be required to produce sufficient force to complete membrane deformation into a coated pit prior to the recruitment of dynamin and subsequent vesicle budding (38; 255). It has been postulated that upon cell surface binding, the viral particles themselves induce membrane tension, thus leading to the recruitment of actin to the forming clathrin-coated vesicle (38; 67; 68; 201).

#### **Rab5, but not Rab7 or Rab11, is required for ABLV G-mediated viral entry**

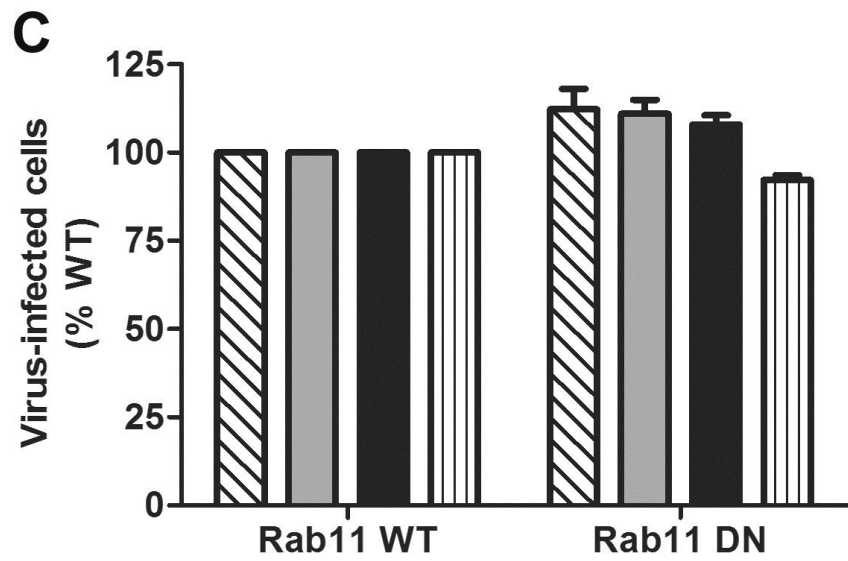
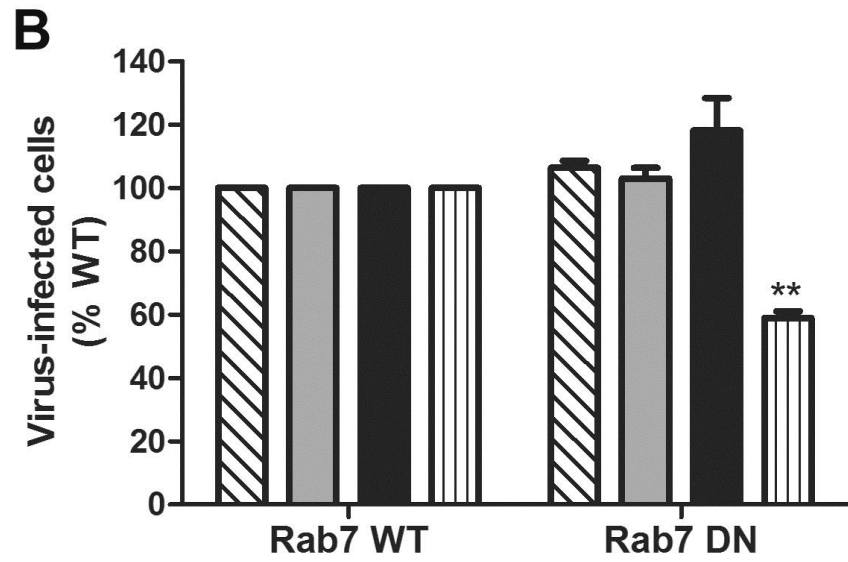
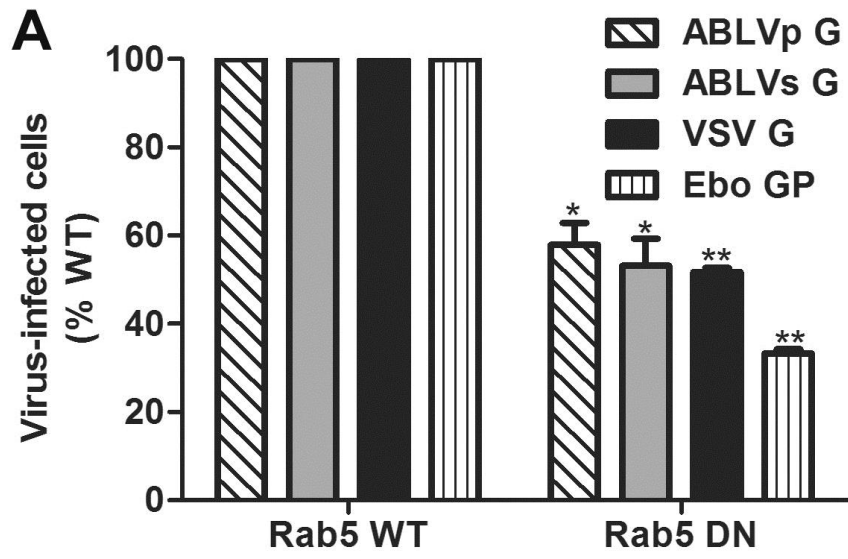
The above data indicate that ABLV G-mediated viral entry into HEK293T cells occurs through a clathrin- and actin-dependent pathway. To investigate the subsequent trafficking route to the site of cytosol penetration, we examined the roles in ABLV entry of the small GTPases Rab5, Rab7, and Rab11, which are involved in vesicular trafficking to early, late, and recycling endosomes, respectively (86; 105; 266). HEK293T cells were transfected with RFP-tagged dominant negative (DN) forms of Rab5 (S34N) (156), Rab7 (T22N) (86), and Rab11 (S25N) (266), which prevent the fusion of endocytic vesicles with early endosomes, prevent movement from early to late endosomes, and prevent movement from early to recycling endosomes, respectively. Transfected cells were infected with rVSV-ABLV G 18-20 hrs post-transfection. Cells were fixed 8 hrs later and analyzed for GFP expression. Reporter viruses that express VSV G and Ebo GP were included as positive controls for Rab5 and Rab7, respectively (187; 227).

As shown in Figure 19A, expression of the Rab5 DN significantly reduced ( $p<0.005$ ) ABLV G-mediated viral entry compared to Rab5 WT, with greater than 40% inhibition for both ABLV variants (Figure 19A) and as previously reported, both VSV G- and Ebo GP-mediated entry was significantly inhibited by Rab5 DN ( $p<0.0001$ ) (Figure 19A) (138; 187; 227). Expression of Rab7 DN and Rab11 DN did not inhibit ABLV G-mediated viral entry, but rather enhanced infection compared to Rab7 and 11 WT plasmids (Figure 19B-C); however, the increase in infectivity was not statistically significant. Expression of the Rab7 DN was sufficient to disrupt trafficking to late endosomes as Ebo GP-mediated viral entry was significantly inhibited ( $p<0.0001$ ) (Figure 19B) (227). In agreement with previous studies, VSV G-mediated viral entry was not inhibited by DN mutants of Rab7 and 11 (Figure 19B-C) (187); similar to results for ABLV G-mediated infection, the apparent increased VSV infectivity of these cells compared to cells expressing WT plasmids was not statistically significant. Rab11 is required for the transport of cargo from the Trans-Golgi network to the plasma membrane (58) and has been shown to play roles in virus assembly/budding (42; 222); however, consistent with our findings, there have been no reports of Rab11 playing a role in viral entry. Nevertheless, both VSV G and RABV G have been shown to colocalize with Rab11 (58; 242) and the expression of the Rab11 DN has previously been shown to lead to accumulation of VSV G in the Golgi (58). These studies suggest that Rab11 may play a post-entry role in trafficking of newly synthesized G from the Golgi to the plasma membrane. It is possible that a similar role for Rab11 in ABLV G trafficking exists, however this has not been investigated. Collectively, these data indicate that ABLV G-mediated fusion of viral and host cell membranes is triggered upon delivery to early

Figure 19. Effect of dominant negative Rab GTPases on ABLV G-mediated viral entry.

HEK293T cells expressing dsRed-tagged WT and DN Rab5, Rab7, and Rab11 were infected with maxGFP encoding rVSV that express ABLVp G, ABLVs G, or VSV G at a MOI=3 for 8 hrs or with rVSV that expresses EboGP at a MOI=15 for 20 hrs and then analyzed as described in Figure 14. At these MOIs, 40-50% of cells transfected with WT Rab plasmids were infected with rVSV viruses. Results are expressed as percent virus-infected cells relative to that of WT Rab controls and represent 3 independent experiments; error bars are SEM. (A) Rab5. (B) Rab7. (C) Rab11. \*\*,  $p<0.0001$ ; \*,  $p<0.005$ .





endosomes and that productive ABLV infection does not require transfer to late or recycling endosomes.

## CONCLUSIONS

In summary, we have used both chemical and molecular approaches to examine the entry pathway utilized by ABLV for internalization into HEK293T cells. The results presented here reveal that ABLV G-mediated viral entry primarily follows a clathrin-dependent pathway that, similar to other rhabdoviruses including RABV, requires actin for complete particle envelopment. Moreover, we show that productive ABLV infection is dependent upon Rab5, but not Rab7 or Rab11, indicating that the mildly acidic environment of the early endosome is sufficient to trigger ABLV G-mediated viral and endosomal membrane fusion and subsequent release of the viral genome into the cytosol.

The identification of specific entry requirements for a given virus is an important first step towards the development of antivirals capable of blocking infection. This study is the first to identify specific host factors required for ABLV entry. Our ongoing studies are aimed at identifying additional host factors required for ABLV infection using a high-throughput siRNA screening approach. Based on the results presented here, which indicate that ABLV follows a similar entry pathway as RABV (201), it is possible that the identification of host factors required for ABLV infection will provide potential targets for the development of therapeutics with the potential of broadspectrum activity against other lyssavirus species.

## **MATERIALS AND METHODS**

### **Cells and viruses**

HEK293T cells were provided by Gerald Quinnan (Uniformed Services University) and were maintained in Dulbecco's modified Eagle's medium (DMEM; Quality Biologicals, Gaithersburg, MD) supplemented with 10% cosmic calf serum (CCS) (Hyclone, Logan, UT) and 2 mM L-glutamine (DMEM-10). Recombinant maxGFP expressing vesicular stomatitis viruses (rVSV) that express ABLV G, Ebola Zaire GP, and VSV (Indiana) G glycoproteins have been previously described (277). VSVΔG-G\*-RFP pseudovirus stocks were kindly provided by Michael Whitt (University of Tennessee). VSVΔG pseudoviruses complemented with ABLV G glycoproteins were prepared by transfecting HEK293T cells with expression plasmids that express ABLVs G and ABLVp G (277). Twenty four hours after transfection, cells were infected with VSVΔG-G\*-RFP at a multiplicity of infection (MOI) of 1 for 1 hr at 37°C. The cells were then washed three times with phosphate buffered saline (PBS) and DMEM-10 was added. After 24 hrs, culture supernatant was collected and cell debris was removed by centrifugation at 2,600 rpm for 10 min. Clarified supernatant was layered on top of 20% sucrose in TNE buffer (10 mM Tris, 135 mM NaCl, 2 mM EDTA) and centrifuged at 27,000 rpm for 2 hrs. Pseudovirus pellets were resuspended in 10% sucrose/TNE buffer. Viral titers were determined by adding serial 10-fold dilutions of virus to HEK293T cells grown on 96-well plates. At 24 hrs post-infection, fluorescent cells were counted under a fluorescent microscope and calculated as infectious units/ml (IU/ml).

## **Drug treatments and cell infection assays**

All chemical inhibitors were purchased from Sigma (St. Louis, MO). Stock solutions were prepared in water (chlorpromazine) or DMSO (dynasore, filipin, EIPA [5-(N-ethyl-N-isopropyl) amiloride], and latrunculin B) and stored, as per manufacturer's recommendation. HEK293T cells were pretreated for 30 min in the presence of dynasore or chlorpromazine or for 1 hr in the presence of filipin, EIPA, or latrunculin B (LatB) at the indicated concentrations and then infected with rVSV viruses (rVSV-ABLV G and -VSV G, MOI=1 or 3 for 20 hrs and 8 hrs infections, respectively; rVSV-EboGP, MOI=15). MOIs were chosen such that 60-70% or 50-60% of untreated (control) cells were productively infected after 20 hrs and 8 hrs, respectively. All drugs and viruses were diluted in OptiMEM® (Invitrogen, Carlsbad, CA) and drugs were maintained for the entire course of infection. Cells were harvested 20 hrs post infection (p.i.) for dynasore, filipin, and EIPA treatments, and 8 hrs p.i. for chlorpromazine and latrunculin B treatments. Single-cell preparations were made and fixed (2% paraformaldehyde (PFA) in PBS) and GFP expression, indicative of productive infection, was analyzed by a Nexcelom Vision cellometer (Nexcelom Bioscience LLC., Lawrence, MA) capable of fluorescence detection. The percent of infected cells was calculated by dividing the number of GFP positive cells by the total number of cells and multiplying by 100. At least 1000 cells were counted per sample for each experiment. Results are expressed as percent virus-infected cells relative to that of untreated controls and represent 3 independent experiments; error bars are standard error of the mean (SEM). Cell viability of drug treated cells was determined by trypan blue staining.

### **Analysis of dominant negative mutants of Eps15, Rab5, Rab7, and Rab11**

Eps15 control (DIIIΔ2) and dominant negative (DN) (EH29) eGFP-tagged plasmids were kindly provided by Robert Davey (Texas Biomedical Research Institute). A plasmid expressing eGFP (pEGFP-C1; Clontech, Mountain View, CA) was used as an additional control in Eps15 experiments. DsRed-tagged Rab7 wild-type (WT) (plasmid #12661) and DN (T22N; plasmid #12662), DsRed-tagged Rab11 WT (plasmid #12679) and DN (S25N; plasmid #12680) (61), and mRFP-tagged Rab5 WT (plasmid #14437) (272) were purchased from Addgene, Cambridge, MA. RFP-tagged Rab5 DN (S34N) was generated by site-directed mutagenesis of Rab5 WT using a QuikChange II site-directed mutagenesis kit (Stratagene, Cedar Creek, TX). HEK293T cells grown to 50% confluence in 24-well tissue culture plates were transfected with plasmids using Lipofectamine LTX (Invitrogen) according to the manufacturer's protocol. Eighteen to twenty hours post transfection, cells were infected with VSVΔG-ABLV G\*-RFP at a MOI=2 for 20 hrs (Eps15 transfected cells) or with rVSV-ABLV G-GFP at a MOI=3 for 8 hrs (Rab transfected cells). VSVΔG-VSV G\*-RFP (MOI=2) was included as a positive control for Eps15 DN functionality. Recombinant VSV-GFP reporter viruses that express VSV G (MOI=3, 8 hrs infection) and EboGP (MOI=15, 20 hrs infection) were included as positive controls for Rab5 DN and Rab7 DN functionality, respectively. The chosen MOIs yielded 25-30% and 40-50% virus-infected cells in controls for the Eps15 and Rab experiments, respectively. Cells were harvested and analyzed for RFP or GFP expression (Eps15 and Rab experiments, respectively) using a Nexcelom Vision cell counter. At least 1000 cells were counted per sample per experiment. Results are expressed as percent virus-infected cells relative to that of controls and represent 3 independent experiments; error bars are SEM. For confocal imaging, HEK293T cells

grown to 30% confluence on 12 mm coverslips were transfected as described above. Cells were fixed with 4% PFA and then the coverslips mounted on slides using SouthernBiotech™ Dapi-Fluoromount-G™ clear mounting media and imaged by confocal microscopy.

### **Cholera toxin B subunit uptake**

HEK293T cells grown on 12 mm coverslips in 24-well tissue culture plates were pretreated with filipin or transfected with Eps15 plasmids as described above and then incubated with Alexa Fluor (AF) 488- or AF 594-conjugated cholera toxin B subunit (Invitrogen) (10 µg/ml) diluted in OptiMEM® for 1 hr at 37°C. Cells were washed twice with PBS and fixed with 4% PFA. The coverslips were mounted on slides using SouthernBiotech™ Dapi-Fluoromount-G™ clear mounting media and imaged by confocal microscopy.

### **Confocal microscopy**

Confocal images were obtained using a 63× oil objective, a Zeiss 710 NLO microscope, and Zen software. LSM files were exported to Adobe Photoshop for cropping and contrast adjustments.

### **Statistical analysis**

Student's *t-test* was used to evaluate the statistical significance levels of the data, with  $p < 0.05$  indicating statistical significance.

### **Acknowledgements**

All confocal images were taken by Eric D. Laing (Uniformed Services University). This work was supported by NIH grant AI057168 to C.C.B.

## **CHAPTER 4: Induction of cross-reactive neutralizing antibodies by a soluble G glycoprotein of Australian bat lyssavirus.**

### **ABSTRACT**

Australian bat lyssavirus (ABLV) is a recently emerged rhabdovirus of the genus *Lyssavirus* that is capable of causing a fatal neurological disease in people indistinguishable from clinical rabies. There are two variants of ABLV, one present in pteropid fruit bats and the other in insectivorous microbats. ABLV infects host cells through receptor-mediated endocytosis and subsequent pH-dependent fusion mediated by its single envelope glycoprotein (G). To characterize ABLV G and to explore its immunogenicity, a soluble form of ABLV G (Gs) was constructed by replacing its transmembrane domain and cytoplasmic tail with the T4 fibrin motif and an S-peptide tag to facilitate purification and detection. Expression of Gs was verified in cell lysates and culture supernatants by S-protein agarose affinity purification. Analysis of purified Gs by native Western blot analysis demonstrated trimeric, dimeric, and monomeric species. Immunization of mice and rabbits with Gs elicited a potent cross-reactive virus neutralizing antibody response against infectious recombinant vesicular stomatitis viruses expressing ABLV G glycoproteins. Results indicate that Gs retained important structural features of native full-length ABLV G and could be an effective diagnostic reagent for the detection of G-specific antibodies in animals or humans or be a useful antigen for the isolation of human anti-ABLV G monoclonal antibodies through phage display technologies.

## INTRODUCTION

Australian bat lyssavirus (ABLV) is an enveloped, non-segmented, negative sense RNA virus belonging to the genus *Lyssavirus* of the family *Rhabdoviridae*. There are two genetically distinct variants of ABLV, the *Pteropus* strain (ABLVp) present in frugivorous flying foxes (genus *Pteropus*), and the *Saccolaimus* strain (ABLVs) present in the insectivorous yellow-bellied sheath-tail bat (genus *Saccolaimus*). Similar to rabies virus (RABV), the prototype member of the *Lyssavirus* genus, ABLV is capable of causing fatal encephalitis in humans (4; 7; 116). Rabies virus post-exposure prophylaxis (PEP) is currently used to treat humans that are exposed to bats suspected of being infected with ABLV and consists of the administration of human rabies immune globulin (HRIG) and a four dose rabies vaccine series (52). Rabies vaccination does not provide complete cross-protection against ABLV in a mouse model of infection; while RABV vaccinated mice were completely protected against intracerebral challenge with ABLVp (129), a separate study found that of RABV vaccinated mice challenged with ABLVs, only 50% and 79% survived intracranial and peripheral challenge, respectively (41).

Lyssaviruses have a single type I membrane envelope glycoprotein (G), organized as a trimer on the virion surface, that mediates attachment to and pH-dependent fusion with host cell membranes (100). The lyssavirus G glycoprotein is a key determinant of the neurotropic and neurovirulent properties of lyssaviruses. It is also the sole viral protein capable of inducing the production of virus-neutralizing antibodies (89). ABLV G, comprised of 507 amino acids, contains a 439 amino acid ectodomain, a 22 amino acid transmembrane domain (TM) and a 46 amino acid cytoplasmic tail (CT); a single N-glycosylation site is present at amino acid 319, which is conserved among all lyssavirus species (107; 275).



To characterize ABLV G and to explore its immunogenicity in animal models, we have developed an S-peptide-tagged version of soluble ABLVs G (ABLVs Gs-GS3T4) that is expressed and secreted from HEK293T cells that stably express Gs. Although production yields were low, data presented below indicate that the Gs produced and secreted from the stable HEK293T-ABLVs Gs-GS3T4 cell line is released from the cells in monomeric, dimeric, and trimeric forms. ABLVs Gs was highly immunogenic in both mice and rabbits and induced a potent cross-reactive virus neutralizing antibody response in immunized animals. Two mouse monoclonal antibodies (MAbs) specific for ABLVs G were isolated and characterized. Both MAbs are conformation dependent and react to native full-length ABLVs G. One of the MAbs, DW11C7 is a potent neutralizer of ABLVs G-mediated viral entry. Taken together, the findings presented herein indicate that ABLVs Gs retains important native structural features, suggesting it may be a useful diagnostic reagent and could also be used as antigen for the panning and isolation of anti-ABLV G human MAbs, which could lead to more effective PEP treatments for individuals exposed to ABLV.

## **RESULTS AND DISCUSSION**

### **Construction and transient expression of soluble ABLV G glycoproteins**

To construct soluble versions of the G glycoprotein (Gs) derived from both the *Saccolaimus* and *Pteropus* ABLV variants, the TM and CT domains of G were replaced with a C-terminal S-peptide tag (Figure 20A). S-protein agarose precipitation followed by SDS PAGE analysis were used to evaluate the expression of Gs from the lysates and cell supernatants harvested from plasmid-transfected cells. Lyssavirus glycoproteins, including ABLV G and RABV G, are organized as trimers on the virion surface.

Previous studies have demonstrated that the soluble ectodomain of RABV G folds in a monomeric conformation that is antigenically distinct from native membrane-anchored glycoprotein (97). Appendage of the GCN trimeric helical domain (GCNt) (117) has been shown to stabilize trimers and enhance secretion of the human immunodeficiency virus type I (HIV-I) truncated envelope glycoprotein gp140 (291; 292) and of soluble F glycoproteins of several paramyxoviruses (54; 251; 278; 295). Thus, a second construct of Gs was designed in which GCNt was added upstream of the S-peptide tag (Figure 20A). Constructs derived from wild-type (WT) ABLVs and ABLVp G coding sequences were expressed in HEK293T cells and could be precipitated and detected in cell lysates, but no ABLVs or ABLVp Gs was released from the cells (Figure 20B). The addition of GCNt did not improve protein secretion (Figure 20B). Codon optimization of both ABLVs and ABLVp Gs constructs significantly enhanced the expression of Gs in HEK293T cells, but did not improve the release of Gs from expressing cells (Figure 20C); due to the enhanced expression levels, codon optimized constructs were used for all subsequent experiments.

These results prompted an extensive literature search of strategies that have been used to promote or improve secretion of recombinant soluble proteins; the various strategies employed for codon optimized ABLV Gs are listed in Table 2. Additionally, various ABLV Gs constructs were expressed in multiple different mammalian cell lines as well as insect cell lines (data not shown). The best expression of Gs occurred in HEK293T cells, thus these cells were used in all subsequent experiments. Most of the strategies listed in Table 2 did not enhance Gs secretion (data not shown). A previous

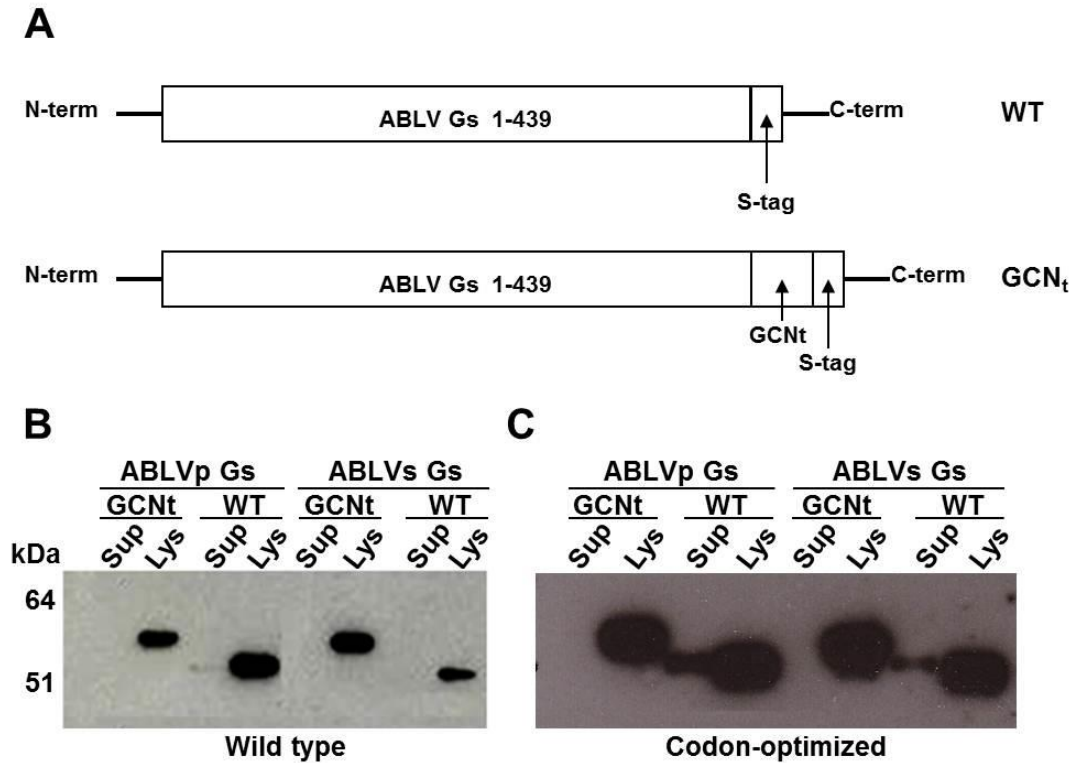


Figure 20. Transient expression of ABLV Gs glycoprotein constructs. (A) Schematic representation of Gs constructs. To construct soluble glycoprotein constructs, the TM and CT domains of ABLV G were replaced by a GCN trimeric helical domain (GCNt) and/or the S-peptide epitope tag at the C-terminus. The Gs constructs were cloned into a modified pcDNA 3.1/Hygro (+) vector (Invitrogen) for expression in mammalian cells. Wild type (WT) (B) and codon-optimized (C) Gs constructs with and without GCNt were transfected into HEK293T cells. At 48 hrs post transfection, culture medium was harvested and cells were lysed and clarified by centrifugation. Clarified cell lysates and supernatants were precipitated with S-protein agarose and the precipitated proteins were resolved by 4-12% BT SDS PAGE. Gs was detected by Western blotting with rabbit anti-S-peptide antibody. Sup, culture supernatant; Lys, cell lysate.

Table 2. Strategies to improve the secretion of ABLV Gs.

Strategy	Citations
Construct Gs-GPI anchor fusion proteins and cleave with phospholipase C or D	Kennard et. al 1999 (139)
Replace native G leader sequence with IgG kappa leader	Bossart et. al 2005 (34)
Mutate hydrophobic residues to decrease the hydrophobicity of G	Martin et. al 2006 (170); Chan et. al 2012 (54)
Construct Gs-human FC domain fusion proteins	Lo et. al 1998 (161)
Fuse Gs with T4 fibrin 'foldon' trimerization motif	Miroshnikov et. al 1998 (188); Sissoeff et. al 2005 (240)
Alter culture conditions/temperature	Swiech et. al 2008 (253)

study found that the lack of secretion of a soluble form of RABV G was due to accumulation of RABV Gs in the rough endoplasmic reticulum (rER); MAb profiling revealed that the Gs protein had adopted an immature or misfolded conformation and was not exported from the ER (257). It is possible that a similar phenomenon was occurring for the ABLV Gs proteins and that they too were being retained in the ER. For numerous proteins, transport from the ER is facilitated not only by correct folding, but also by proper oligomerization (75; 133). Previous studies demonstrated that the T4 fibrin 'foldon' motif (254) provided enhanced stabilization of HIV-1 gp140 trimers compared to the GCNt motif (293) and promoted stable trimers of soluble RABV G (240). Insertion of a linker between the RABV G ectodomain and the T4 fibrin motif enhanced the expression of T4 fibrin, thereby enhancing the stabilization of RABV Gs (240). To test whether the T4 fibrin motif could improve ABLV Gs secretion, ABLV Gs-T4 fusion constructs were designed; two different linkers (G8 and GS3) were inserted between the ABLV G ectodomain and the T4 fibrin motif (Figure 21A). The addition of the T4 fibrin motif to Gs significantly improved the secretion of ABLVs Gs, but not ABLVp Gs (Figure 21B). Expression profiles were the same regardless of the type of linker inserted between the ABLV G ectodomain and the T4 motif. It is unclear why the T4 motif improved secretion of ABLVs Gs, but not that of ABLVp Gs. However, different lyssavirus G glycoproteins have been shown to exhibit differential oligomeric stability (71). It is possible that ABLVp G naturally forms less stable trimers than ABLVs G and that T4 fibrin was simply not sufficient to stabilize ABLVp Gs trimers to a degree that would permit ABLVp Gs escape from the ER, if in fact that is where ABLVp Gs is being accumulated; this has not been experimentally verified.

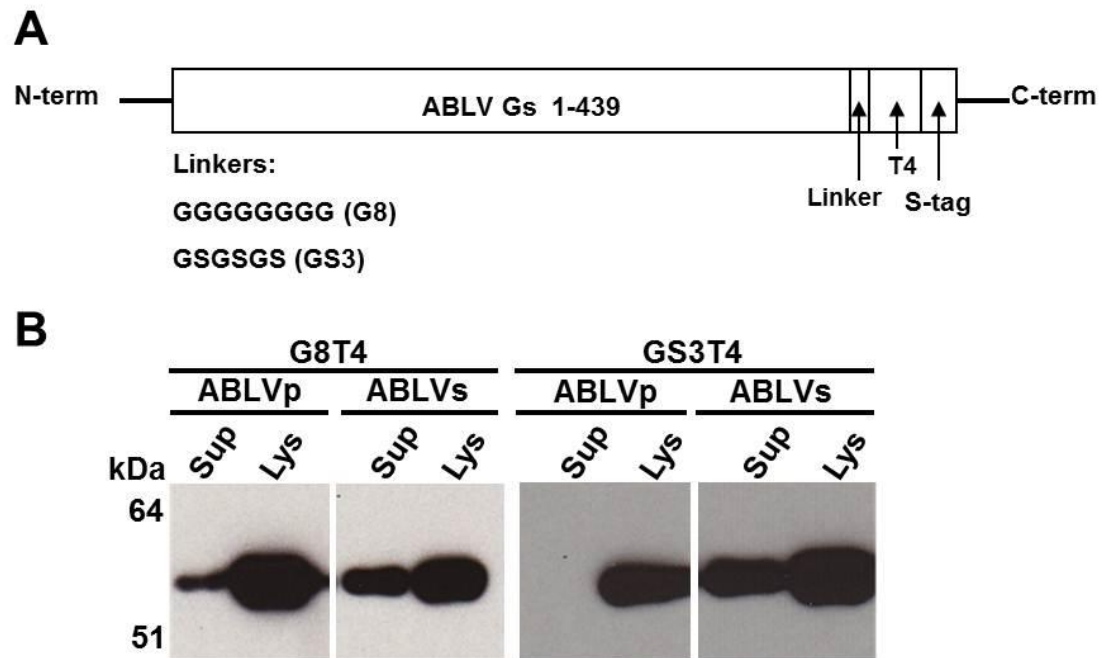


Figure 21. Transient expression of ABLV Gs T4 constructs. (A) Schematic representation of Gs constructs. Constructs were made as described in Figure 1A except instead of GCNt, the bacteriophage T4 fibrin ‘foldon’ trimerization motif preceded by a linker (G8 or GS3) was added to the C-terminus of the ABLV ectodomain upstream of the S-peptide epitope tag. (B) Western blot detection of ABLV GsT4 proteins. Gs constructs were transfected into HEK293T cells and analyzed as described in Figure 20. Sup, culture supernatant; Lys, cell lysate.

## **Large scale production and purification of ABLV Gs**

HEK293T cell lines that stably express ABLVp Gs- G8T4 and ABLVs Gs-GS3T4 were established. S-protein agarose affinity purification of ABLVp Gs-G8T4 and ABLVs Gs-GS3T4 from culture supernatants of stably expressing Gs cell lines revealed that the ABLV Gs constructs produced extremely low protein yields ( $\sim 0.1 \text{ ng}/10^6$  cells and  $0.5 \text{ ng}/10^6$  cells for ABLVp Gs and ABLVs Gs, respectively). Previous studies have shown that decreasing culture temperature can lead to increased production of recombinant proteins, including RABV G (253). Lowering the culture temperature of the ABLV Gs expressing cell lines from  $37^\circ\text{C}$  to  $34^\circ\text{C}$  increased secreted protein production by  $\sim 4$ -fold, but protein yields remained low at  $\sim 0.5$  to  $2 \text{ ng}/10^6$  cells. Protein yields from whole cell lysates of ABLVs Gs-GS3T4 expressing cells were  $\sim 250$  fold higher than those obtained from cell culture supernatant, with yields approaching  $0.25 \mu\text{g}/10^6$  cells.

Low production yields of soluble and secreted G is not unique to ABLV. Although there are several reports of the production of soluble and secreted forms of RABV G, none have reported high yields of Gs (97; 110; 289; 290). The inability to produce high quantities of recombinant soluble G likely explains why a crystal structure of a lyssavirus G glycoprotein has yet to be solved. The only rhabdovirus G crystal structure solved to date is that of vesicular stomatitis virus (VSV) G (213; 215). For those studies, VSV G was cleaved from whole virions by limited proteolysis. This approach has not proven successful for RABV G (97).

Despite numerous attempts, a sufficient amount of purified ABLVp Gs for experimental analysis was not obtained; however, ABLVs Gs was successfully purified in small quantities. SDS PAGE analysis of purified ABLVs Gs indicated that the protein preparation was pure; a single band  $57 \text{ kDa}$  in size, the predicted size of ABLVs Gs, was

detected by Coomassie blue staining (Figure 22A). Native PAGE analysis revealed the presence of 3 to 4 Gs species present within the protein preparation; these species may correspond to monomers, dimers, trimers, and higher order protein aggregates (Figure 22B). This is in agreement with what has been reported for soluble G glycoprotein preparations for both RABV and VSV (2; 240). Fewer aggregates and the absence of Gs monomers in the presence of 1% DDM may be explained by the ability of DDM to better stabilize Gs oligomers compared to digitonin. The differential ability of various detergents to stabilize membrane proteins is well documented [reviewed in (206)].

### **Immunogenicity of recombinant Gs**

To evaluate whether immunization with ABLVs Gs could elicit an immune response, immunization protocols were carried out in mice and rabbits (Figure 23). Immunized animals generated a high titer of immunoreactivity against Gs, with ELISA titers > 1:640,000 in mice (Figure 24A) and > 40,980,000 in rabbits (Figure 24B). Importantly, the immune sera from both mice (immunized with secreted Gs) (Figure 25A) and rabbits (immunized with Gs obtained from cell lysates) (Figure 25B) were able to bind to full-length ABLVs G, as well as cross-react with full-length ABLVp G, as measured by ELISA. The reactivity of the immune sera was specific to ABLV G, as the sera did not react with full-length VSV G (Figure 25A-B). The ability of the immune sera to neutralize replication-competent rVSV encoding and expressing ABLVs G or ABLVp G on the virion surface was also evaluated. Table 3 summarizes the neutralization of rVSV-ABLVp G and rVSV-ABLVs G infection by the mouse and rabbit anti-ABLVs Gs sera. Both mouse and rabbit immune sera were capable of complete neutralization of ABLVs G-mediated viral entry at dilutions of 1:1,600 and



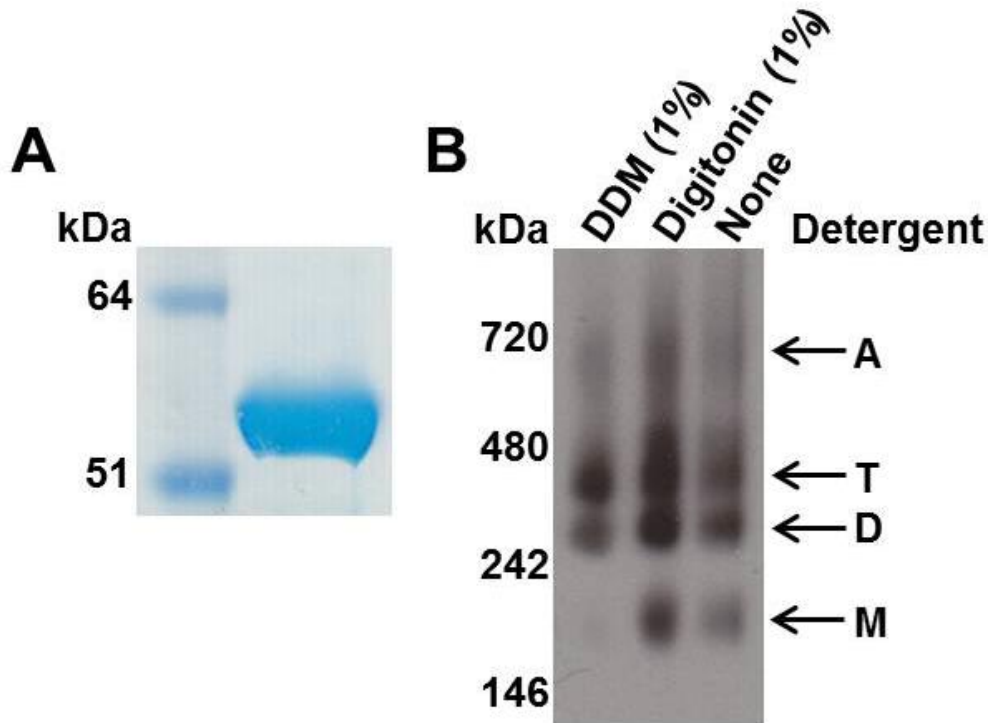


Figure 22. SDS PAGE (A) and Native PAGE (B) analysis of purified ABLVs Gs. (A) Approximately 3 $\mu$ g of purified Gs protein was resolved by 4-12% BT SDS PAGE followed by detection with Coomassie staining. (B) Approximately 190ng of purified Gs was analyzed in the presence or absence of detergent as indicated by 3-12% Native PAGE (Invitrogen) followed by Western blotting with rabbit anti-S-peptide antibody. DDM, n-dodecyl- $\beta$ -D-maltoside; Apparent high molecular mass aggregates (A), trimers (T), dimers (D), and monomers (M) of ABLVs Gs are indicated.

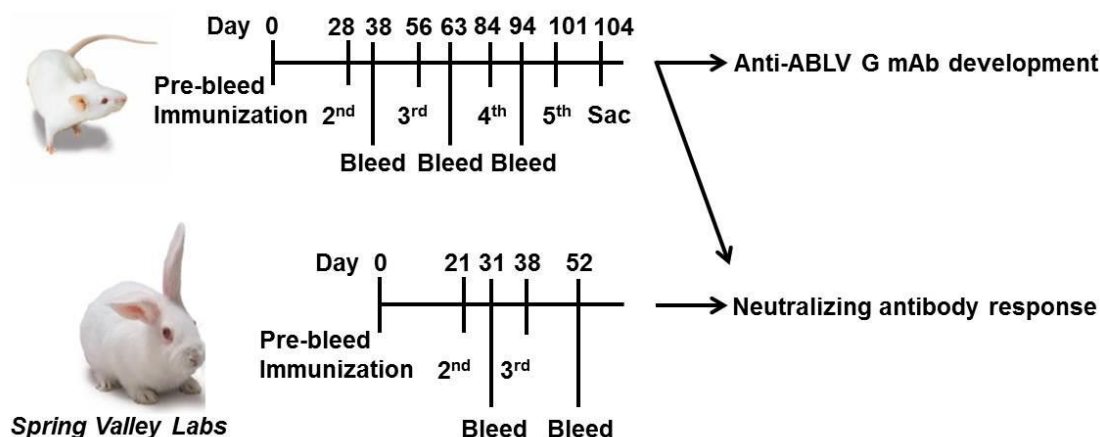


Figure 23. Schematic for mouse and rabbit immunization schedules with purified ABLVs Gs protein. Mice were immunized 5 times with 15 $\mu$ g of Gs (purified from cell supernatants) at the indicated time points. The first 4 were given 28 days apart in a Sigma adjuvant system. A fifth immunization was given without adjuvant 3 days prior to sacrificing the animals. Blood samples were taken 10 days post-boost. Rabbit immunizations were conducted by Spring Valley Labs (Sykesville, MD). A single rabbit was immunized 3 times with 75 $\mu$ g of ABLVs Gs (purified from cell lysates) in a Sigma adjuvant system. Blood samples were collected 10-14 days post-boost. Both mouse and rabbit sera were analyzed for a neutralizing antibody response against ABLV. Immunized mice were used for anti-ABLVs G MAb development.

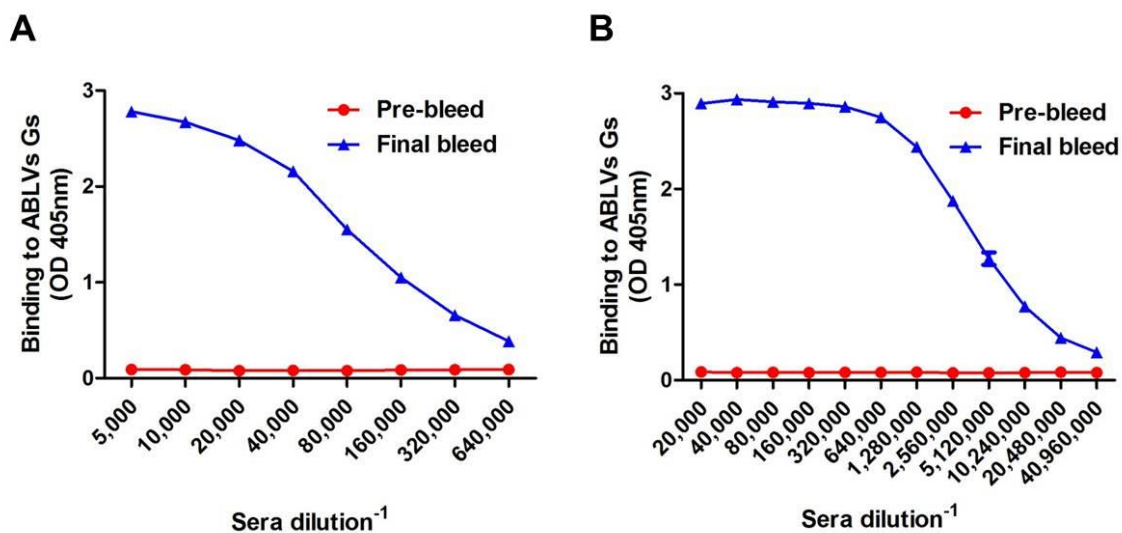


Figure 24. Anti-ABLVs Gs polyclonal antibody response in mice (A) and rabbits (B) immunized with ABLVs Gs as measured by ELISA. Plates were coated with 20ng ABLVs Gs per well. Sera were serially diluted two-fold and HRP-conjugated goat anti-mouse IgG or anti-rabbit IgG was used as the secondary antibody.

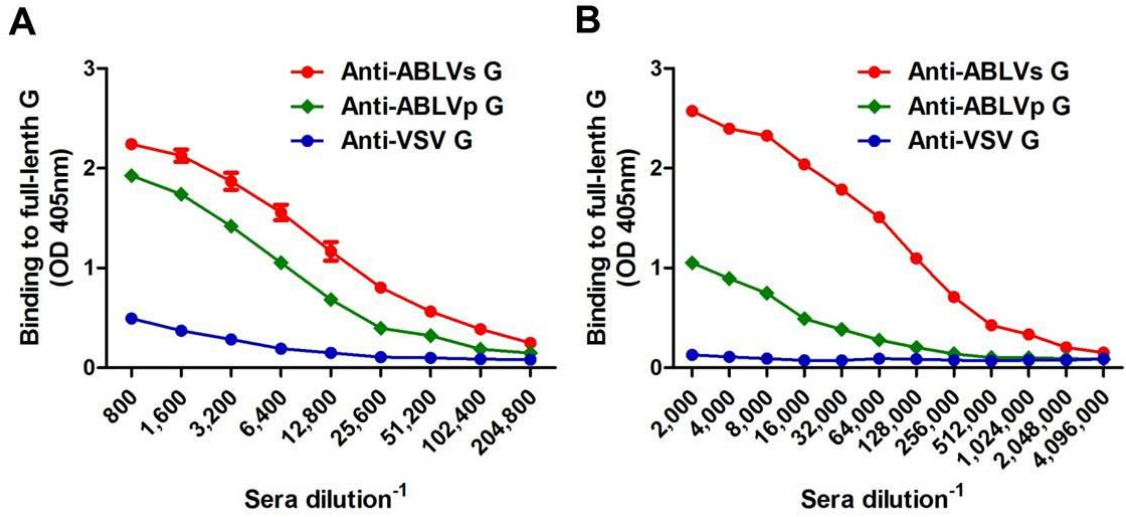


Figure 25. Anti-ABLVs Gs-GS3T4 immune sera binds native full-length ABLV G. ELISA plates were coated with  $10^4$  IU rVSV virus per well. Mouse (A) and rabbit (B) sera were serially diluted two-fold and HRP-conjugated goat anti-mouse IgG was used as the secondary antibody.

Table 3. Neutralization of VSV-ABLV G-GFP infection by anti-ABLVs G polyclonal sera<sup>a</sup>

Dilution	ABLVp G		ABLVs G	
	Mouse	Rabbit	Mouse	Rabbit
1:100	- -	- -	- -	- -
1:200	- -	- -	- -	- -
1:400	- -	- -	- -	- -
1:800	+ +	- +	- -	- -
1:1,600	+ +	+ +	- -	- -
1:3,200	+ +	+ +	+ +	- -
1:6,400	+ +	+ +	+ +	+ -
1:12,800	+ +	+ +	+ +	+ +
1:25,600	+ +	+ +	+ +	+ +

<sup>a</sup>Anti-ABLVs G antisera were generated in mice and rabbits by 5 or 3 inoculations, respectively, with purified ABLVs Gs-GS3T4. Sera collected at 10 days after the final immunization were analyzed in a neutralization assay against VSV-ABLVp G- and VSV-ABLVs G-GFP viruses. Neutralization titers (in duplicate) were determined by the presence of GFP fluorescence (indicated by +) and recorded as the serum dilution where at least one of the duplicate wells showed GFP expression. (-) no GFP expression.

1:3,200, respectively. ABLVp G-mediated viral entry was also neutralized by both immune sera, with complete neutralization at a dilution of 1:400. Pre-immune serum was neutralization negative and VSV G expressing control virus was not neutralized by pre-immune or anti-ABLVs Gs sera (data not shown). Taken together, these results demonstrate that ABLVs Gs, including Gs purified from cell lysates, retains important structural features of native full-length G.

### **Isolation and characterization of mouse anti-ABLVs G MAbs**

Mice immunized against ABLVs Gs were sacrificed and the spleens were harvested for hybridoma development using standard practices. Two anti-ABLV G MAbs, DW8F10 (IgG1) and DW11C7 (IgA), were purified from clonal hybridomas (Figure 26A). Both MAbs displayed a strong affinity for ABLVs Gs, as measured by ELISA, with binding to ABLVs Gs at concentrations less than 0.16 and 0.005  $\mu\text{g/ml}$ , for DW8F10 and DW11C7, respectively (Figure 26B). Neither MAb was capable of detecting ABLVs Gs in Western blot analysis, demonstrating that both are conformation dependent (data not shown). Importantly, the MAbs were able to react with native full-length ABLVs G (Figure 27), as measured by ELISA. DW8F10 displayed some cross reactivity with ABLVp G, though the binding was weak. DW11C7 did not cross react with full-length ABLVp G (Figure 27). As expected, neither MAb reacted with the VSV G control. The ability of the MAbs to neutralize ABLV G expressing rVSV viruses was also evaluated. DW11C7 potentially neutralized ABLVs G-mediated viral entry, with complete neutralization at a concentration of 1.56  $\mu\text{g/ml}$  (Table 4); the vast majority of cells remained uninfected at concentrations as low as 0.1  $\mu\text{g/ml}$  (Appendix C). DW11C7 did not neutralize VSV-ABLVp G virus. Neither virus was neutralized by DW8F10.

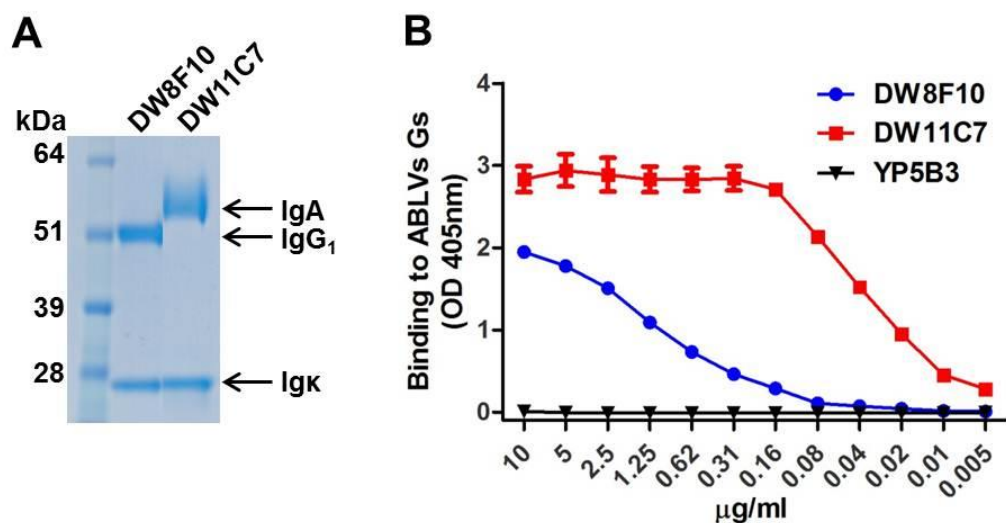


Figure 26. Isolation and purification of mouse anti-ABLVs G MAb. (A) SDS PAGE analysis of purified MAb. Approximately 3μg of purified MAb were resolved by 4-12% BT SDS PAGE followed by detection with Coomassie staining. Antibody isotype and light chain identity, determined by a rapid mouse antibody isotyping kit (Pierce), are indicated on the left. (B) Mouse anti-ABLVs G MAb ELISA titration. Plates were coated with 20ng ABLVs Gs diluted in PBS per well. Mouse MAb were serially diluted two-fold and HRP-conjugated goat anti-mouse IgG was used as the secondary antibody. Mouse monoclonal YP5B3 was used as a negative control.

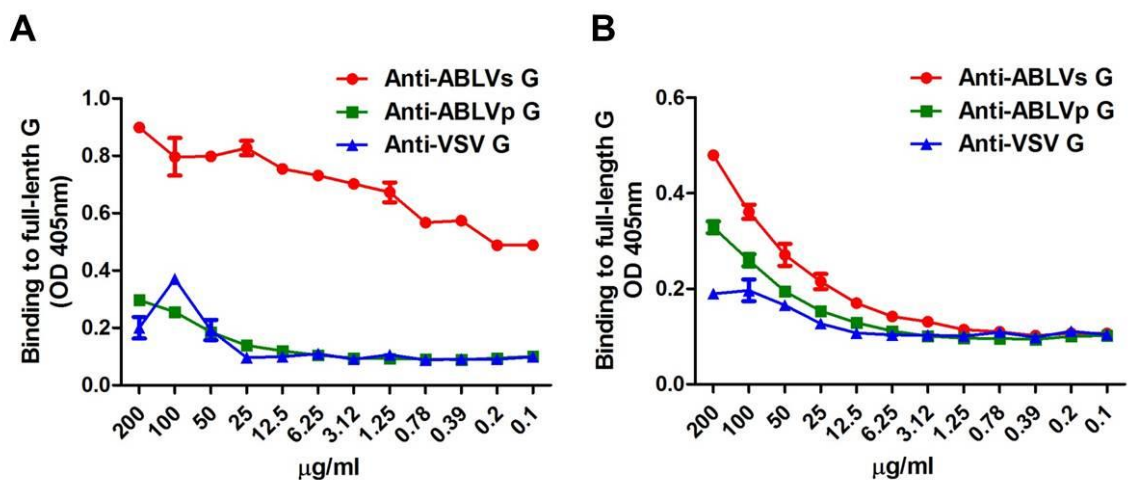


Figure 27. Anti-ABLVs G MAbs bind native full-length ABLVs G. ELISA plates were coated with  $10^4$  IU rVSV virus per well. Mouse MAbs (A) DW11C7 and (B) DW8F10 were serially diluted two-fold and HRP-conjugated goat anti-mouse IgG was used as the secondary antibody.



Table 4. Neutralization of VSV-ABLV G-GFP infection by mouse anti-ABLVs G MAbs<sup>a</sup>

μg/ml	ABLVp G				ABLVs G			
	DW11C7		DW8F10		DW11C7		DW8F10	
200	+	+	+	+	-	-	+	+
100	+	+	+	+	-	-	+	+
50	+	+	+	+	-	-	+	+
25	+	+	+	+	-	-	+	+
12.5	+	+	+	+	-	-	+	+
6.25	+	+	+	+	-	-	+	+
3.12	+	+	+	+	-	-	+	+
1.56	+	+	+	+	-	-	+	+
0.78	+	+	+	+	-	+	+	+
0.39	+	+	+	+	-	+	+	+
0.19	+	+	+	+	+	+	+	+
0.10	+	+	+	+	+	+	+	+

<sup>a</sup>Purified anti-ABLVs G MAbs were analyzed in a neutralization assay against VSV-ABLVp G- and VSV-ABLVs G-GFP viruses. Neutralization titers (in duplicate) were determined by the presence of GFP fluorescence (indicated by +) and recorded as the MAb concentration where at least one of the duplicate wells showed GFP expression. (-) no GFP expression.

## **CONCLUSIONS**

We successfully developed and purified a recombinant soluble and secreted form of ABLV G (Gs). Despite low protein yields, analysis of purified ABLVs Gs revealed that protein preparations were pure and that they were comprised of a mixture of monomers, dimers, and trimers of Gs, which is in agreement with what has been reported for other soluble rhabdovirus G glycoprotein preparations (2; 240). Importantly, immunization of mice and rabbits with ABLVs Gs elicited a potent cross-reactive virus neutralizing antibody response indicating that ABLVs Gs retained important structural features of native full-length ABLVs G. A mouse MAb that potently neutralizes ABLVs G-mediated viral entry was also isolated. The anti-ABLV G immune sera as well as the mouse MAbs will be valuable reagents for future ABLV studies.

The results presented here suggest that ABLVs Gs-GS3T4 could be an effective subunit vaccine against both variants of ABLV; however, the inability to produce high yields of ABLVs Gs makes its use as such impractical. It could however be a useful diagnostic reagent for the detection of ABLV G-specific antibodies in animal or human sera samples using ELISA or luminex platforms, which do not require large quantities of protein, and/or as antigen to pan for anti-ABLVs G hMAbs. Additional strategies to increase ABLV Gs yields, such as cleaving G from specially engineered viruses, are currently being explored.

## **MATERIALS AND METHODS**

### **Cells, viruses, and antibodies**

HEK293T cells were provided by Gerald Quinnan (Uniformed Services University) and were maintained in Dulbecco's modified Eagle's medium (DMEM;

Quality Biologicals, Gaithersburg, MD) supplemented with 10% cosmic calf serum (CCS) (Hyclone, Logan, UT) and 2 mM L-glutamine (DMEM-10). Recombinant maxGFP expressing vesicular stomatitis viruses (rVSV) that express ABLV G glycoproteins have been previously described (277). Rabbit anti-S-peptide-tag antibody, horse radish peroxidase (HRP) conjugated, was from Bethyl Laboratories, Inc., Montgomery, TX. Goat anti-rabbit and anti-mouse IgG (H+L) HRP conjugated secondary antibodies were purchased from Pierce, Rockford, IL.

### **Design of ABLV Gs constructs**

ABLV G cDNA clones of both the *Pteropus* (ABLVp G) (GenBank accession AF426309.1) and *Saccolaimus* (ABLVs G) (GenBank accession AAN63540.1) variants were kindly provided by Lin-Fa Wang (CSIRO, Australia) (111). Full-length ABLV G cDNA sequences for both variants were codon optimized and synthesized by Geneart Inc., Germany. The predicted transmembrane (TM) domain (residues 440-461) and the C-terminal cytoplasmic tail (CT) domain (residues 462-507) (107) of ABLV G were replaced by either by the S-peptide tag (KETAAAKFERQHMDS), or the GCNt motif (MKQIEDKIEEILSKIYHIENEIARIKKLIGE) (117), followed by the S-peptide tag, or the bacteriophage T4 fibritin 'foldon' motif (GYIPEAPRDGQAYVRKDGEWVLLSTFL) (254) preceded by either a G8 linker (GGGGGGGG) or a GS3 linker (GSGSGS), followed by the S-peptide tag, generating ABLV Gs-WT, ABLV Gs-GCNt, ABLV Gs-G8T4, or ABLV Gs-GS3T4. All constructs were cloned into a promoter-modified pcDNA3.1 vector containing a hygromycin selection marker (55).

### **Transient expression and generation of ABLV Gs-expressing stable cell lines**

HEK293T cells were transfected with ABLV Gs plasmid constructs using Fugene (Roche, Indianapolis, IN). Cells grown to 60-70% confluence in 6-well tissue culture plates were transfected with 2 $\mu$ g DNA and 6 $\mu$ l Fugene per well following the manufacturer's instructions. At 48 hrs post transfection, the culture medium was either harvested for S-protein agarose (EMD Biosciences Inc., Madison, WI) precipitation or the culture medium was replaced with selection medium (DMEM-10 supplemented with 150 $\mu$ g/ml of hygromycin B [Invitrogen, Carlsbad, CA]) (DMEM-10H). Hygromycin-resistant cells were subjected to two rounds of limiting dilution cloning to establish stable cell lines that express and secrete ABLV Gs (55).

### **Large scale expression and purification of ABLV Gs**

ABLV Gs was produced from HEK293T stable cell lines grown in serum-free medium and was purified by S-protein agarose affinity purification (55). Briefly, HEK293T cells expressing Gs maintained in DMEM-10H were grown to confluence in a 175-cm<sup>2</sup> tissue culture flask and then harvested and used to seed one 1,700-cm<sup>2</sup> roller bottle in DMEM-10. When cell cultures reached 80-90% confluence, the cell monolayers were washed twice with phosphate-buffered saline (PBS), and the medium was replaced with serum-free OptiMEM® (Invitrogen). Culture medium was collected after 4-5 days and centrifuged at 4°C for 15 min at 14,000 rpm, filtered through a 0.2 $\mu$ m-pore size low-protein-binding membrane (Corning, Inc., Lowell, MA), and passed through an S-protein agarose affinity column. The column was washed with PBS containing 0.1% Triton X-100, and the bound Gs was eluted with 3M MgCl<sub>2</sub>. The eluate was concentrated approximately 10-fold to a volume of 2-3 ml and buffer exchanged into

PBS 0.01% Triton X-100 using Amicon Ultra centrifugal filter units (Millipore, Billerica, MA). For purification of Gs from cell lysates, HEK293T cells expressing Gs were grown to confluence in 160-cm<sup>2</sup> tissue culture flasks, harvested and then treated with lysis buffer (100 mM Tris-HCl (pH 8.0), 100 mM NaCl, 0.5% Triton X-100, 1X complete protease inhibitor cocktail [Roche, Indianapolis, IN]). Cell lysates were clarified by centrifugation at 13,200 rpm for 10 min at 4°C and was then purified by S-protein agarose affinity purification as described above. To assess protein purity, 3-4 µg of purified protein were resolved by 4-12% Bis-Tris SDS PAGE (Invitrogen) under reducing conditions (2% β-mercaptoethanol in NuPAGE sample buffer) and detected by Coomassie staining.

### **Western blot analysis**

Cell culture supernatants and clarified lysates harvested from ABLV Gs expressing cells were precipitated with S-protein agarose. Gs was eluted from the beads by boiling the samples for 5 min and then analyzed by 4-12% Bis-Tris SDS PAGE (Invitrogen) under reducing conditions (2% β-mercaptoethanol in NuPAGE sample buffer). Following transfer to nitrocellulose paper, the blot was probed with HRP-conjugated rabbit anti-S-peptide antibody (1:15,000). For native Western blot analysis of purified ABLVs Gs, approximately 190 ng were analyzed either in the presence of the detergents digitonin (1%) or n-dodecyl-β-D-maltoside (DDM) (1%), or in the absence of detergent by 3-12% Native PAGE (Invitrogen) followed by Western blotting with rabbit anti-S-peptide antibody.

### **Generation of ABLVs G-specific MAbs**

Purified ABLVs Gs-GS3T4 was used to immunize BALB/c mice. All animal studies were conducted under an approved protocol for animal experiments obtained

from the Uniformed Services University Animal Care and Use Committee. Two mice were immunized 4 times, as indicated in Figure 23, with 15µg of Gs protein in a Sigma adjuvant system (Sigma-Aldrich Co. LLC, St. Louis, MO) at intervals of 28 days. Serum samples were taken at 10 days following each boost. Mice were given a fifth immunization without adjuvant 3 days prior to animal sacrifice. Mouse splenic lymphocytes were isolated and fused with SP2/0 cells using polyethylene glycol by standard methods and then distributed by limiting dilution into 96-well tissue culture plates, as previously described (77). Enzyme-linked immunosorbent assay (ELISA) using purified ABLVs Gs-GS3T4 as antigen was used to identify hybridoma supernatants producing ABLVs Gs-specific antibodies. Positive hybridomas were cloned by two rounds of limiting dilution (77). Clonal hybridoma lines were maintained in Iscove's Modified Dubecco's Medium (IMDM; Quality Biologicals) supplemented with 10% CCS, sodium hypoxanthine aminopterin thymidine (HAT; Invitrogen) and 100 U/ml recombinant mouse interleukin 6 (rIL-6; Roche). The anti-ABLVs G MAbs were produced under serum-free conditions using Hyclone SFM4MAb (Thermo Fisher Scientific Inc., Rockford, IL) and were purified by either protein G-Sepharose (GE Healthcare, Piscataway, NJ) or Protein-L-Agarose (Pierce) affinity chromatography. The eluate was concentrated using 50 kDa Amicon Ultra centrifugal filter units and MAb concentrations were determined using a Nanodrop spectrophotometer. MAb isotype and light chain identity were determined using a rapid mouse antibody isotyping kit (Pierce).

## **ELISA**

Anti-ABLV G specific MAbs and serum antibodies were detected using Immulon 2HB microtiter ELISA plates (Fisher Scientific, Hampton, NH) coated overnight at 4°C

with 20 ng of ABLVs Gs-GS3T4 or  $10^4$  infectious units (IU) rVSV per well diluted in PBS. Plates were blocked with PBS containing 5% bovine serum albumin (BSA) and 0.05% Tween-20 (BSA-PBST) for 1 hr at 37°C. A 100 µl aliquot of supernatant from hybridoma colony plates was added, in duplicate, to each well. Serum samples and MAbs were diluted in 1% BSA-PBST in 2-fold series and were assayed in duplicate. Goat anti-mouse IgG HRP (1:10,000 in PBST) was used for detection. For each step, plates were incubated at 37°C for 1 hr and subsequently washed 6 times with PBST. Plates were incubated with ABTS [2,2'-azinobis (3-ethylbenzthiazolinesulfonic acid)] substrate (Roche, Indianapolis, IN) (100µl per well) for 30 min with shaking at room temperature. The absorbance was measured for each well at 405 nm, and the average value was calculated from duplicates.

### **Generation of rabbit antiserum raised against ABLVs Gs**

Rabbit immunizations were carried out by Spring Valley Laboratories, Inc. (Sykesville, MD). A single rabbit was immunized 3 times, as indicated in Figure 23, with 75µg of ABLVs Gs-GS3T4 (purified from cell lysates of Gs expressing HEK293T cells) in a Sigma adjuvant system. Serum samples were taken at 10 days following each boost. A prebleed was collected prior to immunization. Anti-ABLVs G antibody titers were determined by ELISA.

### **Virus neutralization assay**

Sera samples or purified MAbs were serially diluted in DMEM-10, in duplicate wells, in a 96-well tissue culture plate and mixed with  $5 \times 10^4$  IU of either VSV-ABLVp G-, VSV-ABLVs G-, or VSV-VSV G-GFP viruses for 30 min at 37°C. Dilutions of purified MAbs started at 200 µg/ml. A total of  $5 \times 10^4$  HEK293T cells were added to

each well, incubated overnight at 37°C, and observed for GFP expression. Neutralization titers were recorded as the serum dilution or MAb concentration where at least one of the duplicate wells showed GFP expression.

### **Acknowledgements**

We thank Dr. Yee Peng Chan, Lianying Yan, and Yanru Feng (Uniformed Services University) for their help and guidance with the large scale production and purification of ABLV Gs and the production and purification of mouse anti-ABLVs MAbs. This work was supported by NIH grant AI057168 to C.C.B.



## CHAPTER 5: Discussion

### PREFACE

Clinical rabies, a fatal neurological disease caused by all members of the *Lyssavirus* genus (family *Rhabdoviridae*), has been feared by mankind for thousands of years, with the first documented description of canine rabies in 500 B.C. (16).

Lyssaviruses continue to be a global threat to human health causing more than 55,000 deaths annually, mostly in Asia and Africa (282). Australia was one of the few countries considered free of endemic lyssaviruses until the discovery of ABLV in 1996 (93).

ABLV has since caused three fatal human infections manifested as rabies-like encephalitis, the most recent case occurring in February 2013 (4; 7; 116). In May 2013, ABLV spilled over into horses (8), the first occurrence of ABLV in a species other than bats and humans. Accordingly, ABLV is a considerable concern to wildlife, veterinary, and healthcare officials. There is currently no effective treatment for clinical rabies, but disease can be prevented by administration of RABV vaccines to individuals exposed to infected animals. However, currently licensed RABV vaccines do not offer complete protection against ABLV in a mouse model of infection (41).

Like all viruses, lyssaviruses rely on the host cell machinery for replication; thus, understanding virus-host cell interactions such as virus attachment to host cells, receptor-mediated endocytosis, and uncoating provides a means for identifying potential targets for antiviral therapeutics. Studies aimed at identifying host factors essential for lyssavirus host cell entry are limited; for RABV, several host cell molecules have been proposed as receptors, but none have been shown to be essential *in vitro*. One such proposed receptor p75NTR (261) did not interact with the majority of lyssavirus

glycoproteins, including ABLV G (262), and is not essential for RABV infection (264). The role, if any, the other proposed RABV receptors play in the host cell entry of other lyssavirus species is not known. Following G-mediated receptor binding, RABV is internalized via endocytosis. CME has been implicated as the pathway utilized by RABV for internalization, a finding in agreement with entry studies of other rhabdoviruses. Following internalization, the viral cargo is delivered to endosomes where the acidic environment triggers conformational changes in the G glycoprotein that lead to fusion of the viral and endosomal membranes and the subsequent release of the viral genome into the cytosol; however, which endosomal compartment serves as the point of entry has not been specifically investigated, though early endosomes have been implicated for RABV based on co-localization studies with RABV G and EE markers and the optimal pH range for RABV G mediated fusion falls within the pH range of EEs. An understanding of the entry and fusion requirements of ABLV will not only provide clues for the future development of antiviral therapies against this emerging rhabdovirus, but may reveal commonalities between the entry pathways of ABLV and other lyssaviruses, thereby paving the way for the development of broadspectrum lyssavirus therapies. Accordingly, the overall goal of this project was to characterize host cell virus entry mediated by Australian bat lyssavirus G glycoprotein.

## **EXPERIMENTAL RESULTS IN THE CONTEXT OF PROJECT AIMS**

### **Review of Chapter 2 results**

Parts of this section have been published as: **Weir DL, Smith IL, Bossart KN, Wang LF, Broder CC.** 2013. Host cell tropism mediated by Australian bat lyssavirus envelope glycoproteins. *Virology* **444**:21-30

### ***In vitro entry tropism of ABLV***

At the time this study was initiated, there were no confirmed reports of ABLV infection in a species other than bats and humans despite known contacts of domestic dogs with infected flying foxes (173). RABV and other bat lyssaviruses have caused disease in numerous mammalian species (17), suggesting that occasional spillover of ABLV into other animals is likely. Thus, a major question regarding ABLV was its potential for cross-species transmission in terrestrial species other than humans. The first specific aim of this project sought to address this question by defining the host cell infection tropism of ABLV; characterization of tropism would also provide important data for ABLV receptor identification. Both the *Saccolaimus* and *Pteropus* variants were included in this analysis for several reasons. First, the ABLVs and ABLVp G ectodomains differ by 33 amino acids; previous studies have demonstrated that a single amino acid change within a viral glycoprotein can alter cellular tropism (263; 268). Second, the incubation periods of human infections caused by the two variants are very different, ranging from approximately 5 weeks to greater than two years for infections caused by ABLVs and ABLVp, respectively. Third, the lack of overlapping host reservoir species also points to possible tropism differences between ABLVs and ABLVp.

To investigate ABLV tropism we developed and recovered maxGFP-encoding replication competent recombinant vesicular stomatitis viruses (rVSV) that express the G glycoproteins from both ABLVs and ABLVp and used them as infection screening tools to examine infectivity and tropism, as a function of ABLV G. This approach has several advantages over using WT ABLV. First, rVSV-ABLV G viruses are safer and easier to manipulate than WT ABLV. Second, the incorporation of GFP into the viral genome

eliminates the need for traditional fluorescent antibody staining to detect infected cells. Third, the inclusion of rVSV-VSV G as a positive control in all infection assays enabled us to distinguish between actual ABLV G entry blocks and post-entry VSV inhibition. Previous studies that examined *in vitro* RABV tropism and receptor usage did not control for post-entry inhibition (258; 261). Furthermore, because the viral backbones of the rVSV reporter viruses are identical except for the envelope glycoproteins, the tropism differences exhibited by the different viruses can be attributed directly to differences among the G glycoproteins themselves.

In agreement with the broad *in vitro* tropism reported for RABV (258), we found that numerous cell lines derived from several different mammalian species, including multiple species of small rodents, rabbit, human, monkey, and horse, were permissive to viral entry mediated by the G glycoproteins of both ABLV variants. These results indicated that the ABLV host cell receptor is broadly conserved among mammals and suggested that species other than bats and humans could potentially be susceptible to ABLV infection. Importantly, this conclusion proved accurate shortly after submitting the ABLV tropism data for publication in *Virology* when ABLVs infected two horses, representing the first spillover of ABLV into a terrestrial species other than humans. As shown in Chapter 2, our *in vitro* tropism analysis predicted that horses could be susceptible to ABLV as the horse cells included in our study were highly permissive to ABLV G-mediated virus infection.

At present, the risk of human exposure to ABLV is currently believed to be limited to contact with infected bats; however, the recent horse infections demonstrate that other animals could potentially pose a threat. Furthermore, establishment of ABLV

in terrestrial species would significantly increase this risk. Molecular evidence suggests that terrestrial RABV evolved from bat lyssaviruses (15), with dogs being one of the major terrestrial reservoirs of RABV. As recently as 2001, a bat variant of RABV emerged that successfully adapted to skunks (153). Experimental infections of ABLV in terrestrial species are limited. Dogs and cats experimentally infected with a laboratory adapted strain of ABLVp exhibited mild behavioral changes and seroconverted within the three month study, but none succumbed to ABLV and no viral antigen was detected at necropsy (176). However, this study was only carried out for three months and it is possible that this was not sufficient time for the virus to reach the brain; one of the documented human ABLVp infections had an incubation period of more than two years (116). The ability of ABLVs to cause clinical disease in dogs and cats has not been evaluated; however, given the recent spillover of ABLVs into horses and our *in vitro* data demonstrating that cat embryo cells are significantly more susceptible to ABLVs G- than to ABLVp G-mediated infection, it is quite possible that clinical outcomes of dogs and cats inoculated with ABLVs would be much more severe. The *in vitro* tropism analysis presented herein is a first step towards understanding the potential cross-species transmission potential of ABLV. Further work is needed to fully define the potential risk of ABLV transmission and possible adaptation to terrestrial species.

#### ***ABLV variants can exploit alternate host factors for entry***

Although many cell lines were equally permissive to entry mediated by both ABLV variant G glycoproteins, we also identified three cell lines derived from three different species (human, insectivorous bat, and cat) that were moderately permissive to ABLVs G- , but resistant to ABLVp G-mediated viral entry, suggesting that the ABLV

variants can exploit alternate receptors for host cell entry. In further support of this, the polyanionic polysaccharide dextran sulfate (DS) potently inhibited ABLVp G-, but not ABLVs G-mediated viral entry. DS has been reported to have antiviral activity against numerous enveloped RNA and DNA viruses; the mechanism of antiviral action is thought to be mediated by a direct interaction of DS with the viral envelope glycoproteins (288). For human immunodeficiency virus type 1 (HIV-1), DS was shown to bind to the principal neutralizing domain of gp120 (V3) which contains a high local positive charge density (44). Therefore, it seems likely that the mechanism of DS inhibition of ABLVp G-mediated entry is through direct interaction with ABLVp G such that ABLVp G is no longer able to bind to its entry receptor. This interaction could involve direct binding of DS to the ABLVp G receptor binding domain (RBD) or binding to a region of G that prevents a critical conformational change in G required for receptor or co-receptor engagement.

A recent study demonstrated that a peptide comprised of amino acids 330 to 357 of RABV G was sufficient to target recombinant RABV G peptide fusion proteins to the CNS, suggesting that this stretch of amino acids may represent a RABV receptor binding site (94). This region of G is highly conserved among all lyssaviruses and contains two non-overlapping RABV G neutralizing epitopes, one mapped to residues 330-338 (site III) and another to residues 342-343 (minor site a) (21). Additionally, the arginine residue at position 333 has been shown to be critical for RABV virulence *in vivo*; the positive charge is key, as mutants that maintained a positive charge at position 333 were still virulent, but other non-charged mutants were attenuated (73). An X-ray crystal structure for a lyssavirus G glycoprotein has not yet been described, but predicted models

of ABLV G derived by protein threading with the VSV G structure predict that amino acids 330-357 are located at the top of the G globular head. Moreover, this region contains a high local density of positively charged amino acids that are predicted to be surface exposed. The fact that this region of G is so highly conserved among lyssaviruses indicates that these residues are important for some aspect of lyssavirus biology, if not for receptor binding. It would be interesting to examine whether site-directed mutagenesis to reduce the positive charge density of this region would abrogate the ability of DS to inhibit ABLVp G-mediated viral entry.

### ***Identification of cell lines resistant to ABLV G-mediated entry***

A major challenge for the RABV field trying to identify specific host cell receptors required for RABV entry has been the inability to identify RABV resistant cell lines, as fixed strains of RABV can replicate in most immortalized cell lines (258; 261). However, in the present study we were able to identify three cell lines, derived from three different species, that are resistant to ABLV G-mediated viral entry. These cell lines will be invaluable tools for future studies aimed at ABLV receptor identification. With the possible exception of ABLVp G binding to MDBK cells, the low infectivity of ABLV resistant cells did not correlate with lack of host cell attachment suggesting that host cell entry of ABLV may require interaction with two or more co-receptors. Dual- or multi-receptor models have been proposed for a number of viruses (239) as well as the highly neurotropic botulinum and tetanus toxins (203). A multi-receptor model for ABLV entry could explain why treatment of permissive target cells with increasing doses of neuraminidase or protease (pronase, proteinase K, and trypsin) failed to inhibit ABLV G-mediated entry at all concentrations tested (data not shown). If the co-receptors belong to

different classes of macromolecules, as is the case for several bacterial neurotoxins which utilize glycolipid and protein co-receptors to enter neurons (203), then treatment with protease or neuraminidase alone would not reduce viral infection; surface bound virions would interact with functional co-receptors as soon as the enzyme cleaved receptors were recycled and replaced by native ones.

Although we have not investigated the nature of the ABLV attachment factor(s) present on the ABLV resistant cells, heparan sulfate (HS), a glycosaminoglycan (GAG) that is expressed on the surface of most adherent cells (26), serves as an initial attachment receptor for numerous viruses, including the neurotropic  $\alpha$ -herpesviruses (230). The potent inhibition of ABLVp G-mediated entry by dextran sulfate discussed above, suggests that polyanionic molecules on the cell surface such as heparan sulfate, may serve as attachment factors for ABLVp. Biologically relevant to lyssavirus infection *in vivo*, HS is concentrated at the neuromuscular junction (137), the site of lyssavirus entry into motor neurons. Although virus attachment to host cells via HS binding is often considered low affinity binding, pertinent to our binding experiments, the affinity has been shown to be sufficient to withstand PBS washing of inoculated cell monolayers (91; 230). Our data demonstrated that binding of ABLV resistant CHOK1 cells by both ABLVp G and ABLVs G was similar to that of permissive BHK cells. Several mutant CHOK1 cell lines that are deficient in GAG biosynthesis, including HS, have been isolated (80; 81); thus, it would be interesting to examine whether HS plays a role in ABLV G-mediated viral binding to the resistant cells lines by investigating the ability of ABLV G to mediate viral binding to GAG deficient CHOK1 cells.



### ***ABLV and RABV utilize alternate host factors for entry***

Due to the close genetic relationship of ABLV and RABV, an obvious question at the start of this project was whether or not proposed RABV receptors play a role in ABLV entry. As previously mentioned, although it is not clear which host cell factor(s) interact with RABV G to facilitate RABV internalization into host cells, several potential receptors have been identified. Interestingly, ABLV resistant CHOK1 cells were previously reported to be highly permissive to the CVS-11 strain of RABV (258), suggesting that ABLV and RABV may utilize alternate receptors for host cell entry. We confirmed the high susceptibility of CHOK1 cells to RABV CVS-11 G-mediated viral entry and also found PCI-13 cells, another ABLV resistant line, were also highly permissive to RABV G-mediated entry. The expression of the proposed RABV protein receptors nAChR and NCAM was confirmed in both cell lines, indicating that nAChR and NCAM are not sufficient to allow host cell entry of ABLV. Moreover, HeLa-USU cells, which do not express NCAM on the cell surface (data not shown), are permissive to ABLV G-mediated infection further demonstrating that NCAM is not essential for ABLV infection. Rather, ABLV appears to utilize a receptor(s) for host cell entry that remains to be identified. Disruption of lipid raft integrity through sequestration of cholesterol with M $\beta$ CD significantly inhibited ABLV G-mediated entry into HEK293T cells, suggesting that the unknown ABLV receptor(s) may be localized or enriched in lipid rafts.

### **Review of Chapter 3 results**

In the second specific aim of this project, we sought to identify the endocytic pathway and endosomal compartment utilized by ABLV to gain entry into the host cell

cytosol. At the time these studies were initiated, there were no published reports detailing endocytosis and endocytic trafficking of a lyssavirus species, although EM analyses suggested that RABV was internalized via CME (155; 248) and microscopy studies indicated that RABV co-localized with markers for early endosomes (154; 155; 242). Recently, a study was published that used both biochemical and high resolution imaging approaches to show that RABV utilizes CME that is dependent on actin to enter epithelial cells (201). Other rhabdoviruses such as VSV and IHNV also utilize CME for host cell entry and also require actin for complete envelopment (160; 247). We hypothesized that ABLV would similarly utilize a clathrin-mediated pathway that is dependent on actin for internalization with subsequent fusion with early endosomes to gain entry into the cytosol.

To examine the endocytic pathway utilized by ABLV for internalization into HEK293T cells, we used the maxGFP-encoding replication competent recombinant ABLV G-expressing vesicular stomatitis viruses (rVSV) described in Chapter 2 (277). HEK293T cells were chosen as the cell culture model to study ABLV entry due to their recently described neuronal characteristics (119; 167; 237) as well as their ease of handling, robust growth rate, amenability to transfection, and high susceptibility to ABLV G-mediated viral infection (277).

***ABLV G-mediated viral entry occurs through a clathrin-mediated pathway that is dependent on actin***

To assess whether clathrin is required for ABLV entry, we first employed chemical inhibition studies using chlorpromazine, a drug that inhibits CME by blocking the assembly of clathrin coated pits (273). Chlorpromazine inhibited ABLV G-mediated entry in a dose-dependent manner, with >70% inhibition at the highest concentration. To

confirm CME as an entry pathway for ABLV, we examined the effect of the expression of the dominant negative (DN) Eps15 mutant EH29, which blocks CME by preventing clathrin-coated pit formation and does not affect non-clathrin pathways; Eps15 mutant DIIIΔ2, which has no effect on clathrin-coated pit assembly, was included as a negative control for the inhibition of CME (22-24). ABLV G-mediated viral entry was significantly inhibited by EH29 (60%) compared to eGFP and DIIIΔ2 controls. The uptake of cholera toxin B subunit (CTX-B), which is endocytosed by CavME (198), was not inhibited by EH29, demonstrating the specificity of EH29 in inhibiting CME. In agreement with entry studies of other rhabdoviruses, inhibition of actin polymerization with latrunculin B significantly inhibited ABLV G-mediated entry (> 65% inhibition). Taken together, these data suggest that ABLV G-mediated viral entry into HEK293T cells occurs through a clathrin-mediated pathway that is dependent on actin.

***Caveolar-dependent endocytosis and macropinocytosis are not involved in ABLV G-mediated viral entry***

We previously showed that the disruption of lipid rafts through cholesterol depletion significantly reduced ABLV G-mediated entry into HEK293T cells (277), a finding compatible with a clathrin- or caveolae-dependent entry pathway. Some viruses, such as Ebola virus (3; 27; 195; 227), influenza A (57; 225; 238), and reovirus (232), have been reported to utilize more than one type of endocytic pathway to gain entry into host cells. Therefore, we sought to test the possible contribution of pathways other than CME to ABLV G-mediated viral entry into HEK293T cells by using chemical inhibitors of CavME and macropinocytosis. Pretreatment of HEK293T cells with filipin, which disrupts CavME by specifically binding to cholesterol abundant in caveolae (220; 221), did not inhibit ABLV G-mediated entry, but did significantly decrease the uptake of

CTX-B into HEK293T cells. Similarly, pretreatment of HEK293T cells with EIPA, a potent inhibitor of  $\text{Na}^+/\text{H}^+$  exchanger activity required for macropinosome formation (182; 279), had no effect on ABLV G-mediated entry but, as previously reported, drastically inhibited Ebo GP-mediated viral entry (>98%) (195; 227). Taken together, these data indicate that CavME and macropinocytosis do not contribute to ABLV G-mediated entry into HEK293T cells, a finding in agreement with previous studies that show that CavME and macropinocytosis do not play a role in the entry of other rhabdoviruses (160; 201; 227).

***Rab5, but not Rab7 or Rab11, is required for ABLV G-mediated viral entry***

To investigate the subsequent trafficking route to the site of cytosol penetration, we examined the roles in ABLV entry of the small GTPases Rab5, Rab7, and Rab11, which are involved in vesicular trafficking to early, late, and recycling endosomes, respectively (86; 105; 266). Expression of the Rab5 DN significantly reduced ( $p < 0.005$ ) ABLV G-mediated viral entry compared to Rab5 WT, with greater than 40% inhibition for both ABLV variants. In contrast to Rab5, expression of DN mutants of Rab7 and Rab11 DN compared to WT plasmids slightly enhanced ABLV G-mediated viral entry but the increased infectivity was not statistically significant. Together, these data indicate that ABLV G-mediated fusion of viral and host cell membranes is triggered upon delivery to early endosomes and that productive ABLV infection does not require transfer to late or recycling endosomes.

## **Review of Chapter 4 results**

### ***Construction, expression, and purification of ABLV Gs***

To further characterize ABLV G and to explore its immunogenicity in animal models, we sought to develop an S-peptide-tagged version of soluble ABLV G (Gs). Initial attempts to construct soluble G glycoproteins derived from both the *Saccolaimus* and *Pteropus* ABLV variants by replacing the TM and CT domains of G with a C-terminal S-peptide tag were unsuccessful; the protein was expressed within the cell lysate but was not secreted from the cell. Codon optimization of ABLV Gs constructs significantly enhanced the expression of Gs in HEK293T cells, but did not improve the release of Gs from expressing cells. Numerous strategies were undertaken to improve the secretion of codon optimized Gs, most of which did not enhance secretion. A previous study found that the lack of secretion of a soluble form of RABV G was due to accumulation of misfolded RABV Gs in the rough endoplasmic reticulum (rER) (257). It is possible that a similar phenomenon was occurring for the ABLV Gs proteins and that they too were being retained in the ER. For numerous proteins, transport from the ER is facilitated not only by correct folding, but also by proper oligomerization (75; 133). Previous studies demonstrated that the T4 fibrin ‘foldon’ trimerization motif (254) provided enhanced stabilization of HIV-1 gp140 trimers compared to the GCNt motif (293) and promoted stable trimers of soluble RABV G (240). Insertion of a linker between the RABV G ectodomain and the T4 fibrin enhanced the expression of T4 fibrin, thereby enhancing the stabilization of RABV Gs (240). Fusion of the T4 fibrin motif to the ABLV Gs constructs significantly improved the secretion of ABLVs Gs, but not ABLVp Gs. Although it is not clear why the T4 fibrin motif failed to enhance ABLVp Gs secretion, different lyssavirus G glycoproteins have been shown to exhibit

differential oligomeric stability (71). It is possible that ABLVp G naturally forms less stable trimers than ABLVs G and that T4 fibrin was simply not sufficient to stabilize ABLVp Gs trimers to a degree that would permit ABLVp Gs escape from the ER, if in fact that is where ABLVp Gs is being accumulated; this has not been experimentally verified.

HEK293T cell lines that stably express ABLVs Gs-T4 and ABLVp Gs-T4 constructs were established, but protein yields from these cell lines were extremely low; lowering the culture temperature increased secreted protein production by ~4-fold, but protein yields remained low at ~0.5 to 2 ng/10<sup>6</sup> cells for ABLVp Gs and ABLVs Gs, respectively. Despite numerous attempts, a sufficient amount of purified ABLVp Gs for experimental analysis was not obtained; however, ABLVs Gs was successfully purified in small quantities and analysis of purified protein revealed that protein preparations were pure and that they were comprised of a mixture of monomers, dimers, and trimers of Gs, which is in agreement with what has been reported for other soluble rhabdovirus G glycoprotein preparations (2; 240).

Low production yields of soluble and secreted G is not unique to ABLV. Although there are several reports of the production of soluble and secreted forms of RABV G, none have reported high yields of Gs (97; 110; 289; 290). The inability to produce high quantities of recombinant soluble G likely explains why a crystal structure of a lyssavirus G glycoprotein has yet to be solved. The only rhabdovirus G crystal structure solved to date is that of VSV G (213; 215). For those studies, VSV G was cleaved from whole virions by limited proteolysis. This approach has not proven successful for RABV G (97). Additional strategies to increase ABLV Gs yields, such as

cleaving G from specially engineered viruses that express a version of ABLV G that contains a protease cleavage site immediately upstream of the TM domain, are currently being explored.

### ***Immunogenicity of ABLVs Gs and isolation of mouse anti-ABLVs G MAbs***

To evaluate whether immunization with ABLVs Gs could elicit an immune response, immunization protocols were carried out in mice and rabbits. Immunized animals generated a high titer of immunoreactivity against Gs as measured by ELISA and developed a potent cross-reactive virus neutralizing antibody response, indicating that ABLVs Gs retained important structural features of native full-length ABLVs G. These results suggest that ABLVs Gs could be an effective subunit vaccine against both variants of ABLV; however, the inability to produce high yields of ABLVs Gs makes its use as such impractical. It could however be a useful diagnostic reagent for the detection of ABLV G-specific antibodies in animal or human sera samples using ELISA or luminex platforms, which do not require large quantities of protein, and/or as antigen to pan for anti-ABLVs G hMAbs.

Mice immunized against ABLVs G were sacrificed and the spleens were harvested for hybridoma development. Two conformation dependent anti-ABLV G MAbs, DW8F10 (IgG1) and DW11C7 (IgA), that displayed a strong affinity for ABLVs Gs, as measured by ELISA, were purified from clonal hybridomas. Importantly, both MAbs reacted with native full-length ABLVs G, as measured by ELISA, and DW11C7 potently neutralized ABLVs G-mediated viral entry. Both of these MAbs as well as the mouse and rabbit anti-ABLV G immune sera will be valuable reagents for future ABLV studies.

## **Contributions to the field of lyssavirus entry**

All of the ABLV reagents (recombinant viruses and antibodies) used to complete the specific aims described herein were developed and generated as part of this project. These new reagents will be invaluable tools for future ABLV studies. The rVSV-ABLV G reporter viruses in particular, which were used to investigate and characterize the host cell entry of ABLV, will be invaluable for future strategies aimed at identifying the ABLV receptor(s) and additional host factors required for ABLV entry. Additionally, the rVSV-ABLVs G virus was recently used as antigen to pan for human anti-ABLV G monoclonal antibody fragments (Fabs), resulting in the isolation of two neutralizing Fabs that cross-react with ABLVp; the Fabs have since been converted to IgG1 MAbs (Dr. Bang Vu, personal communication). We also successfully developed and produced a secreted version of ABLVs G (Gs) that was used to generate both mouse and rabbit anti-ABLV G polyclonal sera and to produce and isolate mouse anti-ABLVs G MAbs, one of which is a potent neutralizer of ABLVs G-mediated entry.

Prior to this study, the contribution of the proposed RABV receptors to the entry of other lyssaviruses, including ABLV, were not known. Additionally, there was limited information available regarding the cross-species transmission potential of ABLV, which at the start of this project had only spilled over from bats into humans. The host cell infection tropism analyses presented in Chapter 2 indicate that similar to other bat lyssaviruses, ABLV is able to infect cells derived from numerous mammalian species and suggest that other terrestrial species could be productively infected by ABLV. We also showed that the proposed RABV receptors NCAM and nAChR were not sufficient to permit ABLV entry into host cells, highlighting the need for further research on lyssavirus entry. While this project did not result in the discovery of a receptor specific



for ABLV entry, we were able to identify several cell lines resistant to ABLV G-mediated viral entry. This is the first study to successfully identify cell lines resistant to virus entry mediated by a lyssavirus G glycoprotein, overcoming a major obstacle faced by the RABV field when trying to identify specific receptors for RABV entry since fixed strains of RABV are able to replicate in most continuous cell lines (258; 261). Thus, methods that have been successfully used to identify receptors for other viruses could not be used for RABV. ABLV resistant CHOK1 cells in particular, which are easy to transfect with expression plasmids, will be an invaluable tool for future studies aimed at ABLV receptor identification.

The present study also highlights that although ABLV and RABV exhibit unique tropisms and can utilize alternate receptors for host cell virus entry, they utilize similar entry pathways; this suggests that the identification of drug targets for the development of broad spectrum lyssavirus antiviral therapeutics may be possible. However, given that the host factors that have been thus far identified as being required for ABLV and RABV entry, such as clathrin, dynamin, actin, and Rab5, are all critical for host cellular processes, they may not make viable antiviral drug targets. Therapeutics that specifically target the viruses themselves, such as therapeutic antibodies, are much less likely to have undesirable side effects on the host cells. The aforementioned human anti-ABLV G MAbs isolated by Dr. Bang Vu (Uniformed Services University) using the recombinant VSV-ABLVs G virus developed during this study as antigen could lead to the development of more effective prophylactic measures for individuals exposed to ABLV.

## UNANSWERED QUESTIONS

**What is cellular receptor(s) for ABLV? Are different receptors used for initial replication in muscle and epithelial cells, entry into neurons at the NMJ, and neuronal spread within the CNS?**

Although this work did not lead to the discovery of a receptor for ABLV, it nevertheless has provided important information, including the identification of ABLV resistant cell lines, that can be used in future strategies aimed at receptor identification. Three receptor candidate proteins were evaluated as potential receptors for ABLV including neurexin 3 (NRXN3), synaptophysin-like 2 (SYPL2), and fibroblast growth factor receptor 1 (FGFR1). These candidates were chosen based on microarray gene expression data for permissive HEK293T cells and non-permissive PCI-13 cells that was generated by our lab previously and used to identify a functional receptor for Hendra virus and Nipah virus (33). All three candidates were expressed in HEK293T cells but were absent in PCI-13 cells. Additionally, all are transmembrane proteins expressed in neuronal cells at the pre-synaptic membrane, the site of initial lyssavirus entry into the nervous system (11; 142; 157). Flag-tagged cDNA clones of the candidate receptors, including 2-3 splice and/or isotype variants of each, were purchased as expression-ready clones from Origene (Rockville, MD) and were expressed in ABLV resistant CHOK1 cells; expression was verified by Western blotting with HRP-conjugated mouse anti-FLAG MAb M2 (Sigma Aldrich). All candidate receptors were expressed at high levels in CHOK1 cells, but expression did not render CHOK1 cells permissive to ABLV G-mediated viral entry (data not shown). However, multiple splice and isotype variants exist for neurexin 3 and FGFR1; due to limited financial resources and time we were not able to test all variants. Also, if an additional co-receptor or co-factor is required for interaction with ABLV G and its high affinity entry receptor, such as is the case for the

binding of many fibroblast growth factors (FGFs) to FGFRs, and CHOK1 cells lack the co-receptor or co-factor, then expression of the high affinity receptor may not result in productive ABLV infection. Thus, the negative results of these experiments do not necessarily mean that the receptor candidates do not play a role in ABLV entry.

Further complicating receptor discovery for lyssaviruses is that it is possible that different receptors are used to infect different cell types or are used at different stages of infection. For example, the RABV candidate receptor nAchR is located on the postsynaptic muscle membrane and not present on the presynaptic nerve membrane (143); thus, nAchR cannot be the receptor used by RABV to enter nerve cells. While nAchR is not required for RABV infection of neurons (178), it may account for replication of RABV in muscle cells at the site of inoculation (43). The use of multiple receptors by fixed strains of RABV to infect continuous cell lines, most of which express more than one RABV receptor candidate, has hampered RABV receptor discovery. The fact that a cellular receptor essential for RABV infection has not yet been identified further suggests that lyssavirus entry may be complicated, involving the interaction of G with multiple host factors, as is suggested for ABLV entry (Chapter 2). The identification of ABLV resistant cells in the present study will provide a platform for identifying a lyssavirus receptor that has been lacking until now.

### **Is it possible that multiple lyssavirus species utilize a common receptor for host cell entry?**

Although the tropism analyses presented in Chapter 2 demonstrate that proposed RABV receptors are not sufficient to permit ABLV entry into cells, indicating that ABLV requires an alternate receptor for host cell entry, it does not necessarily mean that an as yet unidentified shared receptor does not exist. For phylogroup I lyssaviruses, similar

disease course and pathogenicity, conserved antigenic regions, and the universal requirement of the arginine residue at amino acid position 333 of G for productive infection following intramuscular inoculation (14) suggest that these viruses may utilize a common receptor for initial entry into motor neurons.

Further supporting the idea of a conserved receptor binding domain among lyssavirus G glycoproteins is the highly conserved stretch of amino acids at positions 330-357 of G which have been shown to be sufficient to target fusion proteins to the CNS where they are internalized by receptor-mediated endocytosis (94). Alanine mutagenesis of conserved residues between 330-345 predicted to be surface exposed, reduced the expression of ABLVs G on the cell surface (data not shown) indicating that perhaps these residues are important for proper conformational folding of G. When more conserved mutations were made so that ABLVs G was still expressed on the cell surface, viral entry mediated by the mutant G glycoproteins was reduced (data not shown), further demonstrating the biological importance of this region of G. Perhaps a shared receptor does exist, but some lyssaviruses, such as RABV, have evolved to use additional receptors which expand its tropism to additional cell types in the brain enabling more efficient spread throughout the brain and CNS, thereby enhancing the neurovirulence of the virus. Expanded receptor tropism of RABV G could not only explain the *in vitro* tropism differences exhibited by ABLV G and RABV G, but may also explain the tropism differences exhibited by the two ABLV variants. Perhaps ABLVp G host interactions are simply more restricted than those of ABLVs G.

### **What additional host factors are required for entry? What about post-entry?**

Although we were able to define the entry pathway and subsequent trafficking route followed by ABLV for internalization into HEK293T cells, there is much knowledge yet to be gained regarding not only host factors required specifically for ABLV entry, but also host factors required for later steps in the ABLV life cycle. A more comprehensive examination of host factors required for ABLV infection could lead to the development of antiviral therapies that are not only effective against ABLV, but are also effective against other lyssaviruses. RNAi high-throughput screening technologies have been used to successfully identify host cell factors involved in numerous viral infections [reviewed in (60; 126)]. The recombinant VSV-ABLV G reporter viruses developed in this project will be invaluable tools for identifying host factors specific for ABLV entry through comparison of high throughput screening results with WT VSV reporter viruses. We are currently developing a reverse genetics system for ABLVp. Once rescued, this virus can be used to screen for host factors involved in post-entry events of the ABLV life cycle.

### **FUTURE DIRECTIONS**

Future work will focus on discovering additional host factors required for ABLV entry and infection by using a variety of techniques including loss-of-function screens such as haploid genetic screens (HAP1 screen) or siRNA high-throughput screens, or gain-of-function experiments such as phenotypic screening of a mouse/hamster radiation hybrid panel or cDNA library expression in non-permissive MDBK or CHOK1 cells. The recombinant VSV-ABLV G reporter viruses developed as part of this project will be particularly useful for identifying host factors required specifically for ABLV entry.

Haploid genetic screens are a powerful method for identifying host factors used by pathogens. They involve the use of a large library (~ 1 billion) of insertionally mutagenized transposon-tagged human haploid cells (HAP1 cells) to select for cells that are resistant to virus infection, in our case to VSV-ABLV G infection; cells infected by VSV-based viruses die within 1-2 days due to the cytopathic effect of VSV replication. Disrupted genes responsible for the viral resistance are then identified by mapping the integration sites of the resistant cells and comparing the distribution and frequency of the integration sites of these cells to the sites in the parental mutagenized library. This work will be done in collaboration with Drs. Paul Bates and Rick Bushman (University of Pennsylvania). Similar screens have been used to identify host factors required for Ebola virus entry (46; 47). We have already demonstrated that the parental HAP1 cells are highly permissive to ABLV G-mediated infection (data not shown).

High-throughput siRNA screening is another approach to identifying host factors required for pathogen infection. This approach will involve the use of a 9,000 gene siRNA library (four siRNAs per gene) in human osteosarcoma U2OS cells and will be done in collaboration with Dr. Sara Cherry (University of Pennsylvania). Preliminary data indicate that U2OS cells are permissive to ABLV-G mediated infection and a protocol for siRNA transfection into these cells has been optimized (data not shown).

Another approach that looks promising for identifying host factors required for ABLV entry is phenotypic screening of a mouse/Chinese hamster radiation hybrid (RH) panel (174). RH panels are generated by exposing donor cells from the species of interest to X-rays to generate small chromosomal fragments. These DNA fragments are then rescued through fusion with recipient hamster cells. Because Chinese hamster cells are

refractive to infection by many viruses, including ABLV, this is a powerful approach for mapping receptor genes and has been successfully used to identify cellular receptors for Jaagsiekte sheep retrovirus (JSRV) (208) and mouse mammary tumor virus (MMTV) (218). From this screen of approximately 100 hybridomas, which have each been typed for chromosomal framework markers, the chromosomal placement of the receptor is determined via an RH database server. Bacterial artificial chromosomes (BACs) from the candidate region can then be transfected into a resistant cell line for gain-of-function experiments; positive BAC clones may then be sequenced to identify the gene of interest. Alternatively, gain-of-function experiments in which ABLV resistant MDBK or CHOK1 cells are transduced or transfected with a cDNA expression library (commercially available), followed by infection with VSV-ABLV G reporter viruses, could be performed; cDNA clones that render resistant cells permissive to infection could then be isolated and sequenced.

We are also developing a reverse genetics system for WT ABLVp. A full-length ABLVp genome clone and ABLV N, P, and L expression plasmids have been constructed in collaboration with Dr. Ina Smith (CSIRO). Experiments to rescue ABLV are set to commence within the next few weeks. Once rescued, the WT ABLV virus can be used in high-throughput siRNA screens to identify host factors required for stages of the ABLV life cycle beyond initial entry.

Future work also includes further characterization of the mouse and human anti-ABLV G MAbs that have been isolated and produced during this study (the human MAbs were isolated by Dr. Bang Vu, Uniformed Services University). The VSV-ABLV G reporter viruses can be used to isolate additional human Fabs in order to generate a panel

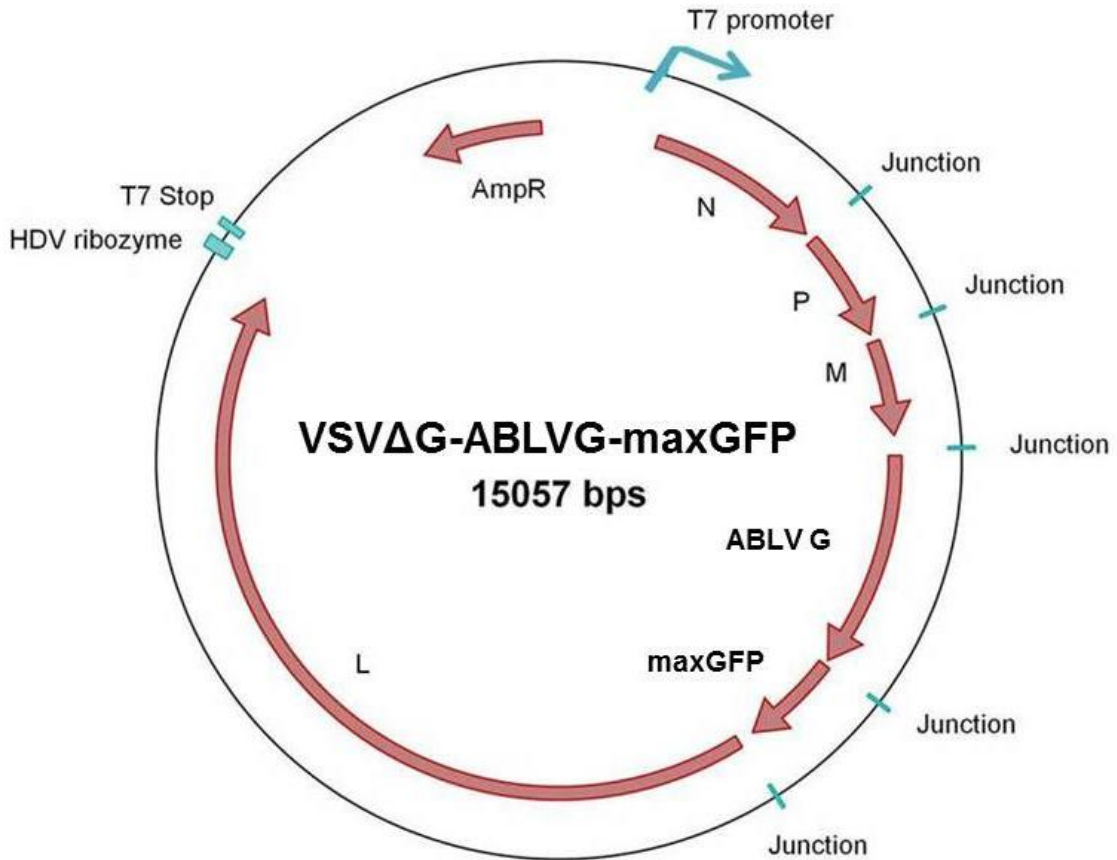
of antibodies that will not only be valuable research tools for future ABLV studies, but may lead to the development of improved therapeutics for individuals exposed to ABLV infected animals.

## **CONCLUSIONS**

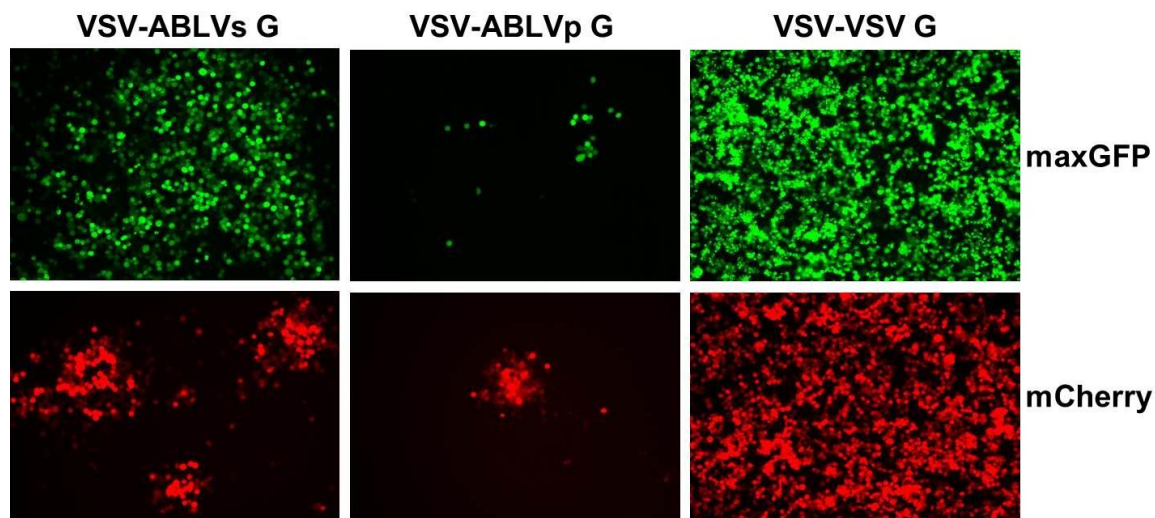
In summary, we have developed replication-competent rVSV maxGFP reporter viruses that encode ABLV G envelope glycoproteins and have used them to characterize ABLV host cell virus entry as a function of G. The results indicate that the unknown ABLV host cell receptor(s) is broadly conserved among mammalian species and may localize to lipid rafts. A clathrin- and actin-dependent endocytic pathway and subsequent fusion with early endosomes appears to be the predominant entry pathway utilized by ABLV to gain entry into HEK293T cells. The identification of cell lines resistant to ABLV infection, which to date has not been successful for RABV, will be an invaluable asset for strategies aimed at identifying the ABLV receptor. Furthermore, the recombinant VSV-ABLV G reporter viruses and other reagents that were developed during this project will be important tools for future studies that will yield new information about ABLV and lyssavirus biology and entry mechanisms.



## APPENDICES

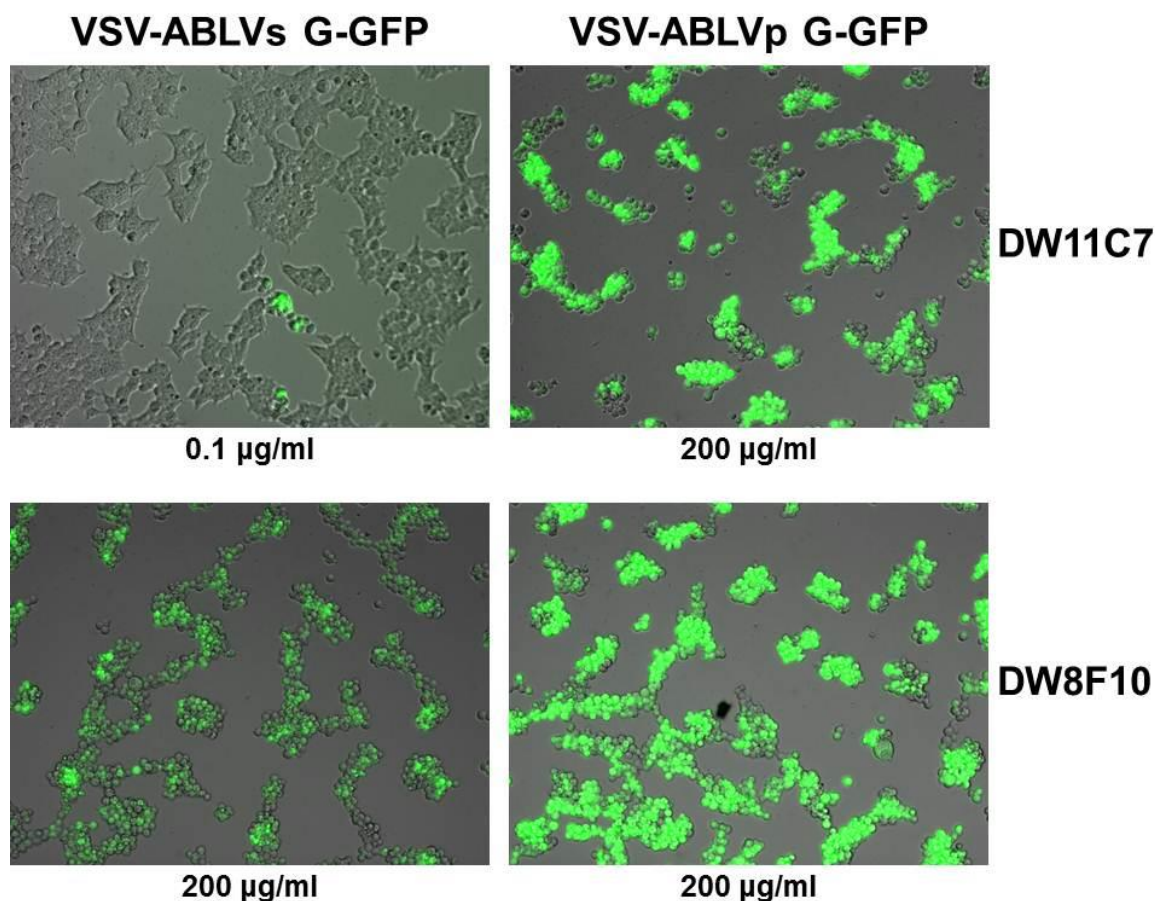


Appendix A. Plasmid map of the full-length cDNA clone of VSVΔG-ABLVG-maxGFP. Encodes full-length antigenomic (positive-sense) viral RNA (VSV Indiana N, P, M, and L genes and ABLV G) and the maxGFP green fluorescent protein under control of bacteriophage T7 promoter at 5' end and the self-cleaving Hepatitis delta virus ribozyme at 3' end. Similar plasmids were constructed that encode the mCherry red fluorescent protein in place of maxGFP.



#### Appendix B. Rescue of recombinant VSV-ABLV G and WT VSV-reporter viruses.

HEK293T cells at 75% confluence were transfected with plasmids encoding VSV N (2.5  $\mu$ g), P (2.5  $\mu$ g), and L (0.5  $\mu$ g), and 2.5  $\mu$ g of plasmids encoding the recombinant VSV-ABLV G-maxGFP or VSV-ABLV G-mCherry antigenomic RNA (2.5  $\mu$ g) using Lipofectamine LTX (Invitrogen). 4 hrs post transfection cells were washed with PBS and infected with MVA-T7 (MOI of 5). 1 hr post infection cells washed with PBS and 1.5 ml of fresh DMEM-10 added. After 48 hrs cells and supernatants were collected and freeze-thawed 3x (-80°C, 37°C) to release cell-associated virus. Lysates were clarified by centrifugation at 1300xg for 10 min. The supernatant was added to HEK293T cells in a 6-well plate. After 48 hrs cells were examined for maxGFP or mCherry expression and CPE by microscopy (10x objective).



Appendix C. Mouse anti-ABLVs G MAb DW11C7 potently neutralizes ABLVs G-, but not ABLVp G-mediated viral entry. MAbs were serially diluted in DMEM-10, in duplicate wells, in a 96-well tissue culture plate and mixed with  $5 \times 10^4$  IU of either VSV-ABLVp G-, VSV-ABLVs G-, or VSV-VSV G-GFP viruses for 30 min at 37°C. Dilutions of purified MAbs started at 200 µg/ml. A total of  $5 \times 10^4$  HEK293T cells were added to each well, incubated overnight at 37°C, and observed for GFP expression (Table 4). Representative microscopic fields of viruses pre-incubated with the indicated MAbs concentrations. DW8F10, which does not recognize a neutralizing epitope of ABLVs G, was included as a negative control. Even at the lowest concentration tested (0.1 µg/ul), the majority of VSV-ABLVs G virus was neutralized by DW11C7.

## REFERENCES

1. Albertini AA, Baquero E, Ferlin A, Gaudin Y. 2012. Molecular and cellular aspects of rhabdovirus entry. *Viruses* 4:117-39
2. Albertini AA, Merigoux C, Libersou S, Madiona K, Bressanelli S, et al. 2012. Characterization of monomeric intermediates during VSV glycoprotein structural transition. *PLoS Pathog* 8:e1002556
3. Aleksandrowicz P, Marzi A, Biedenkopf N, Beimforde N, Becker S, et al. 2011. Ebola virus enters host cells by macropinocytosis and clathrin-mediated endocytosis. *J Infect Dis* 204 Suppl 3:S957-67
4. Allworth A, Murray K, Morgan J. 1996. A human case of encephalitis due to a lyssavirus recently identified in fruit bats. *Commun. Dis. Intellig.* 20:504
5. Alvarez L, Fajardo R, Lopez E, Pedroza R, Hemachudha T, et al. 1994. Partial recovery from rabies in a nine-year-old boy. *Pediatr Infect Dis J* 13:1154-5
6. Anonymous. 2012. Milwaukee Protocol, version 4.0, Children's Hospital of Wisconsin, Milwaukee
7. Anonymous. 2013. Australian bat lyssavirus - Australia (02): Queensland, human fatality *Rep. 20130323.1600266*, International Society for Infectious Diseases
8. Anonymous. 2013. AUSTRALIAN BAT LYSSAVIRUS - AUSTRALIA (04): EQUINE FATALITIES. *Rep. 20130517.1720540*, International Society for Infectious Diseases
9. Anonymous. 2013. RABIES - INDIA (06): (MADHYA PRADESH): CANINE, HUMAN-TO-HUMAN TRANSMISSION SUSPECTED, International Society for Infectious Diseases
10. Anonymous. 2013. Rabies - USA (02): (Maryland) Organ Transplant. *Rep. 20130316.1589941*, International Society for Infectious Diseases
11. Aoto J, Martinelli DC, Malenka RC, Tabuchi K, Sudhof TC. 2013. Presynaptic neurexin-3 alternative splicing trans-synaptically controls postsynaptic AMPA receptor trafficking. *Cell* 154:75-88
12. Arguin PM, Murray-Lillibridge K, Miranda ME, Smith JS, Calaor AB, Rupprecht CE. 2002. Serologic evidence of Lyssavirus infections among bats, the Philippines. *Emerg Infect Dis* 8:258-62
13. Baba M, Snoeck R, Pauwels R, de Clercq E. 1988. Sulfated polysaccharides are potent and selective inhibitors of various enveloped viruses, including herpes

- simplex virus, cytomegalovirus, vesicular stomatitis virus, and human immunodeficiency virus. *Antimicrob Agents Chemother* 32:1742-5
14. Badrane H, Bahloul C, Perrin P, Tordo N. 2001. Evidence of two Lyssavirus phylogroups with distinct pathogenicity and immunogenicity. *J Virol* 75:3268-76
  15. Badrane H, Tordo N. 2001. Host switching in Lyssavirus history from the Chiroptera to the Carnivora orders. *J Virol* 75:8096-104
  16. Baer GM, ed. 1991. *The Natural History of Rabies*. Boca Raton: CRC Press. 2nd ed.
  17. Banyard AC, Hayman D, Johnson N, McElhinney L, Fooks AR. 2011. Bats and lyssaviruses. *Advances in virus research* 79:239-89
  18. Barrett J. 2004. *Australian Bat Lyssavirus*. University of Queensland
  19. Bashkirov PV, Akimov SA, Evseev AI, Schmid SL, Zimmerberg J, Frolov VA. 2008. GTPase cycle of dynamin is coupled to membrane squeeze and release, leading to spontaneous fission. *Cell* 135:1276-86
  20. Belikov SI, Leonova GN, Kondratov IG, Romanova EV, Pavlenko EV. 2009. Isolation and genetic characterisation of a new lyssavirus strain in the Primorskiy kray. *East Siberian J. Infect. Pathol.* 16:68-9
  21. Benmansour A, Leblois H, Coulon P, Tuffereau C, Gaudin Y, et al. 1991. Antigenicity of rabies virus glycoprotein. *J Virol* 65:4198-203
  22. Benmerah A, Bayrou M, Cerf-Bensussan N, Dautry-Varsat A. 1999. Inhibition of clathrin-coated pit assembly by an Eps15 mutant. *J Cell Sci* 112 ( Pt 9):1303-11
  23. Benmerah A, Lamaze C, Begue B, Schmid SL, Dautry-Varsat A, Cerf-Bensussan N. 1998. AP-2/Eps15 interaction is required for receptor-mediated endocytosis. *J Cell Biol* 140:1055-62
  24. Benmerah A, Poupon V, Cerf-Bensussan N, Dautry-Varsat A. 2000. Mapping of Eps15 domains involved in its targeting to clathrin-coated pits. *J Biol Chem* 275:3288-95
  25. Bernard E, Solignat M, Gay B, Chazal N, Higgs S, et al. 2010. Endocytosis of chikungunya virus into mammalian cells: role of clathrin and early endosomal compartments. *PLoS ONE* 5:e11479
  26. Bernfield M, Gotte M, Park PW, Reizes O, Fitzgerald ML, et al. 1999. Functions of cell surface heparan sulfate proteoglycans. *Annu Rev Biochem* 68:729-77

27. Bhattacharyya S, Warfield KL, Ruthel G, Bavari S, Aman MJ, Hope TJ. 2010. Ebola virus uses clathrin-mediated endocytosis as an entry pathway. *Virology* 401:18-28
28. Bingham J, van der Merwe M. 2002. Distribution of rabies antigen in infected brain material: determining the reliability of different regions of the brain for the rabies fluorescent antibody test. *J Virol Methods* 101:85-94
29. Blanchard E, Belouzard S, Goueslain L, Wakita T, Dubuisson J, et al. 2006. Hepatitis C virus entry depends on clathrin-mediated endocytosis. *J Virol* 80:6964-72
30. Blanco JC, Pletneva LM, Wieczorek L, Khetawat D, Stantchev TS, et al. 2009. Expression of Human CD4 and chemokine receptors in cotton rat cells confers permissiveness for productive HIV infection. *Virol J* 6:57
31. Blondeau F, Ritter B, Allaire PD, Wasiak S, Girard M, et al. 2004. Tandem MS analysis of brain clathrin-coated vesicles reveals their critical involvement in synaptic vesicle recycling. *Proc Natl Acad Sci U S A* 101:3833-8
32. Blumenthal R, Bali-Puri A, Walter A, Covell D, Eidelman O. 1987. pH-dependent fusion of vesicular stomatitis virus with Vero cells. Measurement by dequenching of octadecyl rhodamine fluorescence. *J Biol Chem* 262:13614-9
33. Bonaparte MI, Dimitrov AS, Bossart KN, Crameri G, Mungall BA, et al. 2005. Ephrin-B2 ligand is a functional receptor for Hendra virus and Nipah virus. *Proc Natl Acad Sci U S A* 102:10652-7
34. Bossart KN, Crameri G, Dimitrov AS, Mungall BA, Feng YR, et al. 2005. Receptor binding, fusion inhibition, and induction of cross-reactive neutralizing antibodies by a soluble G glycoprotein of Hendra virus. *J Virol* 79:6690-702
35. Bossart KN, Wang LF, Eaton BT, Broder CC. 2001. Functional expression and membrane fusion tropism of the envelope glycoproteins of Hendra virus. *Virology* 290:121-35
36. Botvinkin A, Selnikova OP, Anotonova LA, Moiseeva AB, Nesterenko EY. 2005. Human rabies case caused from a bat bite in Ukraine. *Rabies Bull. Eruope* 29:5-7
37. Boucrot E, Saffarian S, Massol R, Kirchhausen T, Ehrlich M. 2006. Role of lipids and actin in the formation of clathrin-coated pits. *Exp Cell Res* 312:4036-48
38. Boulant S, Kural C, Zeeh JC, Ubelmann F, Kirchhausen T. 2011. Actin dynamics counteract membrane tension during clathrin-mediated endocytosis. *Nat Cell Biol* 13:1124-31
39. Bourhy H, Kissi B, Tordo N. 1993. Molecular diversity of the Lyssavirus genus. *Virology* 194:70-81

40. Bronnert J, Wilde H, Tepsumethanon V, Lumlertdacha B, Hemachudha T. 2007. Organ transplantations and rabies transmission. *J Travel Med* 14:177-80
41. Brookes SM, Parsons G, Johnson N, McElhinney LM, Fooks AR. 2005. Rabies human diploid cell vaccine elicits cross-neutralising and cross-protecting immune responses against European and Australian bat lyssaviruses. *Vaccine* 23:4101-9
42. Bruce EA, Stuart A, McCaffrey MW, Digard P. 2012. Role of the Rab11 pathway in negative-strand virus assembly. *Biochem Soc Trans* 40:1409-15
43. Burrage TG, Tignor GH, Smith AL. 1985. Rabies virus binding at neuromuscular junctions. *Virus Res* 2:273-89
44. Callahan LN, Phelan M, Mallinson M, Norcross MA. 1991. Dextran sulfate blocks antibody binding to the principal neutralizing domain of human immunodeficiency virus type 1 without interfering with gp120-CD4 interactions. *J Virol* 65:1543-50
45. Cantin C, Holguera J, Ferreira L, Villar E, Munoz-Barroso I. 2007. Newcastle disease virus may enter cells by caveolae-mediated endocytosis. *J Gen Virol* 88:559-69
46. Carette JE, Guimaraes CP, Varadarajan M, Park AS, Wuethrich I, et al. 2009. Haploid genetic screens in human cells identify host factors used by pathogens. *Science* 326:1231-5
47. Carette JE, Raaben M, Wong AC, Herbert AS, Obernosterer G, et al. 2011. Ebola virus entry requires the cholesterol transporter Niemann-Pick C1. *Nature* 477:340-3
48. CDC. 1977. Rabies in a laboratory worker - New York, MMWR 26:183-184
49. CDC. 2004. Recovery of a patient from clinical rabies--Wisconsin, 2004. *MMWR Morb Mortal Wkly Rep* 53:1171-3
50. CDC. 2010. Presumptive abortive human rabies - Texas, 2009. *MMWR Morb Mortal Wkly Rep* 59:185-90
51. CDC. 2012. Recovery of a patient from clinical rabies--California, 2011. *MMWR Morb Mortal Wkly Rep* 61:61-5
52. CDNA. 2012. CDNA National guidelines for public health units: rabies virus and other lyssavirus (including Australian bat lyssavirus) exposures and infections, Communicable Disease Network Australia
53. Ceballos NA, Moron, S. V., Berciano, J. M., Nicolas, O., Lopez, C. A., Juste, J., Nevado, C. R., Setien, A. A., and Echevarria, J. E. 2013. Novel Lyssavirus in Bat, Spain. *Emerg Infect Dis* 19:793-5

54. Chan YP, Lu M, Dutta S, Yan L, Barr J, et al. 2012. Biochemical, conformational, and immunogenic analysis of soluble trimeric forms of henipavirus fusion glycoproteins. *J Virol* 86:11457-71
55. Chan YP, Yan L, Feng YR, Broder CC. 2009. Preparation of recombinant viral glycoproteins for novel and therapeutic antibody discovery. *Methods Mol Biol* 525:31-58, xiii
56. Charlton KM. 1984. Rabies: spongiform lesions in the brain. *Acta Neuropathol* 63:198-202
57. Chen C, Zhuang X. 2008. Epsin 1 is a cargo-specific adaptor for the clathrin-mediated endocytosis of the influenza virus. *Proc Natl Acad Sci U S A* 105:11790-5
58. Chen W, Feng Y, Chen D, Wandinger-Ness A. 1998. Rab11 is required for trans-golgi network-to-plasma membrane transport and a preferential target for GDP dissociation inhibitor. *Mol Biol Cell* 9:3241-57
59. Cheng Y, Boll W, Kirchhausen T, Harrison SC, Walz T. 2007. Cryo-electron tomography of clathrin-coated vesicles: structural implications for coat assembly. *J Mol Biol* 365:892-9
60. Cherry S. 2011. RNAi screening for host factors involved in viral infection using *Drosophila* cells. *Methods Mol Biol* 721:375-82
61. Choudhury A, Dominguez M, Puri V, Sharma DK, Narita K, et al. 2002. Rab proteins mediate Golgi transport of caveola-internalized glycosphingolipids and correct lipid trafficking in Niemann-Pick C cells. *J Clin Invest* 109:1541-50
62. Chu JJ, Leong PW, Ng ML. 2006. Analysis of the endocytic pathway mediating the infectious entry of mosquito-borne flavivirus West Nile into *Aedes albopictus* mosquito (C6/36) cells. *Virology* 349:463-75
63. Chu JJ, Ng ML. 2004. Infectious entry of West Nile virus occurs through a clathrin-mediated endocytic pathway. *J Virol* 78:10543-55
64. Clemente R, de la Torre JC. 2009. Cell entry of Borna disease virus follows a clathrin-mediated endocytosis pathway that requires Rab5 and microtubules. *J Virol* 83:10406-16
65. Constantine DG. 1962. Rabies transmission by nonbite route. *Public Health Rep* 77:287-9
66. Conti C, Superti F, Tsiang H. 1986. Membrane carbohydrate requirement for rabies virus binding to chicken embryo related cells. *Intervirology* 26:164-8



67. Cureton DK, Massol RH, Saffarian S, Kirchhausen TL, Whelan SP. 2009. Vesicular stomatitis virus enters cells through vesicles incompletely coated with clathrin that depend upon actin for internalization. *PLoS Pathog* 5:e1000394
68. Cureton DK, Massol RH, Whelan SP, Kirchhausen T. 2010. The length of vesicular stomatitis virus particles dictates a need for actin assembly during clathrin-dependent endocytosis. *PLoS Pathog* 6:e1001127
69. Dean DJ, Baer GM, Thompson WR. 1963. Studies on the local treatment of rabies-infected wounds. *Bull World Health Organ* 28:477-86
70. Deborde S, Perret E, Gravotta D, Deora A, Salvarezza S, et al. 2008. Clathrin is a key regulator of basolateral polarity. *Nature* 452:719-23
71. Desmezieres E, Maillard AP, Gaudin Y, Tordo N, Perrin P. 2003. Differential stability and fusion activity of Lyssavirus glycoprotein trimers. *Virus Res* 91:181-7
72. Dietzschold B, Tollis M, Rupprecht CE, Celis E, Koprowski H. 1987. Antigenic variation in rabies and rabies-related viruses: cross-protection independent of glycoprotein-mediated virus-neutralizing antibody. *J Infect Dis* 156:815-22
73. Dietzschold B, Wunner WH, Wiktor TJ, Lopes AD, Lafon M, et al. 1983. Characterization of an antigenic determinant of the glycoprotein that correlates with pathogenicity of rabies virus. *Proc Natl Acad Sci U S A* 80:70-4
74. Dolman CL, Charlton KM. 1987. Massive necrosis of the brain in rabies. *Can J Neurol Sci* 14:162-5
75. Doms RW, Lamb RA, Rose JK, Helenius A. 1993. Folding and assembly of viral membrane proteins. *Virology* 193:545-62
76. Dube D, Schornberg KL, Stantchev TS, Bonaparte MI, Delos SE, et al. 2008. Cell adhesion promotes Ebola virus envelope glycoprotein-mediated binding and infection. *J Virol* 82:7238-42
77. Earl PL, Broder CC, Long D, Lee SA, Peterson J, et al. 1994. Native oligomeric human immunodeficiency virus type 1 envelope glycoprotein elicits diverse monoclonal antibody reactivities. *J Virol* 68:3015-26
78. Ehrlich M, Boll W, Van Oijen A, Hariharan R, Chandran K, et al. 2004. Endocytosis by random initiation and stabilization of clathrin-coated pits. *Cell* 118:591-605
79. Elferink JG. 1979. Chlorpromazine inhibits phagocytosis and exocytosis in rabbit polymorphonuclear leukocytes. *Biochem Pharmacol* 28:965-8

80. Esko JD. 1991. Genetic analysis of proteoglycan structure, function and metabolism. *Curr Opin Cell Biol* 3:805-16
81. Esko JD, Stewart TE, Taylor WH. 1985. Animal cell mutants defective in glycosaminoglycan biosynthesis. *Proc Natl Acad Sci U S A* 82:3197-201
82. Familusi JB, Moore DL. 1972. Isolation of a rabies related virus from the cerebrospinal fluid of a child with 'aseptic meningitis'. *Afr J Med Sci* 3:93-6
83. Familusi JB, Osunkoya BO, Moore DL, Kemp GE, Fabiyi A. 1972. A fatal human infection with Mokola virus. *Am J Trop Med Hyg* 21:959-63
84. Fekadu M. 1988. Pathogenesis of rabies virus infection in dogs. *Rev Infect Dis* 10 Suppl 4:S678-83
85. Fekadu M, Shaddock JH, Sanderlin DW, Smith JS. 1988. Efficacy of rabies vaccines against Duvenhage virus isolated from European house bats (*Eptesicus serotinus*), classic rabies and rabies-related viruses. *Vaccine* 6:533-9
86. Feng Y, Press B, Wandinger-Ness A. 1995. Rab 7: an important regulator of late endocytic membrane traffic. *J Cell Biol* 131:1435-52
87. Field H, McCall B, Barrett J. 1999. Australian bat lyssavirus infection in a captive juvenile black flying fox. *Emerg Infect Dis* 5:438-40
88. Field HE. 2005. *Australian bat lyssavirus*. University of Queensland
89. Flamand A, Raux H, Gaudin Y, Ruigrok RW. 1993. Mechanisms of rabies virus neutralization. *Virology* 194:302-13
90. Flores-Rodriguez N, Rogers SS, Kenwright DA, Waigh TA, Woodman PG, Allan VJ. 2011. Roles of dynein and dynactin in early endosome dynamics revealed using automated tracking and global analysis. *PLoS ONE* 6:e24479
91. Flynn SJ, Ryan P. 1996. The receptor-binding domain of pseudorabies virus glycoprotein gC is composed of multiple discrete units that are functionally redundant. *J Virol* 70:1355-64
92. Fooks AR, McElhinney LM, Pounder DJ, Finnegan CJ, Mansfield K, et al. 2003. Case report: isolation of a European bat lyssavirus type 2a from a fatal human case of rabies encephalitis. *J Med Virol* 71:281-9
93. Fraser GC, Hooper PT, Lunt RA, Gould AR, Gleeson LJ, et al. 1996. Encephalitis caused by a Lyssavirus in fruit bats in Australia. *Emerg Infect Dis* 2:327-31
94. Fu A, Wang Y, Zhan L, Zhou R. 2012. Targeted delivery of proteins into the central nervous system mediated by rabies virus glycoprotein-derived peptide. *Pharm Res* 29:1562-9

95. Fujimoto LM, Roth R, Heuser JE, Schmid SL. 2000. Actin assembly plays a variable, but not obligatory role in receptor-mediated endocytosis in mammalian cells. *Traffic* 1:161-71
96. Gaudin Y. 2000. Rabies virus-induced membrane fusion pathway. *J Cell Biol* 150:601-12
97. Gaudin Y, Moreira S, Benejean J, Blondel D, Flamand A, Tuffereau C. 1999. Soluble ectodomain of rabies virus glycoprotein expressed in eukaryotic cells folds in a monomeric conformation that is antigenically distinct from the native state of the complete, membrane-anchored glycoprotein. *J Gen Virol* 80 ( Pt 7):1647-56
98. Gaudin Y, Raux H, Flamand A, Ruigrok RW. 1996. Identification of amino acids controlling the low-pH-induced conformational change of rabies virus glycoprotein. *J Virol* 70:7371-8
99. Gaudin Y, Ruigrok RW, Knossow M, Flamand A. 1993. Low-pH conformational changes of rabies virus glycoprotein and their role in membrane fusion. *J Virol* 67:1365-72
100. Gaudin Y, Ruigrok RW, Tuffereau C, Knossow M, Flamand A. 1992. Rabies virus glycoprotein is a trimer. *Virology* 187:627-32
101. Gaudin Y, Tuffereau C, Durrer P, Flamand A, Ruigrok RW. 1995. Biological function of the low-pH, fusion-inactive conformation of rabies virus glycoprotein (G): G is transported in a fusion-inactive state-like conformation. *J Virol* 69:5528-34
102. Gaudin Y, Tuffereau C, Segretain D, Knossow M, Flamand A. 1991. Reversible conformational changes and fusion activity of rabies virus glycoprotein. *J Virol* 65:4853-9
103. Gilbert AT, Petersen BW, Recuenco S, Niezgodka M, Gomez J, et al. 2012. Evidence of rabies virus exposure among humans in the Peruvian Amazon. *Am J Trop Med Hyg* 87:206-15
104. Gorfien SFU, Fike, Richard M. (US), Dzimian, Joyce L. (US), Godwin, Glenn P. (US), Price, Paul J. (US), Epstein, David A. (US), Gruber, Dale (US), McClure, Don (US). 2004.
105. Gorvel JP, Chavrier P, Zerial M, Gruenberg J. 1991. rab5 controls early endosome fusion in vitro. *Cell* 64:915-25
106. Gould AR, Hyatt AD, Lunt R, Kattenbelt JA, Hengstberger S, Blacksell SD. 1998. Characterisation of a novel lyssavirus isolated from Pteropid bats in Australia. *Virus Res* 54:165-87

107. Gould AR, Kattenbelt JA, Gumley SG, Lunt RA. 2002. Characterisation of an Australian bat lyssavirus variant isolated from an insectivorous bat. *Virus Res* 89:1-28
108. Graham FL, Smiley J, Russell WC, Nairn R. 1977. Characteristics of a human cell line transformed by DNA from human adenovirus type 5. *J Gen Virol* 36:59-74
109. Gruenberg J. 2009. Viruses and endosome membrane dynamics. *Curr Opin Cell Biol* 21:582-8
110. Gupta PK, Sharma S, Walunj SS, Chaturvedi VK, Raut AA, et al. 2005. Immunogenic and antigenic properties of recombinant soluble glycoprotein of rabies virus. *Vet Microbiol* 108:207-14
111. Guyatt KJ, Twin J, Davis P, Holmes EC, Smith GA, et al. 2003. A molecular epidemiological study of Australian bat lyssavirus. *J Gen Virol* 84:485-96
112. Hall L, Richards G. 2000. *Flying Foxes: Fruit and Blossom Bats of Australia*. Sydney: University of New South Wales Press
113. Halpin K, Young PL, Field HE, Mackenzie JS. 2000. Isolation of Hendra virus from pteropid bats: a natural reservoir of Hendra virus. *J Gen Virol* 81:1927-32
114. Hanham CA, Zhao F, Tignor GH. 1993. Evidence from the anti-idiotypic network that the acetylcholine receptor is a rabies virus receptor. *J Virol* 67:530-42
115. Hanlon CA, Kuzmin IV, Blanton JD, Weldon WC, Manangan JS, Rupprecht CE. 2005. Efficacy of rabies biologics against new lyssaviruses from Eurasia. *Virus Res* 111:44-54
116. Hanna JN, Carney IK, Smith GA, Tannenberg AE, Deverill JE, et al. 2000. Australian bat lyssavirus infection: a second human case, with a long incubation period. *Med. J. Aust.* 172:597-9
117. Harbury PB, Kim PS, Alber T. 1994. Crystal structure of an isoleucine-zipper trimer. *Nature* 371:80-3
118. Hattwick MA, Weis TT, Stechschulte CJ, Baer GM, Gregg MB. 1972. Recovery from rabies. A case report. *Ann Intern Med* 76:931-42
119. He B, Soderlund DM. 2010. Human embryonic kidney (HEK293) cells express endogenous voltage-gated sodium currents and Na v 1.7 sodium channels. *Neurosci Lett* 469:268-72
120. Heldwein EE, Lou H, Bender FC, Cohen GH, Eisenberg RJ, Harrison SC. 2006. Crystal structure of glycoprotein B from herpes simplex virus 1. *Science* 313:217-20

121. Hellenbrand W, Meyer C, Rasch G, Steffens I, Ammon A. 2005. Cases of rabies in Germany following organ transplantation. *Euro Surveill* 10:E050224 6
122. Hemachudha T, Phanuphak P, Sriwanthana B, Manutsathit S, Phanthumchinda K, et al. 1988. Immunologic study of human encephalitic and paralytic rabies. Preliminary report of 16 patients. *Am J Med* 84:673-7
123. Hemachudha T, Phuapradit P. 1997. Rabies. *Curr Opin Neurol* 10:260-7
124. Henne WM, Boucrot E, Meinecke M, Evergren E, Vallis Y, et al. 2010. FCHo proteins are nucleators of clathrin-mediated endocytosis. *Science* 328:1281-4
125. Hinshaw JE, Schmid SL. 1995. Dynamin self-assembles into rings suggesting a mechanism for coated vesicle budding. *Nature* 374:190-2
126. Hirsch AJ. 2010. The use of RNAi-based screens to identify host proteins involved in viral replication. *Future Microbiol* 5:303-11
127. Hollinshead M, Johns HL, Sayers CL, Gonzalez-Lopez C, Smith GL, Elliott G. 2012. Endocytic tubules regulated by Rab GTPases 5 and 11 are used for envelopment of herpes simplex virus. *EMBO J* 31:4204-20
128. Hooper PT, Fraser GC, Foster RA, Storie GJ. 1999. Histopathology and immunohistochemistry of bats infected by Australian bat lyssavirus. *Aust Vet J* 77:595-9
129. Hooper PT, Lunt RA, Gould AR, Samaratunga H, Hyatt AD, et al. 1997. A new lyssavirus: the first endemic rabies-related virus recognized in Australia. *Bull. Inst. Pasteur* 95:209-18
130. Houff SA, Burton RC, Wilson RW, Henson TE, London WT, et al. 1979. Human-to-human transmission of rabies virus by corneal transplant. *N Engl J Med* 300:603-4
131. Hu WT, Willoughby RE, Jr., Dhonau H, Mack KJ. 2007. Long-term follow-up after treatment of rabies by induction of coma. *N Engl J Med* 357:945-6
132. Hurst EW, Pawan JL. 1959. An outbreak of rabies in Trinidad without history of bites, and with the symptoms of acute ascending myelitis. *Caribb Med J* 21:11-24
133. Hurtley SM, Helenius A. 1989. Protein oligomerization in the endoplasmic reticulum. *Annu Rev Cell Biol* 5:277-307
134. Hussain KM, Leong KL, Ng MM, Chu JJ. 2011. The essential role of clathrin-mediated endocytosis in the infectious entry of human enterovirus 71. *J Biol Chem* 286:309-21

135. Iversen TG, Frerker N, Sandvig K. 2012. Uptake of ricinB-quantum dot nanoparticles by a macropinocytosis-like mechanism. *J Nanobiotechnology* 10:33
136. Jackson AC. 2003. Rabies virus infection: an update. *J Neurovirol* 9:253-8
137. Jenniskens GJ, Veerkamp JH, van Kuppevelt TH. 2006. Heparan sulfates in skeletal muscle development and physiology. *J Cell Physiol* 206:283-94
138. Johannsdottir HK, Mancini R, Kartenbeck J, Amato L, Helenius A. 2009. Host cell factors and functions involved in vesicular stomatitis virus entry. *J Virol* 83:440-53
139. Kennard ML, Lizee GA, Jefferies WA. 1999. GPI-Anchored Fusion Proteins. 8:187-200. Number of 187-200 pp.
140. Kim C, Bergelson JM. 2012. Echovirus 7 entry into polarized intestinal epithelial cells requires clathrin and Rab7. *MBio* 3
141. Krishnan MN, Sukumaran B, Pal U, Agaisse H, Murray JL, et al. 2007. Rab 5 is required for the cellular entry of dengue and West Nile viruses. *J Virol* 81:4881-5
142. Kwon SE, Chapman ER. 2011. Synaptophysin regulates the kinetics of synaptic vesicle endocytosis in central neurons. *Neuron* 70:847-54
143. Lafon M. 2005. Rabies virus receptors. *J Neurovirol* 11:82-7
144. Lafon M, Bourhy H, Sureau P. 1988. Immunity against the European bat rabies (Duvenhage) virus induced by rabies vaccines: an experimental study in mice. *Vaccine* 6:362-8
145. Lafon M, Herzog M, Sureau P. 1986. Human rabies vaccines induce neutralising antibodies against the European bat rabies virus (Duvenhage). *Lancet* 2:515
146. Lakadamyali M, Rust MJ, Zhuang X. 2004. Endocytosis of influenza viruses. *Microbes Infect* 6:929-36
147. Lakadamyali M, Rust MJ, Zhuang X. 2006. Ligands for clathrin-mediated endocytosis are differentially sorted into distinct populations of early endosomes. *Cell* 124:997-1009
148. Lawson ND, Stillman EA, Whitt MA, Rose JK. 1995. Recombinant vesicular stomatitis viruses from DNA. *Proc Natl Acad Sci U S A* 92:4477-81
149. Lee E, Knecht DA. 2002. Visualization of actin dynamics during macropinocytosis and exocytosis. *Traffic* 3:186-92

150. Lee RC, Hapuarachchi HC, Chen KC, Hussain KM, Chen H, et al. 2013. Mosquito cellular factors and functions in mediating the infectious entry of chikungunya virus. *PLoS Negl Trop Dis* 7:e2050
151. Lentz TL, Burrage TG, Smith AL, Crick J, Tignor GH. 1982. Is the acetylcholine receptor a rabies virus receptor? *Science* 215:182-4
152. Lentz TL, Wilson PT, Hawrot E, Speicher DW. 1984. Amino acid sequence similarity between rabies virus glycoprotein and snake venom curaremimetic neurotoxins. *Science* 226:847-8
153. Leslie MJ, Messenger S, Rohde RE, Smith J, Cheshier R, et al. 2006. Bat-associated rabies virus in Skunks. *Emerg Infect Dis* 12:1274-7
154. Lewis P, Fu Y, Lentz TL. 1998. Rabies virus entry into endosomes in IMR-32 human neuroblastoma cells. *Exp Neurol* 153:65-73
155. Lewis P, Lentz TL. 1998. Rabies virus entry into cultured rat hippocampal neurons. *J Neurocytol* 27:559-73
156. Li G, Barbieri MA, Colombo MI, Stahl PD. 1994. Structural features of the GTP-binding defective Rab5 mutants required for their inhibitory activity on endocytosis. *J Biol Chem* 269:14631-5
157. Li PP, Chen C, Lee CW, Madhavan R, Peng HB. 2011. Axonal filopodial asymmetry induced by synaptic target. *Mol Biol Cell* 22:2480-90
158. Libersou S, Albertini AA, Ouldali M, Maury V, Maheu C, et al. 2010. Distinct structural rearrangements of the VSV glycoprotein drive membrane fusion. *J Cell Biol* 191:199-210
159. Lin SX, Gundersen GG, Maxfield FR. 2002. Export from pericentriolar endocytic recycling compartment to cell surface depends on stable, detyrosinated (glu) microtubules and kinesin. *Mol Biol Cell* 13:96-109
160. Liu H, Liu Y, Liu S, Pang DW, Xiao G. 2011. Clathrin-mediated endocytosis in living host cells visualized through quantum dot labeling of infectious hematopoietic necrosis virus. *J Virol* 85:6252-62
161. Lo KM, Sudo Y, Chen J, Li Y, Lan Y, et al. 1998. High level expression and secretion of Fc-X fusion proteins in mammalian cells. *Protein Eng* 11:495-500
162. Lopez A, Miranda P, Tejada E, Fishbein DB. 1992. Outbreak of human rabies in the Peruvian jungle. *Lancet* 339:408-11
163. Lumio J, Hillbom M, Roine R, Ketonen L, Haltia M, et al. 1986. Human rabies of bat origin in Europe. *Lancet* 1:378

164. Luscher-Mattli M, Gluck R, Kempf C, Zanoni-Grassi M. 1993. A comparative study of the effect of dextran sulfate on the fusion and the in vitro replication of influenza A and B, Semliki Forest, vesicular stomatitis, rabies, Sendai, and mumps virus. *Arch Virol* 130:317-26
165. Lyles DS, Rupprecht CE. 2007. *Rhabdoviridae*. In *Fields virology*, ed. DM Knipe, PM Howley, DE Griffin, RA Lamb, MA Martin, et al:1363-408. Philadelphia, PA.: Lippincott/The Williams & Wilkins Co. Number of 1363-408 pp.
166. Macia E, Ehrlich M, Massol R, Boucrot E, Brunner C, Kirchhausen T. 2006. Dynasore, a cell-permeable inhibitor of dynamin. *Dev Cell* 10:839-50
167. Madhusudana SN, Sundaramoorthy S, Ullas PT. 2010. Utility of human embryonic kidney cell line HEK-293 for rapid isolation of fixed and street rabies viruses: comparison with Neuro-2a and BHK-21 cell lines. *Int J Infect Dis* 14:e1067-71
168. Mani CS, Murray DL. 2006. Rabies. *Pediatr Rev* 27:129-36; quiz 36
169. Maritzen T, Haucke V. 2010. Gadkin: A novel link between endosomal vesicles and microtubule tracks. *Commun Integr Biol* 3:299-302
170. Martin D, Calder LJ, Garcia-Barreno B, Skehel JJ, Melero JA. 2006. Sequence elements of the fusion peptide of human respiratory syncytial virus fusion protein required for activity. *J Gen Virol* 87:1649-58
171. May RC, Machesky LM. 2001. Phagocytosis and the actin cytoskeleton. *J Cell Sci* 114:1061-77
172. McCall BJ, Epstein JH, Neill AS, Heel K, Field H, et al. 2000. Potential exposure to Australian bat lyssavirus, Queensland, 1996-1999. *Emerg Infect Dis* 6:259-64
173. McCall BJ, Field HE, Smith GA, Storie GJ, Harrower BJ. 2005. Defining the risk of human exposure to Australian bat lyssavirus through potential non-bat animal infection. *Commun Dis Intell* 29:202-5
174. McCarthy LC, Terrett J, Davis ME, Knights CJ, Smith AL, et al. 1997. A first-generation whole genome-radiation hybrid map spanning the mouse genome. *Genome Res* 7:1153-61
175. McColl KA, Chamberlain T, Lunt RA, Newberry KM, Middleton D, Westbury HA. 2002. Pathogenesis studies with Australian bat lyssavirus in grey-headed flying foxes (*Pteropus poliocephalus*). *Aust Vet J* 80:636-41
176. McColl KA, Chamberlain T, Lunt RA, Newberry KM, Westbury HA. 2007. Susceptibility of domestic dogs and cats to Australian bat lyssavirus (ABLV). *Vet Microbiol* 123:15-25



177. McColl KA, Gould AR, Selleck PW, Hooper PT, Westbury HA, Smith JS. 1993. Polymerase chain reaction and other laboratory techniques in the diagnosis of long incubation rabies in Australia. *Aust Vet J* 70:84-9
178. McGehee DS, Role LW. 1995. Physiological diversity of nicotinic acetylcholine receptors expressed by vertebrate neurons. *Annu Rev Physiol* 57:521-46
179. McMahon HT. 1999. Endocytosis: an assembly protein for clathrin cages. *Curr Biol* 9:R332-5
180. McMahon HT, Boucrot E. 2011. Molecular mechanism and physiological functions of clathrin-mediated endocytosis. *Nat Rev Mol Cell Biol* 12:517-33
181. Mercer J, Helenius A. 2008. Vaccinia virus uses macropinocytosis and apoptotic mimicry to enter host cells. *Science* 320:531-5
182. Mercer J, Helenius A. 2009. Virus entry by macropinocytosis. *Nat Cell Biol* 11:510-20
183. Mercer J, Schelhaas M, Helenius A. 2010. Virus entry by endocytosis. *Annu Rev Biochem* 79:803-33
184. Mifune K, Ohuchi M, Mannen K. 1982. Hemolysis and cell fusion by rhabdoviruses. *FEBS Lett* 137:293-7
185. Mills RP, Swanepoel R, Hayes MM, Gelfand M. 1978. Dumb rabies: its development following vaccination in a subject with rabies. *Cent Afr J Med* 24:115-7
186. Milzani A, DalleDonne I. 1999. Effects of chlorpromazine on actin polymerization: slackening of filament elongation and filament annealing. *Arch Biochem Biophys* 369:59-67
187. Mire CE, White JM, Whitt MA. 2010. A spatio-temporal analysis of matrix protein and nucleocapsid trafficking during vesicular stomatitis virus uncoating. *PLoS Pathog* 6:e1000994
188. Miroshnikov KA, Marusich EI, Cerritelli ME, Cheng N, Hyde CC, et al. 1998. Engineering trimeric fibrous proteins based on bacteriophage T4 adhesins. *Protein Eng* 11:329-32
189. Morimoto K, Foley HD, McGettigan JP, Schnell MJ, Dietzschold B. 2000. Reinvestigation of the role of the rabies virus glycoprotein in viral pathogenesis using a reverse genetics approach. *J Neurovirol* 6:373-81
190. Morimoto K, Patel M, Corisdeo S, Hooper DC, Fu ZF, et al. 1996. Characterization of a unique variant of bat rabies virus responsible for newly emerging human cases in North America. *Proc Natl Acad Sci U S A* 93:5653-8

191. Mrak RE, Young L. 1994. Rabies encephalitis in humans: pathology, pathogenesis and pathophysiology. *J Neuropathol Exp Neurol* 53:1-10
192. Mulherkar N, Raaben M, de la Torre JC, Whelan SP, Chandran K. 2011. The Ebola virus glycoprotein mediates entry via a non-classical dynamin-dependent macropinocytic pathway. *Virology* 419:72-83
193. Murphy FA. 1977. Rabies pathogenesis. *Arch Virol* 54:279-97
194. Murray K, Selleck P, Hooper P, Hyatt A, Gould A, et al. 1995. A morbillivirus that caused fatal disease in horses and humans. *Science* 268:94-7
195. Nanbo A, Imai M, Watanabe S, Noda T, Takahashi K, et al. 2010. Ebolavirus is internalized into host cells via macropinocytosis in a viral glycoprotein-dependent manner. *PLoS Pathog* 6:e1001121
196. Nel LH, Markotter W. 2007. Lyssaviruses. *Crit Rev Microbiol* 33:301-24
197. Niwa H, Yamamura K, Miyazaki J. 1991. Efficient selection for high-expression transfectants with a novel eukaryotic vector. *Gene* 108:193-9
198. Orlandi PA, Fishman PH. 1998. Filipin-dependent inhibition of cholera toxin: evidence for toxin internalization and activation through caveolae-like domains. *J Cell Biol* 141:905-15
199. Pasqual G, Rojek JM, Masin M, Chatton JY, Kunz S. 2011. Old world arenaviruses enter the host cell via the multivesicular body and depend on the endosomal sorting complex required for transport. *PLoS Pathog* 7:e1002232
200. Pawan JL. 1959. Rabies in the vampire bat of Trinidad, with special reference to the clinical course and the latency of infection. *Caribb Med J* 21:137-56
201. Piccinotti S, Kirchhausen T, Whelan SP. 2013. Uptake of rabies virus into epithelial cells by clathrin-mediated endocytosis depends upon actin. *J Virol*
202. Plitzko JM, Rigort A, Leis A. 2009. Correlative cryo-light microscopy and cryo-electron tomography: from cellular territories to molecular landscapes. *Curr Opin Biotechnol* 20:83-9
203. Popoff MR, Poulain B. 2010. Bacterial toxins and the nervous system: neurotoxins and multipotential toxins interacting with neuronal cells. *Toxins (Basel)* 2:683-737
204. Porras C, Barboza JJ, Fuenzalida E, Adaros HL, Oviedo AM, Furst J. 1976. Recovery from rabies in man. *Ann Intern Med* 85:44-8
205. Preuss MA, Faber ML, Tan GS, Bette M, Dietzschold B, et al. 2009. Intravenous inoculation of a bat-associated rabies virus causes lethal encephalopathy in mice

- through invasion of the brain via neurosecretory hypothalamic fibers. *PLoS Pathog* 5:e1000485
206. Prive GG. 2007. Detergents for the stabilization and crystallization of membrane proteins. *Methods* 41:388-97
  207. Quirin K, Eschli B, Scheu I, Poort L, Kartenbeck J, Helenius A. 2008. Lymphocytic choriomeningitis virus uses a novel endocytic pathway for infectious entry via late endosomes. *Virology* 378:21-33
  208. Rai SK, DeMartini JC, Miller AD. 2000. Retrovirus vectors bearing jaagsiekte sheep retrovirus Env transduce human cells by using a new receptor localized to chromosome 3p21.3. *J Virol* 74:4698-704
  209. Raiborg C, Bache KG, Mehlum A, Stang E, Stenmark H. 2001. Hrs recruits clathrin to early endosomes. *EMBO J* 20:5008-21
  210. Razani B, Woodman SE, Lisanti MP. 2002. Caveolae: from cell biology to animal physiology. *Pharmacol Rev* 54:431-67
  211. Rey FA, Heinz FX, Mandl C, Kunz C, Harrison SC. 1995. The envelope glycoprotein from tick-borne encephalitis virus at 2 Å resolution. *Nature* 375:291-8
  212. Rink J, Ghigo E, Kalaidzidis Y, Zerial M. 2005. Rab conversion as a mechanism of progression from early to late endosomes. *Cell* 122:735-49
  213. Roche S, Bressanelli S, Rey FA, Gaudin Y. 2006. Crystal structure of the low-pH form of the vesicular stomatitis virus glycoprotein G. *Science* 313:187-91
  214. Roche S, Gaudin Y. 2002. Characterization of the equilibrium between the native and fusion-inactive conformation of rabies virus glycoprotein indicates that the fusion complex is made of several trimers. *Virology* 297:128-35
  215. Roche S, Rey FA, Gaudin Y, Bressanelli S. 2007. Structure of the prefusion form of the vesicular stomatitis virus glycoprotein G. *Science* 315:843-8
  216. Roine RO, Hillbom M, Valle M, Haltia M, Ketonen L, et al. 1988. Fatal encephalitis caused by a bat-borne rabies-related virus. Clinical findings. *Brain* 111 ( Pt 6):1505-16
  217. Rojek JM, Sanchez AB, Nguyen NT, de la Torre JC, Kunz S. 2008. Different mechanisms of cell entry by human-pathogenic Old World and New World arenaviruses. *J Virol* 82:7677-87
  218. Ross SR, Schofield JJ, Farr CJ, Bucan M. 2002. Mouse transferrin receptor 1 is the cell entry receptor for mouse mammary tumor virus. *Proc Natl Acad Sci U S A* 99:12386-90

219. Roth I. 2013. CVO bulletin to NSW veterinarians re Australian Bat Lyssavirus (ABLV), Veterinary Practitioners Board of New South Wales
220. Rothberg KG, Heuser JE, Donzell WC, Ying YS, Glenney JR, Anderson RG. 1992. Caveolin, a protein component of caveolae membrane coats. *Cell* 68:673-82
221. Rothberg KG, Ying YS, Kamen BA, Anderson RG. 1990. Cholesterol controls the clustering of the glycosphospholipid-anchored membrane receptor for 5-methyltetrahydrofolate. *J Cell Biol* 111:2931-8
222. Rowe RK, Suszko JW, Pekosz A. 2008. Roles for the recycling endosome, Rab8, and Rab11 in hantavirus release from epithelial cells. *Virology* 382:239-49
223. Royle SJ, Bright NA, Lagnado L. 2005. Clathrin is required for the function of the mitotic spindle. *Nature* 434:1152-7
224. Rupprecht CE, Hanlon CA, Hemachudha T. 2002. Rabies re-examined. *Lancet Infect Dis* 2:327-43
225. Rust MJ, Lakadamyali M, Zhang F, Zhuang X. 2004. Assembly of endocytic machinery around individual influenza viruses during viral entry. *Nat Struct Mol Biol* 11:567-73
226. Sabharanjak S, Sharma P, Parton RG, Mayor S. 2002. GPI-anchored proteins are delivered to recycling endosomes via a distinct cdc42-regulated, clathrin-independent pinocytic pathway. *Dev Cell* 2:411-23
227. Saeed MF, Kolokoltsov AA, Albrecht T, Davey RA. 2010. Cellular entry of ebola virus involves uptake by a macropinocytosis-like mechanism and subsequent trafficking through early and late endosomes. *PLoS Pathog* 6:e1001110
228. Saffarian S, Cocucci E, Kirchhausen T. 2009. Distinct dynamics of endocytic clathrin-coated pits and coated plaques. *PLoS Biol* 7:e1000191
229. Samaratunga H, Searle JW, Hudson N. 1998. Non-rabies Lyssavirus human encephalitis from fruit bats: Australian bat Lyssavirus (pteropid Lyssavirus) infection. *Neuropathol Appl Neurobiol* 24:331-5
230. Schneider-Schaulies J. 2000. Cellular receptors for viruses: links to tropism and pathogenesis. *J Gen Virol* 81:1413-29
231. Schnell MJ, McGettigan JP, Wirblich C, Papaneri A. 2010. The cell biology of rabies virus: using stealth to reach the brain. *Nat Rev Microbiol* 8:51-61
232. Schulz WL, Haj AK, Schiff LA. 2012. Reovirus uses multiple endocytic pathways for cell entry. *J Virol* 86:12665-75

233. Selimov MA, Tatarov AG, Botvinkin AD, Klueva EV, Kulikova LG, Khismatullina NA. 1989. Rabies-related Yuli virus; identification with a panel of monoclonal antibodies. *Acta Virol* 33:542-6
234. Semerdjieva S, Shortt B, Maxwell E, Singh S, Fonarev P, et al. 2008. Coordinated regulation of AP2 uncoating from clathrin-coated vesicles by rab5 and hRME-6. *J Cell Biol* 183:499-511
235. Shah WA, Peng H, Carbonetto S. 2006. Role of non-raft cholesterol in lymphocytic choriomeningitis virus infection via alpha-dystroglycan. *J Gen Virol* 87:673-8
236. Shankar SK, Mahadevan A, Sapico SD, Ghodkirekar MS, Pinto RG, Madhusudana SN. 2012. Rabies viral encephalitis with probable 25 year incubation period! *Ann Indian Acad Neurol* 15:221-3
237. Shaw G, Morse S, Ararat M, Graham FL. 2002. Preferential transformation of human neuronal cells by human adenoviruses and the origin of HEK 293 cells. *FASEB J* 16:869-71
238. Sieczkarski SB, Whittaker GR. 2002. Influenza virus can enter and infect cells in the absence of clathrin-mediated endocytosis. *J Virol* 76:10455-64
239. Sieczkarski SB, Whittaker GR. 2005. Viral entry. *Curr Top Microbiol Immunol* 285:1-23
240. Sissioeff L, Mousli M, England P, Tuffereau C. 2005. Stable trimerization of recombinant rabies virus glycoprotein ectodomain is required for interaction with the p75NTR receptor. *J Gen Virol* 86:2543-52
241. Srinivasan A, Burton EC, Kuehnert MJ, Rupprecht C, Sutker WL, et al. 2005. Transmission of rabies virus from an organ donor to four transplant recipients. *N Engl J Med* 352:1103-11
242. St Pierre CA, Leonard D, Corvera S, Kurt-Jones EA, Finberg RW. 2011. Antibodies to cell surface proteins redirect intracellular trafficking pathways. *Exp Mol Pathol* 91:723-32
243. Stenmark H. 2009. Rab GTPases as coordinators of vesicle traffic. *Nat Rev Mol Cell Biol* 10:513-25
244. Stimpson HE, Toret CP, Cheng AT, Pauly BS, Drubin DG. 2009. Early-arriving Syp1p and Edelp function in endocytic site placement and formation in budding yeast. *Mol Biol Cell* 20:4640-51
245. Subtil A, Gaidarov I, Kobylarz K, Lampson MA, Keen JH, McGraw TE. 1999. Acute cholesterol depletion inhibits clathrin-coated pit budding. *Proc Natl Acad Sci U S A* 96:6775-80

246. Suksanpaisan L, Susantad T, Smith DR. 2009. Characterization of dengue virus entry into HepG2 cells. *J Biomed Sci* 16:17
247. Sun X, Yau VK, Briggs BJ, Whittaker GR. 2005. Role of clathrin-mediated endocytosis during vesicular stomatitis virus entry into host cells. *Virology* 338:53-60
248. Superti F, Derer M, Tsiang H. 1984. Mechanism of rabies virus entry into CER cells. *J Gen Virol* 65 ( Pt 4):781-9
249. Superti F, Hauttecoeur B, Morelec MJ, Goldoni P, Bizzini B, Tsiang H. 1986. Involvement of gangliosides in rabies virus infection. *J Gen Virol* 67 ( Pt 1):47-56
250. Sutter G, Ohlmann M, Erfle V. 1995. Non-replicating vaccinia vector efficiently expresses bacteriophage T7 RNA polymerase. *FEBS Lett* 371:9-12
251. Swanson K, Wen X, Leser GP, Paterson RG, Lamb RA, Jardetzky TS. 2010. Structure of the Newcastle disease virus F protein in the post-fusion conformation. *Virology* 402:372-9
252. Sweitzer SM, Hinshaw JE. 1998. Dynamin undergoes a GTP-dependent conformational change causing vesiculation. *Cell* 93:1021-9
253. Swiech K, Rossi N, Astray RM, Suazo CA. 2008. Enhanced production of recombinant rabies virus glycoprotein (rRVGP) by *Drosophila melanogaster* S2 cells through control of culture conditions. *Cytotechnology* 57:67-72
254. Tao Y, Strelkov SV, Mesyanzhinov VV, Rossmann MG. 1997. Structure of bacteriophage T4 fibrin: a segmented coiled coil and the role of the C-terminal domain. *Structure* 5:789-98
255. Taylor MJ, Perrais D, Merrifield CJ. 2011. A high precision survey of the molecular dynamics of mammalian clathrin-mediated endocytosis. *PLoS Biol* 9:e1000604
256. Tebar F, Sorkina T, Sorkin A, Ericsson M, Kirchhausen T. 1996. Eps15 is a component of clathrin-coated pits and vesicles and is located at the rim of coated pits. *J Biol Chem* 271:28727-30
257. Thirapanmethee K, Ootaki N, Sakai M, Lien CK, Kawai A. 2005. Further studies on the soluble form (gs) of rabies virus glycoprotein (g): molecular structure of gs protein and possible mechanism of the shedding. *Microbiol Immunol* 49:733-43
258. Thoulouze MI, Lafage M, Schachner M, Hartmann U, Cremer H, Lafon M. 1998. The neural cell adhesion molecule is a receptor for rabies virus. *J Virol* 72:7181-90

259. Tignor GH, Shope RE. 1972. Vaccination and challenge of mice with viruses of the rabies serogroup. *J Infect Dis* 125:322-4
260. Tsiang H, Ceccaldi PE, Lycke E. 1991. Rabies virus infection and transport in human sensory dorsal root ganglia neurons. *J Gen Virol* 72 ( Pt 5):1191-4
261. Tuffereau C, Benejean J, Blondel D, Kieffer B, Flamand A. 1998. Low-affinity nerve-growth factor receptor (P75NTR) can serve as a receptor for rabies virus. *EMBO J* 17:7250-9
262. Tuffereau C, Desmeziers E, Benejean J, Jallet C, Flamand A, et al. 2001. Interaction of lyssaviruses with the low-affinity nerve-growth factor receptor p75NTR. *J Gen Virol* 82:2861-7
263. Tuffereau C, Leblois H, Benejean J, Coulon P, Lafay F, Flamand A. 1989. Arginine or lysine in position 333 of ERA and CVS glycoprotein is necessary for rabies virulence in adult mice. *Virology* 172:206-12
264. Tuffereau C, Schmidt K, Langevin C, Lafay F, Dechant G, Koltzenburg M. 2007. The rabies virus glycoprotein receptor p75NTR is not essential for rabies virus infection. *J Virol* 81:13622-30
265. Ugolini G. 1995. Specificity of rabies virus as a transneuronal tracer of motor networks: transfer from hypoglossal motoneurons to connected second-order and higher order central nervous system cell groups. *J Comp Neurol* 356:457-80
266. Ullrich O, Reinsch S, Urbe S, Zerial M, Parton RG. 1996. Rab11 regulates recycling through the pericentriolar recycling endosome. *J Cell Biol* 135:913-24
267. Ungewickell E, Ungewickell H, Holstein SE, Lindner R, Prasad K, et al. 1995. Role of auxilin in uncoating clathrin-coated vesicles. *Nature* 378:632-5
268. Vahlenkamp TW, Verschoor EJ, Schuurman NN, van Vliet AL, Horzinek MC, et al. 1997. A single amino acid substitution in the transmembrane envelope glycoprotein of feline immunodeficiency virus alters cellular tropism. *J Virol* 71:7132-5
269. van der Schaar HM, Rust MJ, Waarts BL, van der Ende-Metselaar H, Kuhn RJ, et al. 2007. Characterization of the early events in dengue virus cell entry by biochemical assays and single-virus tracking. *J Virol* 81:12019-28
270. Van Dyke S, Strahan R, eds. 2008. *The Mammals of Australia*. Brisbane: New Holland / Queensland Museum. Third ed.
271. Veiga E, Guttman JA, Bonazzi M, Boucrot E, Toledo-Arana A, et al. 2007. Invasive and adherent bacterial pathogens co-Opt host clathrin for infection. *Cell Host Microbe* 2:340-51

272. Vonderheit A, Helenius A. 2005. Rab7 associates with early endosomes to mediate sorting and transport of Semliki forest virus to late endosomes. *PLoS Biol* 3:e233
273. Wang LH, Rothberg KG, Anderson RG. 1993. Mis-assembly of clathrin lattices on endosomes reveals a regulatory switch for coated pit formation. *J Cell Biol* 123:1107-17
274. Warrell DA. 1976. The clinical picture of rabies in man. *Trans R Soc Trop Med Hyg* 70:188-95
275. Warrilow D. 2005. Australian bat lyssavirus: a recently discovered new rhabdovirus. *Curr Top Microbiol Immunol* 292:25-44
276. Watanabe S, Hirose M, Miyazaki A, Tomono M, Takeuchi M, et al. 1988. Calmodulin antagonists inhibit the phagocytic activity of cultured Kupffer cells. *Lab Invest* 59:214-8
277. Weir DL, Smith IL, Bossart KN, Wang LF, Broder CC. 2013. Host cell tropism mediated by Australian bat lyssavirus envelope glycoproteins. *Virology* 444:21-30
278. Wen X, Krause JC, Leser GP, Cox RG, Lamb RA, et al. 2012. Structure of the human metapneumovirus fusion protein with neutralizing antibody identifies a pneumovirus antigenic site. *Nat Struct Mol Biol* 19:461-3
279. West MA, Bretscher MS, Watts C. 1989. Distinct endocytotic pathways in epidermal growth factor-stimulated human carcinoma A431 cells. *J Cell Biol* 109:2731-9
280. White J, Matlin K, Helenius A. 1981. Cell fusion by Semliki Forest, influenza, and vesicular stomatitis viruses. *J Cell Biol* 89:674-9
281. WHO. 2010. Current WHO guide for rabies pre and post-exposure prophylaxis in humans, World Health Organization
282. WHO. 2013. Rabies; Fact Sheet No. 99, World Health Organization
283. Willoughby RE, Jr. 2009. "Early death" and the contraindication of vaccine during treatment of rabies. *Vaccine* 27:7173-7
284. Willoughby RE, Jr., Tieves KS, Hoffman GM, Ghanayem NS, Amlie-Lefond CM, et al. 2005. Survival after treatment of rabies with induction of coma. *N Engl J Med* 352:2508-14
285. Wilson DE, Reeder DM, eds. 2005. *Mammal Species of the World. A Taxonomic and Geographic Reference*: Johns Hopkins University press. 2,142 pp. 3rd ed.



286. Wilson IA, Skehel JJ, Wiley DC. 1981. Structure of the haemagglutinin membrane glycoprotein of influenza virus at 3 Å resolution. *Nature* 289:366-73
287. Winkler WG, Fashinell TR, Leffingwell L, Howard P, Conomy P. 1973. Airborne rabies transmission in a laboratory worker. *JAMA* 226:1219-21
288. Witvrouw M, De Clercq E. 1997. Sulfated polysaccharides extracted from sea algae as potential antiviral drugs. *Gen Pharmacol* 29:497-511
289. Wojczyk B, Shakin-Eshleman SH, Doms RW, Xiang ZQ, Ertl HC, et al. 1995. Stable secretion of a soluble, oligomeric form of rabies virus glycoprotein: influence of N-glycan processing on secretion. *Biochemistry* 34:2599-609
290. Wojczyk BS, Czerwinski M, Stwora-Wojczyk MM, Siegel DL, Abrams WR, et al. 1996. Purification of a secreted form of recombinant rabies virus glycoprotein: comparison of two affinity tags. *Protein Expr Purif* 7:183-93
291. Yang X, Farzan M, Wyatt R, Sodroski J. 2000. Characterization of stable, soluble trimers containing complete ectodomains of human immunodeficiency virus type 1 envelope glycoproteins. *J Virol* 74:5716-25
292. Yang X, Florin L, Farzan M, Kolchinsky P, Kwong PD, et al. 2000. Modifications that stabilize human immunodeficiency virus envelope glycoprotein trimers in solution. *J Virol* 74:4746-54
293. Yang X, Lee J, Mahony EM, Kwong PD, Wyatt R, Sodroski J. 2002. Highly stable trimers formed by human immunodeficiency virus type 1 envelope glycoproteins fused with the trimeric motif of T4 bacteriophage fibritin. *J Virol* 76:4634-42
294. Yao Q, Chen J, Cao H, Orth JD, McCaffery JM, et al. 2005. Caveolin-1 interacts directly with dynamin-2. *J Mol Biol* 348:491-501
295. Yin HS, Wen X, Paterson RG, Lamb RA, Jardetzky TS. 2006. Structure of the parainfluenza virus 5 F protein in its metastable, prefusion conformation. *Nature* 439:38-44
296. Young PL, Halpin K, Selleck PW, Field H, Gravel JL, et al. 1996. Serologic evidence for the presence in Pteropus bats of a paramyxovirus related to equine morbillivirus. *Emerg Infect Dis* 2:239-40